Daylight Availability and Manual Lighting Control in Office Buildings – Simulation Studies and Analysis of Measurements

Dissertation towards the Attainment of

the academic degree of

Doctor of Engineering (Dr.-Ing.)

from the Faculty of Architecture

at the University of Karlsruhe, Germany

by

Christoph F. Reinhart, Dipl.-Phys., M.Sc.

from Düsseldorf, Germany

Date of oral exam:	October 8th 2001
Committee Chair	Professor Dr. sc. techn. Niklaus Kohler
Senior Supervisor	Professor Andreas Wagner
External Examiner	Professor Dr. Jean-Louis Scartezzini, Lausanne
Further committee member	Professor Rüdiger Kramm

The stone age did not end because of a lack of stone same as the oil age will not end because we will run out of oil.

Sheik Ahmed Naki Yamani[1] *2000*

[1] *OPEC consultant and Saudi Arabia's oil minister from 1962 to 1986*

Abstract

This thesis aims to encourage a wider usage of daylighting design features in office buildings. The two major outputs are a *dynamic daylight simulation method* and a *manual lighting control model*. While the former method predicts the annual daylight availability in buildings, the latter model also considers occupant behavioral patterns to predict the temporary status of the artificial lighting and blind system.

The first part of this thesis concentrates on the development and validation of a reliable but easy-to-use dynamic daylight simulation method, which is based on the backward raytracer RADIANCE and the concept of daylight coefficients. The performance of the method is compared to conventional dynamic daylight simulation methods and simulation results are compared to illuminance measurements in a full scale test-bed under more than 10,000 sky conditions. The method also features a stochastic model which generates the short-time-step dynamics of natural daylight based on hourly mean direct and diffuse irradiances. The method is able to predict the annual daylight availability in arbitrary buildings with complicated facade geometries and advanced shading devices such as external venetian blinds.

While daylight simulations predict the physically available amount of daylight in a building, field studies are necessary to understand how people tend to respond to changing indoor illuminance distributions, i.e. how and when they operate their artificial lighting and blind systems. Therefore, a literature review of past studies has been carried out and a new monitoring procedure has been designed and installed in an office building in Southern Germany. The collected data are used to validate and refine behavioral switching patterns, which in turn form the basis of a manual lighting control model. The model combines simulated indoor illuminance and occupancy profiles with probabilistic switching patterns to predict the electric energy demand for artificial lighting in a work place.

Both methods have been implemented into a C-program which can be readily integrated into existing building simulation programs and is available upon request from the author[2].

keywords: *daylight simulations, daylight coefficients, RADIANCE, occupant behavior, manual lighting control, blind control*

[2] christoph.reinhart@nrc.ca

Dedication

To Diana, my one and only.

Acknowledgement

This thesis presents research results from my work as a junior researcher at the Solar Building Design Group of the Fraunhofer Institute for Solar Energy Systems (ISE) in Freiburg, Germany, which lasted from August 1998 to January 2001. The data analysis and development of the manual lighting control model (chapter 7 and 8) was carried out in spring 2001 at the Institute for Research in Construction of the National Research Council Canada in Ottawa, Canada. I am indebted to both Institutes for providing me with excellent research facilities and an inspiring and friendly working environment.

My work at the Fraunhofer ISE has been funded through the German Research Foundation under the contract number LU 204/10-2 and I am grateful to Joachim Luther and Volker Wittwer for enabling me to carry out such a long-term research project without the need to acquire short-term revenues. The monitoring equipment for the pilot study which is described in part B of this work has been funded by the Federal German Ministry of Economics and Technology under the contract number 033506U.

First of all, I want to thank Andreas Wagner for accepting me as a Ph.D. student at the Department of Architecture of the Technical University of Karlsruhe, Germany, as well as Jean-Louis Scartezzini for acting as the external examiner and Niklaus Kohler for chairing my defense committee.

Concerning the research itself, I want to express my very special thanks to my supervisor at the Fraunhofer ISE, Karsten Voss, for guiding me towards the formulation and realization of an in-depth research project. Karsten was a constant source of inspiration and motivation – always willing to critically review my results and play Volleyball.

The comparison of different dynamic daylight simulation methods (chapter 3) is the result of many fruitful discussions with Sebastian Herkel who was a competent colleague and friend.

The work for chapter 4 and 5 was accomplished in collaboration with Oliver Walkenhorst whom I had the pleasure to accompany through his first research project which lead to the successful completion of this Master Thesis in Physics at the Albert-Ludwigs Universität Freiburg, Germany. Oliver, working with you has always been rewarding and a lot of fun.

Special thanks to Christian Reise for providing the external irradiance and illuminance data for Freiburg and to Jan Wienold for letting me use the daylighting test facilities at the Fraunhofer ISE.

Clint Johnson assisted me during the development of the experimental setup for the pilot study described in chapter 6 as a part of his five month internship with the Fraunhofer ISE. He carefully assembled and tested the monitoring devices which have been reliable working throughout the whole monitoring period.

Many thanks to Peter Schossig, Peter Jäckle and Peter Apian-Bennewitz for providing amazing computer support for the remote monitoring and data acquisition setup in Weilheim. The system did not fail once during measurement period except when the monitoring PC was accidentally switched off.

The cooperation with Peter Seeberger and Uwe Bauer from the Fachhochschule Stuttgart was also a thoroughly pleasant experience. Thanks a lot Peter for saving me several maintenance trips to Weilheim!

Finally, I feel privileged to have been given the opportunity to be a member of the Solar Building Design Group and work in a professional team in which everybody works on exciting research projects.

Thanks to Karsten Voss, Guy Newsham and my wife Diana for proof-reading this thesis and providing valuable comments which greatly enhanced the quality of the work.

Di, I very much appreciated your patience when I was obsessed with the completion of this work in the months proceeding our move to Canada. The future will see a lot more work-free weekends.

Thanks to everybody who takes the time to read this thesis. It will be my great delight to discuss its content with you.

Ottawa, Canada, November 5, 2001

Table of Content

Chapter 1 Introduction

The energy related carbon emissions of the European building stock are substantial. To address this problem an *integrated design approach* aims to reduce the energy demand of a building via a performance assessment of various energy efficiency measures during the design phase. Such an approach requires reliable simulation methods to enable architects and building engineers to compare different design options.

Accordingly, the first part of this thesis concentrates on the development of a reliable but easy-to-use dynamical RADIANCE-based daylight simulation method to model the annual daylight availability in a building. The second part presents a field study of a building in Southern Germany in which the manual control of the artificial lighting and blind system has been monitored and analyzed. Based on the observed user behavior and previous findings a manual lighting control model is proposed which predicts the energy demand of a manually operated lighting system.

1.1. Energy and Buildings

Buildings fulfill multiple proposes. They provide shelter and aim to create adequate working and living conditions for their inhabitants. Apart from these functional aspects, buildings serve as a means of cultural identification and social representation. To satisfy all these diverse expectations, financial, material and energy resources are required to construct and maintain a building. Despite the diversity of individual life styles in the EU member states, about a third of the total energy use in these countries is used to heat, cool, ventilate and light buildings. Fig. 1-1 shows the resulting individual energy related annual carbon emissions per capita for all EU member states. The accompanying costs in the domestic and tertiary sector correspond to roughly 4% of the gross domestic product of the European Union (EU)[3].

Traditionally, a country's consumption figures have been determined by living standards, economic growth rates and energy prices but the recent development in several EU member states shows that emission levels can be decoupled from the economic output and to a certain degree from the climatic boundary conditions. If more sustainable building practices were fostered, the future carbon emissions of all EU countries could fall well below the lowest levels found in Fig. 1-1.

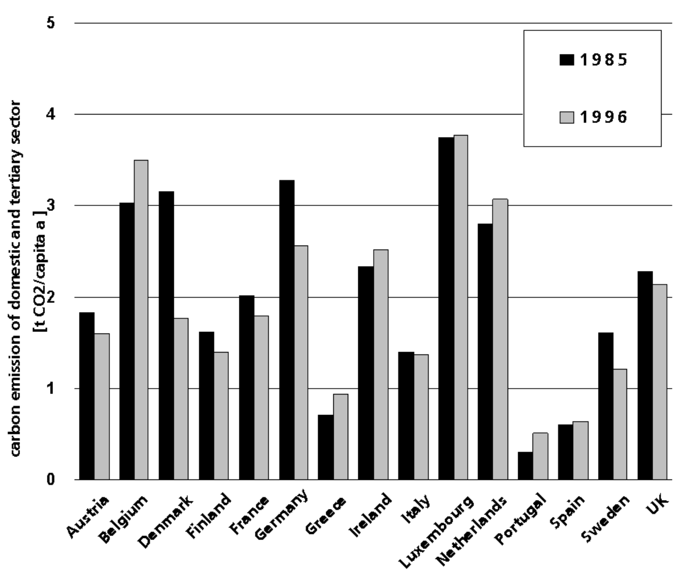

Fig. 1-1: Energy related carbon emission in the domestic and tertiary sector in the EU member states [ESAP98].

1.2. Energy Use in Office Buildings

Nowadays, more than 50% of the workforce in Western societies works in offices [red97] and as a consequence the total office area has risen in the past decades. Fig. 1-2 shows that at the same time the total primary energy demand per net floor area in offices has also risen. The figure reveals that the mean annual heating demand in Swiss and Swedish office buildings has fallen by a factor of two while the electricity demand doubled. As the primary energy content of electrical energy is roughly 2.6 times[4] higher than that of thermal energy, this development has lead to the surprising fact that the energy consumption in many commercial buildings is nowadays dominated by the electricity demand for lighting, ventilation, cooling and office suppliants – even in traditionally heating dominated climates. Several circumstances have contributed to this development:

[3] The number has been estimated from the energy demand weighted with the European mean costs for oil, gas, coal and electricity in 1996[ESAP 98].
[4] number valid for the German energy mix [tem97]

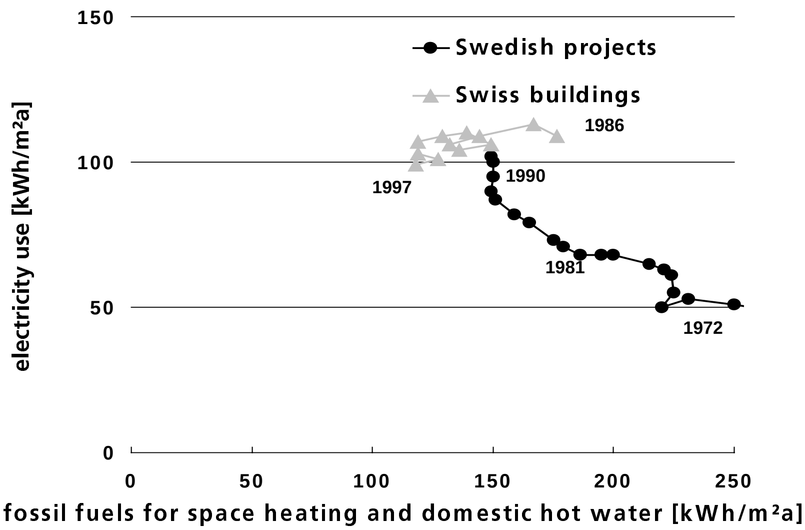

Fig. 1-2: Development of the electricity use and demand for fossil fuel for space heating and domestic hot water in Swedish and Swiss office building from 1972 to 1997 [nil97, web99].

stricter building codes: The reduced energy demand for space heating has been mainly initiated by stricter building codes which progressively refined over the years and have lead to an enhanced thermal quality of building envelopes.

changing office environments: The seventies and eighties have seen a rising numbers of open plan office environments in several central European countries. These work spaces provide centrally controlled artificial lighting and mechanical ventilation with very limited or no control for the individual. The resulting energy intensive building automation system aims to create a time- and site-independent indoor climate which approaches a narrow, *trans*-global norm for what are considered to be adequate working conditions [bak99]. As a collective standard reduces the tolerance range for indoor climatic conditions, the need for HVAC[5] equipment rises together with the energy demand. While open plan office environments are nowadays still widely used in North America [new01], they seem to have become less popular in Europe over the past decades.

more electrical office equipment: Modern office buildings have experienced an explosive increase in the use of electrically powered office equipment like PCs, printers and other technical devices. This lead to rising internal loads and the necessity to mechanically cool offices even in moderate climates. Nowadays, more energy efficient appliances are finding their way into offices, e.g. LCD computer displays and fluorescent lamps but the energy benefit of these devices is often outweighed by extended stand-by periods.

design aspects: Commercial buildings communicate the corporate identity of the building inhabitants to the outside and place a building in context with its neighboring surroundings. This important function of buildings has lead to build examples which ignore their climatic boundary conditions for the sake of a desired visual impression. Particularly, the trend towards an extended use of glazings often causes unwanted solar gains which may drastically increase the cooling load of office buildings.

The diversity of these issues highlights the complexity of the phenomena of rising electrical energy demands in office buildings. The usage of energy-efficient office equipment and better-sized HVAC systems should become a high priority concern for building owners and could be promoted either via higher energy prices or via extended building codes which feature electrical *and* thermal energy benchmarks. To promote the use of energy saving measures which involve the overall building design, it is important to teach the necessary design techniques to architects and to introduce them to the concept of *integrated design* [sch96].

[5] HVAC: heating ventilation air-conditioning

1.3. Integrated Design

The goal of an integrated design approach is to construct a so-called *lean building* which harmonizes with its given climatic boundary conditions and exploits naturally available energy sinks and sources in order to provide increased visual and thermal comfort for its inhabitants while reducing the energy demand. To realize the ambitious goals of constructing a lean building, a more thorough planning compared to a conventional building is required. Ideally, the building owner initially formulates a catalogue of requirements for the future building. Certain weights should be assigned to the different items in the catalogue which reflect personal preferences, the available economical resources, the anticipated working conditions for the users and the sustainability of the resulting building. The composition of the design team should reflect the earlier chosen preferences so that the interrelations between the building and the HVAC system design can be addressed and possibly exploited. In the latter case, the extra costs created in the planning phase can be counterbalanced by reduced initial investments or lower future operation costs, i.e. costs are shifted from the investment into the planning phase [vos01].

Innovative building designs require a careful assessment of the energy flows as well as the resulting thermal and visual conditions in the future building. These quantities can only be predicted during the conceptual design phase if reliable simulation methods are available. Various building simulation programs are already widely used to model the energy flows within buildings. Prominent examples are TRNSYS [bec94], ESP-R [cla97] and ENERGYPLUS (former BLAST and DOE2) [cra01]. These programs feature sophisticated physical models to simulate thermal energy flows but they fail to provide reliable predictions of the indoor daylight availability for advanced building designs. There is an even greater insecurity about how the users of a building might react towards changing indoor illuminance and temperature conditions. This ignorance can introduce substantial errors in building simulations as the status of shading devices and the artificial lighting greatly influences the incoming solar gains and internal loads. Accordingly, the present work aims to enrich the catalogue of existing simulation tools with methods which yield reliable predictions of annual indoor illuminance levels due to daylight and which provide some insight into how the users of an office building tend to react towards changing indoor illuminance levels.

1.4.Thesis Outline

Fig. 1-3 sketches the content of this thesis. In part A a *dynamic* daylight simulation tool to predict the indoor illuminance distribution due to daylight and artificial lighting over an extended period of time is developed. An introduction into daylight simulations is given in chapter 2 followed by a performance evaluation of a new and several conventional RADIANCE-based dynamic daylight simulation methods in chapter 3. In chapter 4 the new simulation method is validated against actually measured data. The influence of the underlying time-step interval for simulations of the annual daylight availability is discussed in chapter 5.

In Part B a manual lighting control model is proposed. A field study has been carried out in which occupancy and working conditions in 10 offices as well as the status of the outer blind system and the artificial lighting system have been collected over a nine-month period in an office building situated in Weilheim, Germany. The experimental procedure is presented in chapter 6 and results are analyzed and discussed in chapter 7. In chapter 8, a manual lighting control model is integrated with the dynamical daylight simulation method from part A and an example application is presented.

Chapter 9 summarizes the results of this thesis.

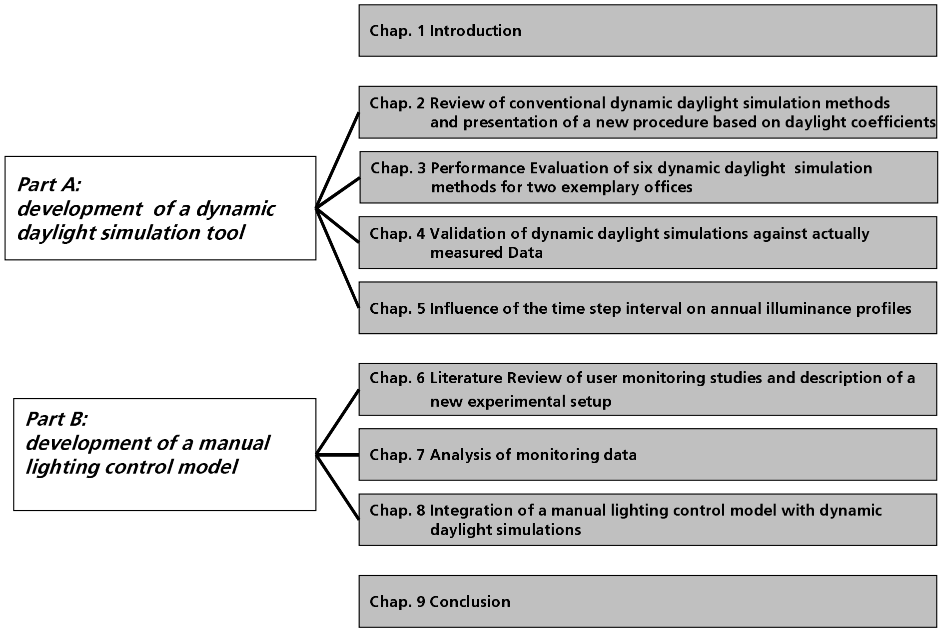

Fig.1-3: Thesis Outline.

1.5. Hypotheses

The research presented in this thesis is based on the assumption that it is *useful* and *possible* to develop a planning simulation tool that predicts annual indoor illuminance profiles and yields the status of the shading device and the artificial lighting based on occupancy and illuminance profiles. This conviction is founded on the following hypotheses which will be discussed in the concluding chapter 9:

<u>feasibility:</u>

- The short-time-step dynamics of indoor illuminance levels due to daylight can be accurately simulated for a range of climatic boundary conditions and building geometries.
- People consciously and consistently operate their blinds and artificial lighting system and tend to follow a number of basic behavioral patterns. These patterns can be used to estimate electric energy demands of a manually operated lighting system.

<u>justifiable effort:</u>

- The required effort and working hours to produce such simulations can be justified by the additional insight gained from the results.

<u>relevance:</u>

- The implementation of behavioral patterns into lighting simulation programs yields more accurate simulation results which can help to judge daylighting strategies and products during the conceptual design phase of a building.

Part A Dynamic Simulations of the Daylight Availability in Buildings

In part A of this thesis a new dynamic, RADIANCE-based daylight simulation method is developed, compared to conventional simulation methods and validated against reality. Complementary to the daylight simulation method a stochastic model has been implemented that generates the short-time-step development of direct and diffuse irradiances from hourly mean values. Linked together, both approaches yield a reliable tool to model the short-time-step dynamics of indoor illuminances in buildings for arbitrary sites on earth. Part A comprises chapters 2 to 5.

Chapter 2 Daylight Simulation Methods

Following an introduction into daylighting theory, an overview of existing static and dynamic daylight simulation methods is presented. Afterwards a new dynamic method is described which has been implemented into the RADIANCE simulation environment and which uses the concept of daylight coefficients according to Tregenza.

2.1. Aspects of the Theory of Daylighting

Daylighting is the immediate exploitation of solar energy and an established building design aspect. It strives to optimize the availability of glare-free natural daylight to light the interior of a building. The term is predominantly used in the context of commercial buildings in which the times of daylight availability and building occupation largely overlap. The benefits of a carefully planned daylighting concept range from an enhanced *lighting quality* for the inhabitants to a reduced artificial lighting consumption. While annual indoor illuminance levels as well as the electric energy demand for artificial lighting are measurable entities, *lighting quality* still lacks a clear definition and a common metric. It can be paraphrased as the "effect of the luminous environment on the occupants of a building" [vei95, sic99] and involves design as well as health aspects. *Daylighting* a building has far-reaching consequences for the inhabitants and some key features of daylight are described in the following like

- its effect on the human body,
- its role as an architectural design element,
- its interaction with the climatisation concept and
- its role in official norms and building codes.

<u>daylight and the human body:</u> Most humans experience daylight as more pleasing and stimulating than artificial lighting and there is an overall consensus that a satisfactorily daylit work place positively influences the productivity of a person. This hypothesis still lacks a scientifically sound proof as the experience of *visual comfort* is highly individual. So far no consent has even been reached of how much daylight is necessary to perform a specific task and which external stimuli are apt to describe the quality of a daylit space. Among the physically measurable quantities which have been proposed are

- illuminance levels and illuminance uniformity,
- the luminance distribution within the view of the spectator,
- the readability of a screen and
- the color rendering and spectral power distribution of the light source.

The influence of such external stimuli on the visual perception of a space does probably not only depend on the performed task and individual differences but also on cultural and historical expectations [vei96]. This complexity makes it difficult - maybe impossible – to predict the visual perception of a daylit space even though numerous research efforts are carried out worldwide [cak00, vei96, vel99, wie99].

Concerning the physiological reaction of humans to daylight, it is well established, that daylight influences the daily and yearly rhythm of certain hormones of which melatonin is the most widely investigated. The secretion of melatonin is characterized by high nocturnal and low diurnal levels, i.e. it is closely entangled with the cardiac wake-sleep cycle in humans. The secretion of melatonin is stopped if light of sufficient intensity is incident on the eye. This effect is stronger for daylight than for conventional artificial lighting as its spectral composition exactly matches the receptivity of the human eye [ken91, pic91, vel99].

Collins reviewed research on psychological reactions to windows [col76]. She found that the main qualities of windows are view, sunshine, daylight and spaciousness. Concerning the impact of windowless working environments on the human psyche, Collins noted that people general express a desire for windows even though the intellectual and academic performance of some students in a school in California "was neither impaired not improved by a windowless classroom". She also found that the absence of windows is often urgently experienced in static environments and for people with monotonous working tasks.

Collins results stand in contrast to a recent study by the California-based Heshong Mohane Group [hes99]. The researchers investigated the performance of over 21,000 school kids in California, Colorado and Washington on standardized tests and found a significant and positive correlation between a daylight rating code for class rooms and the relative academic progress of school kids that were taught in these class rooms. According to the study "students in a California school district with the most daylight in their class rooms progressed 20% faster on math tests and 26% on reading tests than those with the least". The validity of these dramatic effects is currently tested in a further-going set of studies.

daylight as a design element: The history of daylighting and the history of architecture were one until the second half of the twentieth century when the development of inexpensive electrical lighting sources allowed to replace daylight by artificial lighting [tur00,ben90]. The new possibilities lead to different building designs which cumulated in factories and offices without any windows [col76]. Daylighting degraded from a necessary mean of lighting a space to a light source of choice. Since the early seventies daylight is regaining importance as a design element, partly to substitute electrical energy for lighting but also due to a rising concern towards the physiological and psychological benefits which are attributed to daylight: A window establishes visual contact with the outside and a room with a view provides a feeling of spaciousness and suppresses feelings of isolation [col76]. Therefore, a space near a window is a highly desired architectural feature in most professional environments [ino88]. Another bonus of natural daylight is its dynamics. The resulting continuously changing lighting conditions are a stimulating effect which is usually not provided by conventional artificial lighting[6].

The strong influence of light – particularly daylight – on the perception of a room together with the strong historic ties of daylighting and architecture cause that daylighting is often perceived as an exclusively architectural domain, a pure matter of design. Such a one-dimensional interpretation of daylight can lead to buildings in which the lighting designer "creates a pleasant space and then sees if there is enough light to see by" [wag85, vei95]. Under such conditions, the interactions of daylight with the remaining energy flows in a building are neglected.

daylight and solar gains: The daylighting concept strongly interacts with the air-conditioning concept of a building as daylight is always accompanied by solar gains. Usually the goal is to admit sufficient daylight but to avoid solar gains in the cooling period. This apparent contradiction can often be resolved, as usually only scattered, diffuse daylight can be used for lighting. Direct sunlight is a heat and glare source and can only be used for lighting a computer work place if it is well distributed and does not create excessively high illumination levels[7]. Usually the heat load resulting from daylight is less than from electric light due to the high luminous efficacy of daylight (see also glossary). Therefore, the daylighting and climatisation concepts can be compatible unless unfavorable boundary conditions are set either by an unsuitable building design, e.g. through oversized glazings, or in the case of uncommon working requirements [DIA92].

daylight and its role in official norms: Norms have been implemented for numerous years to ensure work place safety and adequate ergonomic working conditions in Western Societies e.g. [DIN 5035, VBG95]. Some of these legally advising design guidelines promote the use of daylight in buildings based on the common notion that daylight is beneficial to employees' health and enhances the productivity. The German DIN 5035 identifies daylight to be able to "counteract premature fatigue and to promote attentiveness" [Cak00, Din5035]. To ensure adequate lighting conditions, such documents usually rely on measurable physical parameters.

[6] The lighting company Luxmate® (http://www.luxmate.com/) is presently in the process of introducing a new artificial lighting systems whose output varies with time and aims to provide a stimulating effect for the users.

[7] Numerous shading and glare protection devices have found their way into the market in recent years which are designed to reduce unwanted solar gains while still maintaining visual contact with the outside and admitting sufficient daylight to the inside for lighting. Examples are found under [hüp00,war00].

Prominent requirements are minimum illuminance levels at work plane height and maximum luminance levels and contrasts within direct view of a PC work place to avoid glare [Din5035].

Innovative building codes like the Swiss SIA 380/4 code also list maximum installed artificial lighting power densities in work spaces to limit the electricity demand in commercial buildings and encourage the use of daylight to substitute artificial lighting[8]. This energy efficiency aspect of daylight is receiving growing attention and has been identified by the California based Pacific Gas & Electric Company as "the single largest ´new´ opportunity for saving energy in commercial lighting today" [tur00].

This above list of various daylighting features shows that for a daylighting concept *quality differs from quantity* [vei95]. Nevertheless, it is also not debatable, that the prediction of the future daylight availability in a building is a necessary condition for the assessment of a design variant. Simple calculation methods and spreadsheets are available to estimate the daylight availability for straightforward building geometries [DIN5034, IESNA00]. If more detailed information are required, some architects and lighting engineers employ modern computing facilities to evaluate different design options. The necessary daylight simulation tools are usually employed if an investigated design

- makes extensive use of daylight,
- involves complex building geometries,
- features a complicated shading situation due to surrounding buildings or landscape,
- includes innovative daylight elements and/or
- requires a careful management of solar gains due to a reduced HVAC system.

Design guidelines for good daylighting

The success of a daylighting concept for a specific site depends on its geographic position, the local climate, the shading situation due to surrounding objects and the overall building design. The ultimately available quantity and quality of daylight in a building is decisively influenced at several design stages:

- The early design phase is crucial during which the distribution of the building masses on the site, the orientation of the building, the room depths and ceiling heights as well as the horizontal and vertical *openness* of the building are defined.
- Later in the design process, the suitability of a facade for daylighting is determined by the position and size of apertures, the width of the window frames and the utilized types of glazing. Further important parameters are the photometrical properties of the surfaces of the ceilings and walls, the utilized shading devices and finally the artificial lighting system.
- The latter should play the role of a backup system for the available daylight. While artificial lighting contributes about a third to the total electrical energy use in an office building, an efficient lighting design can principally reduce this value by up to 70% [vol98,kno98]. This can be achieved by introducing a control system which activates and dims the lighting as needed, based on occupancy and indoor or outdoor illuminance sensors. Other saving options are the usage of lamps with higher luminous efficacies and advanced reflectors.

2.2. Daylight Simulations

A daylight simulation is a computer-based calculation which aims to predict the lighting situation in a building under a specific daylight situation. A daylight simulation program requires

- information on the building,
- information on the prevailing sky conditions and
- a simulation algorithm which calculates indoor illuminances and luminances based on the former two data complexes (Fig. 2-1).

[8] Such extended legal obligations are viewed as unnecessary and even dangerous limitations by some lighting designers. Nevertheless, they constitute an important step towards holistic building codes which address all energy demand categories of a building.

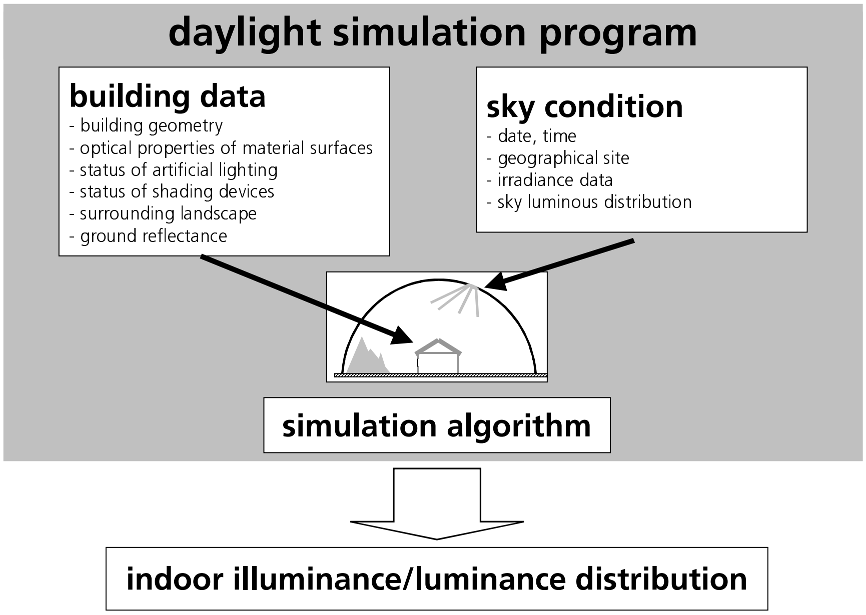

Fig. 2-1: A daylight simulation tool requires information on the building and the prevailing sky conditions to calculate indoor illuminance or luminance distributions.

building data: The description of a building for a daylight simulation comprises the geometry of the building, information on the optical properties of the involved material surfaces in the building and on the surrounding landscape. The building geometry is usually generated with CAD related design and construction tools. These programs are graphical interfaces which feature extended libraries of architectural objects like ceilings, walls, doors and windows to build two or three dimensional virtual models of a building. The optical properties like color, reflection and transmission of the involved building materials are either provided by implemented libraries or can be demanded from the manufacturers of glazings, paint or furniture. Opaque surfaces are usually characterized by their diffuse and specular reflection properties while for glazing systems the angle dependant visible transmission is needed.

Exemplary 3-dimensional CAD construction tools are AutoCAD 2000 and ArchiCAD 6.0 [aut00,arc99]. Such commercial programs are nowadays widely used by architects to support the design process of a building (see also gray box on page 17). Many CAD tools also feature simple rendering algorithms which yield visualizations of the building model. The drawback of the rendering algorithms which are presently common in such tools is that they have been designed to quickly generate photo-realistic images and not to yield physically based results. Desktop RADIANCE is an exemption which is under current development at Lawrence Berkeley National Laboratories as it aims to combine the simulation power of the validated backward raytracer RADIANCE with AutoCAD[9].

sky conditions: To calculate indoor illuminance levels due to daylight for a specific sky condition, the luminous distribution of the celestial hemisphere is required for this sky condition. This physical quantity is usually presented by a two dimensional function which yields luminance values in different sky directions. The sky luminous distribution can be either directly measured with a sky scanner or modeled using a sky model. A sky scanner is an optical device which measures luminances in different sky directions either with a number of discrete luminous sensors which aim at different sky directions or with a single sensor which is mechanically moved [Ine94]. Typical sky scanning data is recorded in 15-minute intervals and reliable data sets for a year or several months only exist for a very limited number of sites on earth as a sky scanner requires intense maintenance[10].

---

[9] see also: http://radsite.lbl.gov/radiance

[10] With the rising of modern CCD technologies chances are that low-cost sky scanners will be available in the near

As sky scanner data is very scarce, practical daylight simulation methods use theoretical sky models based on widely available input data. Until the beginning of the 1990s the CIE sky model was the most widely used sky model [doi73]. The charm of the model is that only data on date, time, site as well as monthly mean Linke turbidity factors[11] are required to yield a specific sky luminous distribution. The model differentiates between clear and overcast skies.

Since then a number of luminous efficacy models has been developed. Vartiainen from the Helsinki University of Technology in Finland used measured data from Otaniemi, Finland, to estimate the quality of six luminous efficacy models [var00, var00_a]. The models he compared had been developed by Littlefair [lit98], Perez *et al.* [per90], Olseth and Skartveit [ols89], Chung [chu92] and Muneer and Kinghorn [mun98_a]. Vartiainen found that the Perez sky luminous efficacy model yielded the lowest root mean square errors and mean bias errors with respect to the measured data. He also pointed out, that using a constant value of 110 lm/W as a simplified luminous efficacy model is not accurate enough for daylight calculations: in a climate with a high proportion of overcast sky conditions such a model underestimates the diffuse illuminance by some 13% [var00]. These results underline the importance of using a reliable sky model for daylight simulations. The Perez model which yielded the best results in Vartiainen's study is also used by the daylight simulation method which is developed in this thesis. Therefore, the following paragraph describes the model in more detail.

The *Perez all weather sky luminance model* has been developed in the early nineties by Richard Perez *et al.* and requires date, time, site and direct and diffuse irradiance values to calculate the sky luminous distribution for a given sky condition. The model consists of two independent models:

- The Perez *luminous efficacy model* calculates the mean luminous efficacy of the diffuse and the direct sunlight for a considered sky condition. Input parameters are the solar zenith angle, solar altitude, direct and diffuse illuminances as well as the atmospheric precipitable water content[12] [per90,duf91].
- The Perez *sky luminous distribution model* yields the sky luminous distribution based on date, time, direct and diffuse illuminances. The model comprises five parameters which influence the darkening or brightening of the horizon, the luminance gradient near the horizon, the relative intensity of the circumsolar region, the width of the circumsolar region and the relative intensity of light back-scattered from the earth's surface [per93].

Fig. 2-2 shows (a) a clear sky modeled with Perez and a bright overcast sky modeled with (b) Perez and (c) CIE. The comparison of the latter two sky conditions reveals the superiority of the Perez sky model compared to the CIE model. While the former distinguishes between dark and bright overcast skies and provides some details in the sky luminous distribution, the CIE overcast sky is rotationally invariant. The correct modeling of overcast skies is a crucial quality aspect of a sky model, as in mid-European climates 45% to 55% of all appearing sky conditions are overcast[13]. For very dark or bright sky conditions the Perez sky model reduces to the CIE overcast or clear sky. A limitation of the Perez model – as for any presently available sky model which is only based on direct and diffuse irradiances - is that it cannot resolve details like clouds in the sky luminous distribution.

---

future which consist of a frog-eye lens and a high resolution CCD camera. Such devices could principally yield physically correct sky luminous distributions at a high time resolution and would require little maintenance due to the absence of movable parts.

[11] For further information on the Linke turbidity factor and the atmospheric precipitable water content please refer to the glossary or [ayd81].

[12] see glossary

[13] numbers are based on the German TRYs

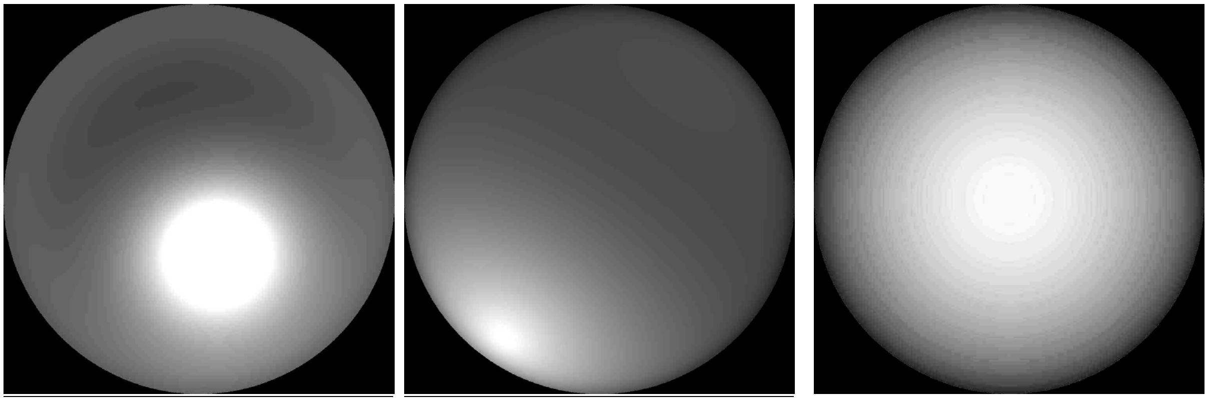

Fig. 2-2:
(a) Perez clear sky (June 21st 1 p.m.)
(b) Perez overcast sky (Jan 1st 10 a.m.)
(b) CIE overcast sky (Jan 1st 10 a.m.)

Test reference years (TRY) are available for many sites on earth and usually provide hourly mean values of the ambient temperature, wind direction and velocity, precipitation and direct and diffuse irradiances. TRYs are published by various state agencies. The German TRYs are based on sequences of several year's measurements of global irradiances. Hourly mean direct and diffuse contributions are simulated from global irradiances [blü86]. The Swiss data base METEONORM provides meteorological irradiance data for over 930 sites worldwide [met97]. For Germany METEONORM simulates hourly irradiances from monthly measurements. The European Union Project Satellight[14] provides yet another European database of daylight and solar radiation based on satellite pictures. In case there is no radiation data available for a site of interest, Munner and Gul *et al.* from Napier University in Edinburgh, Scotland, have proposed several first-principal models for obtaining solar radiation from meteorological data like sunshine duration, dry- and wet bulb temperature or the cloud amount [gul98, mun98].

Daylight simulation algorithms: As mentioned above, the task of a daylight simulation algorithm is to predict indoor illuminances and luminances based on a given sky luminance distribution and a building model. Two main different numerical approaches have been identified in the past to simulate illuminances in three dimensional space: *radiosity* and *raytracing*.

Radiosity has been originally developed to solve problems involving radiative heat transfer in various forms between surfaces based on form factors. Since the 80's it is also applied to computer graphics to calculate illuminance levels due to artificial lighting or daylight. A form-factor defines the fraction of energy leaving a given surface to that which arrives at a second surface directly [co93]. In radiosity each surface is treated like a perfectly diffuse reflector with a constant luminance so that the radiation exchange between two surfaces can be described by a single number which depends on the reflective properties of the surfaces and the scene geometry. To calculate the indoor luminance distribution in a room due to daylight, the incoming luminous flux through all transparent parts of the building envelope is set equal to the available flux within the building. This assumption defines a set of equations that uniquely determine the luminances of all considered surfaces. The basic radiosity approach can be coupled with a finite element approach which detects regions with a large luminance gradient between neighboring surface patches and subsequently subdivides the affected surfaces into sub-surfaces. A detailed description of radiosity methods can be found under [mül96, co93].

The idea behind *(backward) raytracing* is to simulate individual light rays in space to calculate the luminous distribution in a room from a given viewpoint. Therefore, rays are emitted from the point of interest and traced backwardly until they either hit a light source or another object. In

[14] http://www.physik.uni-oldenburg.de/ehf/meteo/satellight_engl.html

the former case the luminance distribution function of the light source determines the luminance contribution at the view point. If a ray hits an object, the luminance of the object needs to be calculated by secondary rays which are emitting from the object. The angular distribution under which secondary rays are *spawned* depends on the optical properties of the object. Conceptually, raytracing allows for arbitrarily complex surfaces including purely specular surfaces like mirrors, Lambertian surfaces like regular walls, transparent surfaces like glazings as well as arbitrary mixtures of these basic surface types. A ray paths is usually aborted if an certain number of reflective bounces is reached or if the weight of a ray falls below a threshold value[15]. [tsa97, war88].

An advantage of radiosity compared to raytracing is that it requires less calculation times for straightforward geometries which do not contain too many surface elements. This advantage of radiosity diminishes with rising model complexity. According to Tregenza the calculation time in radiosity increases with the square of the number of considered elements while in raytracing this relation is roughly linear [tre83]. A radiosity calculation yields the total luminance distribution in a room independent of the point of view of the spectator. Therefore, a walk-through a scene can be faster realized with radiosity than with raytracing as each new viewpoint requires a new raytracing run.

As has been pointed out by several authors, a decisive advantage of raytracing over radiosity is that only the former approach is able to simulate specular and partly specular materials [tsa97, war88]. This aspect is less crucial if only visual impressions of a given scene are desired, but if physically correct results are needed only raytracing based methods can succeed as most real surfaces exhibit specular components. Especially daylighting elements like blinds, light-shelves or prisms exhibit extremely non-diffuse surface properties and their correct modeling is crucial as all incoming daylight passes through them.

A basic problem of all daylight simulation algorithms is that they provide no estimate of the remaining calculation errors. This can turn out to be a real problem as simulation results can lie above *or* below the true illuminance levels. Simulation results are too low if a raytracer misses a small window or skylight in a room and therefore grossly underestimates the real illuminance. Results are too high if a raytracer interpolates between two bright luminances directions, e.g. from two neighboring windows, and ignores that a wall lies in the interpolated region. Michael Donn has noted that systematic quality assurance methods are seldom used by computer based simulations. New consistency checks are needed to provide the users of daylight simulation tools with more confidence into their simulation results [don99]. Obviously, the experience of the simulator is crucial. The right numerical algorithm needs to be employed for the right question and all simulation parameters need to be set carefully so that reliable results are obtained under justifiable calculation times and working efforts.

While radiosity is preferable for solving problems which only involve diffusing surfaces, raytracing tools gain importance for more advanced building designs which involve daylighting elements and features. As the latter building class is the focus of this work, a raytracing algorithm was chosen as the underlying calculation engine for all presented daylight simulations. Among the spectrum of available raytracing tools, RADIANCE is considered a *state-of-the-art* backward raytracer which is based on a mixed stochastic and deterministic raytracing approach [war88, war98]. Simulation results with RADIANCE have been physically validated for a range of building geometries and shading devices [mar97,mar95]. Further details on RADIANCE are provided in the Appendix A.2.1.

[15] The weight assigned to a single ray usually depends on the optical properties of the material from which it has been reflected before as well as the number of reflections since the primary ray has been emitted form the view point of the spectator.

Limitations of daylight simulations

Before being exposed to various daylight simulation methods in the following sections and chapters, the reader should recall that an intrinsic limitation of daylight simulations and measurements is that they are difficult to interpret. While simulation techniques have become increasingly efficient and accurate, there is still a surprising lack of suitable parameters that define "good" daylighting practice. Intuitively one might think that the luminance distribution in the field of view of an office worker is a more suitable parameter than desktop illuminances to judge the visual quality of a work place. Unfortunately, there have been too few data collected so far to support this hypothesis.

computer simulations vs. model measurements

Computer based daylight simulations compete with scaled 3-dimensional building models in which indoor illuminances are measured either under artificial or real skies. Scaled models are long established elements of the educational colloquia of most Architecture Departments and widely used during the design of larger buildings. They indicate the daylit appearance of a building from multiple view points and underline a building's task to communicate a visual impression. In contrast to a scaled model, a computer simulation only allows for a 2 dimensional inspection of a building from various view points.
The ability of both methods to predict indoor illuminance levels are equally limited by incertitudes of the photometric properties of the building surfaces and the dimensional accuracy of the building model [can97]. Nowadays, the optical properties of a growing number of building products are being provided by the manufactures so that model incertitudes will partly diminish in the future. Cannon-Brookes suggested prediction errors of indoor illuminances in refined scaled models in the order of 20% [can97]. This accuracy roughly corresponds to the accuracies which have been archived with RADIANCE simulations by Mardaljevic [mar97].
A bonus of CAD models is that they are becoming a certain standard in large commercial buildings for various planning purposes so that the specific costs of daylight simulations decrease. Both methods presently require comparable planning costs if a single building variant is investigated, but an intrinsic advantage of computer simulations is that different building variants can be investigated at little extra costs. The future will show whether both presentational modes will keep their legitimacy[16].

Photo of the building

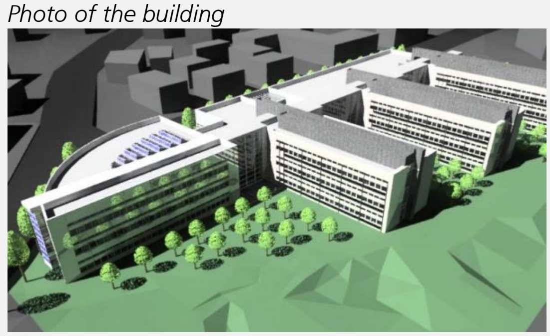

RADIANCE visualization

3-dimensional scaled model

2.2.1. Static Daylight Simulations

Daylight simulations can be divided into *static* and *dynamic* methods depending on whether they consider a single or a series of consecutive sky conditions. The results of a static daylight simulation are commonly expressed either in the form of photo-realistic images (Fig. 2-3) or in the form of illuminance values at certain points of interest in a building under a reference sky.

[16] A note for the reader: in 1990 "over 75% of the American architects [surveyed] could not *name* a CAD system they had used in the past"; in 1999 over 90% of architects, lighting consultants and electrical engineers *used* some type of CAD tool in their commercial design work. [tur00]

Static daylight simulations usually concentrate on the indoor illuminance distribution under overcast sky conditions. The daylight factor, DF, is the most common parameter to characterize the daylight situation in buildings. It is defined as the ratio of the indoor illuminance E(x) at point x to the outdoor horizontal illuminance, $E_{hor\ outside}$, under the overcast CIE sky.

$$DF(x) = \frac{E(x)}{E_{hor\ outside}} \qquad \text{(equ. 2-1)}$$

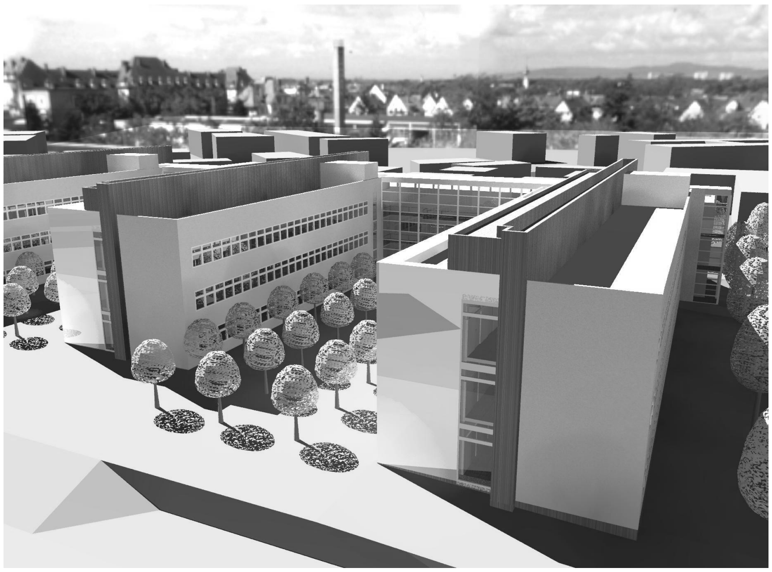

Fig. 2-3: RADIANCE visualization of the new building of the Fraunhofer Institute for Solar Energy Systems in Freiburg, Germany (architects Dissing & Weitling, Copenhagen, Denmark); by mapping a photograph of the neighboring buildings onto the celestial hemisphere the future building is set into context with its urban surroundings.

The daylight factor enjoys considerable popularity since it is an intuitive quantity which can be measured and/or calculated either based on calculation tables or more refined simulations with RADIANCE in the case of advanced building geometries and material surfaces. The major weakness of the daylight factor is that the orientation of the investigated building does not influence the daylight factor since the reference sky is rotationally invariant and independent of the geographical latitude of the investigated building (Fig. 2-2) [lit90]. Another shortcoming of the daylight factor approach is that the CIE overcast sky tends to underestimate real horizontal illuminances, causing up to 100% discrepancies between simulated and measured illuminances both above and below the simulated value [tre80]. The daylight factor provides a feeling of how "bright" or "dark" a given building is, but since it is based on a single sky luminance distribution, its credibility to judge the overall daylight situation in a given building is intrinsically limited. Fig. 2-4 presents the distribution of the daylight factor in the work plane of an exemplary office.

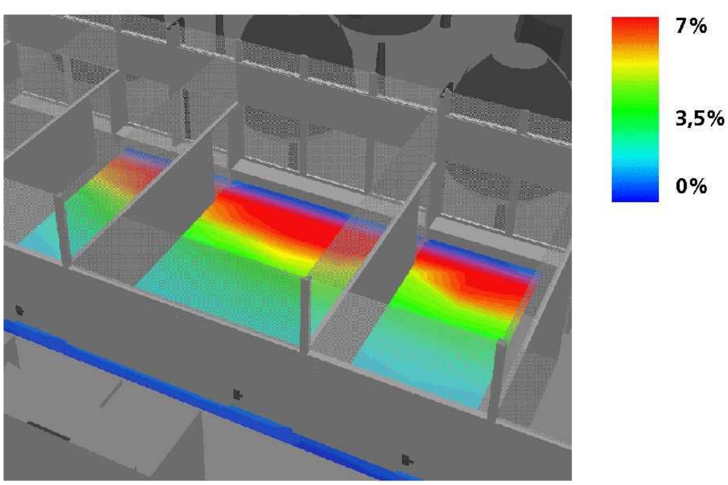

Fig. 2-4: False color picture of the distribution of the daylight factor in the work plane level of a row for South facing offices. The daylight calculations have carried out with the backward raytracer RADIANCE [Ward88] while the visualization has been done with the program RSHOW developed at the Fraunhofer Institute for Solar Energy Systems [api97].

2.2.2. Dynamic Daylight Simulations

As natural daylight is extremely dynamic and cannot be stored, static daylight simulations are only of limited usage. Usually it is necessary to calculate the daily and seasonal development of indoor illuminances and/or luminances in order to evaluate the effectiveness of a given daylighting concept. Dynamic daylight simulation methods yield the time development of indoor illuminances under multiple sky conditions and the resulting *Annual Daylighting Profiles*[17] may serve as a basis to

- quantify the energy saving potential and hence the cost effectiveness of different manual and automated artificial lighting strategies,
- avoid the appearance of glare by testing different shading strategies,
- avoid unwanted thermal loads in the cooling period while still exploiting solar radiation in the heating period,
- estimate the thermal and visual comfort at office work places by coupling the results with thermal simulation programs and/or
- predict how the overall daylight situation might be perceived by the users.[18]

Several dynamic daylight simulation methods have been proposed in the past which yield hourly mean indoor illuminances for a given building geometry. The most basic method relies on the *daylight factor* method while more advanced, integrated thermal and daylighting simulation tools like ADELINE [sze96] and ESP-R [jan97] use refined methods like the *statistical sky* and *daylight coefficients* (see below). While all these methods yield annual hourly mean indoor illuminances, they require various calculation times and yield different accuracies. To judge the suitability of a method to serve as a design tool for the actual *day-to-day* building design process a dynamic simulation method should satisfy a number of requirements. It should

(R1) yield reliable results for complex building geometries as well as for Lambertian, specular and partly specular material surfaces.
(R2) run under calculation times in the order of minutes to hours to allow for an interactive design process.
(R3) be able to model short-time-step variances of the available daylight. This requirement is necessary to successfully model the performance of automated lighting concepts based on illuminance and occupancy sensors.

Due to the reliability criteria (R1), only methods based on the RADIANCE raytracing algorithm are considered in the following.

2.3. A Review of dynamic RADIANCE-based Daylight Simulation Methods

At least five RADIANCE-based dynamic daylight simulation methods have been proposed in the past. None of these methods fulfills all of the above listed requirements, i.e. excellent accuracy under convincing simulation times with the possibility of introducing shorter time-steps. Therefore, a new method to perform annual daylight simulations based on the daylight coefficient method according to Tregenza [tre83] has been developed. The new method is termed DAYSIM and differs from the way daylight coefficients have been introduced into ESP-R with respect to accuracy and required calculation times. In chapter 3, the method is compared to a set of five popular annual daylight simulation tools, namely:

---

[17] Although in this work only Annual Daylighting Profiles of indoor *illuminances* are simulated, compared and discussed, the various dynamic daylight simulation methods could also be used to calculated annual indoor *luminance* distributions. This has not been done explicitly, as the accuracy of the different simulation methods is identical for luminance and illuminance calculations.

[18] Several of these applications are further discussed in part B of this study.

(1) complete year runs based on multiple static daylight simulations
(2) the daylight factor method according to Littlefair [lit90]
(3) ADELINE 2.0 [sze96, sze96_2] [19]
(4) classified weather data based on Herkel *et al.* [her97]
(5) ESP-R version 9 series [cla98]

Since all these different simulation approaches are based on RADIANCE, their results can be readily compared. In the rest of this chapter the underlying physical concepts of the five above listed conventional methods and DAYSIM are described.

2.3.1. Complete Year-Runs

The highest amount of accuracy for an annual dynamic daylight simulation is achieved by carrying out a static daylight simulation, i.e. a single raytracing run, for every hourly mean sky condition of the year. This great number of sky conditions can be modeled by the Perez sky model in conjunction with a TRY. *Complete year runs* are extremely time and hardware demanding and they are only considered here to serve as a reference case in chapter 3 to quantify the accuracy of the other dynamic daylight simulation methods.

2.3.2. The Daylight Factor Method

Annual illuminance distributions based on the daylight factor are traditionally performed by scaling the cumulative distribution of horizontal external diffuse illuminances with the daylight factor at the point of interest inside the building [lit90]. The weakness of this definition is that many TRYs only provide direct and diffuse irradiances *not* illuminances. For the performance evaluation of the different methods in chapter 3 the Perez luminous efficacy model has been used to get the diffuse illuminances from irradiances of the German TRY for Freiburg. This procedure ensures that the results are comparable to the reference case. The simulation results for the different methods presented in chapter 3 will show that the utilized luminous efficacy model decisively influences the quality of an indoor illuminance simulation.

Annual daylight simulations based on the daylight factor method serve as a *worst case scenario* of the annual daylight availability, since direct sunlight is discarded. To overcome the rotational invariance of the daylight factor, linear correction factors for different facade orientations have been proposed which consider the facade orientation of the investigated building [hun79]. For the daylight factor simulation in chapter 3, an orientation factor of R_{of}=1.2 taken from [lit90] for a southern facade has been used. The hourly mean illuminance, E(x), at a point, x, under a diffuse horizontal illuminance, L, is given by:

$$E(x) = DF(x) \cdot R_{of} \cdot L^{diffuse} \qquad \text{(equ. 2-2)}$$

2.3.3. ADELINE

Yet, another approach has been developed within the Task 21 of the Solar Heating and Cooling Program of the International Energy Agency and has been integrated into the lighting simulation environment ADELINE [sze96]. The program can be coupled to thermal building simulation tools. The physical basis of annual daylight simulations with ADELINE is the concept of the statistical sky according to Szerman [sze94]. The simulations are carried out in two steps. At first, the

[19] According to a recent paper from Erhorn *et al.* [erh97] the operating algorithm of the RADLINK program has not been changed in ADELINE 3.0. RADLINK is a RADIANCE-based program within the ADELINE family which generates annual illuminance distributions form a set of daylight situations.

development of indoor illuminance levels under the CIE overcast and clear skies with and without the sun are calculated for the 15th day of all months of the year with one hour time-steps. This theoretically leads to a total of

$$12 \text{ months} \times 24 \text{ hours} \times 3 \text{ sky conditions} = 864 \text{ sky conditions} \quad \text{(equ. 2-3)}$$

for which raytracing has to be carried out before the annual indoor illuminance simulation starts. The actual number of raytracing calculations is considerably smaller than 864 since no raytracing is necessary in the absence of daylight. The site-dependent turbidity values for the clear CIE skies change on a monthly basis. In the ADELINE simulation in chapter 3 actual values for Freiburg have been taken from [sze96].

In a second simulation step, hourly mean illuminance levels are approximated by mixing the corresponding clear and overcast skies depending on the *effective sunshine probability* of the hour. The effective sunshine probability for a given time interval is the ratio of the actual length of sunshine to the length of the time interval [sze96]. A sunshine probability of zero means that the sky was overcast throughout the hour whereas a sunshine probability of one corresponds to continuously clear sky conditions. To obtain this ratio, ADELINE uses the direct normal radiation data from a meteorological input file (e.g. the TRY of the considered site) and divides this value by the simulated maximum direct normal radiation for the geographical location and ambient atmosphere. As will be elaborated in section 3.3, a decisive drawback of this approach is that ADELINE does not consider diffuse horizontal irradiances for the input data file. Therefore, an hour with a vanishing sunshine probability is always modeled as a dark standard overcast CIE sky. Fig. 2-2 shows the significant differences between a bright overcast sky modeled by the Perez instead of the CIE sky model.

2.3.4. Classified Weather Data

To reduce the over 4700 hourly mean daylight situations, considered for a complete year-run, Herkel *et al.* have proposed a method to classify this ensemble into a set of some 450 classes [her97]. In this method similar sets of daytime, sun position, direct and diffuse illuminances are grouped into classes which represent all appearing sky distributions during the course of a year. The classification leaves the mean global irradiances unaltered. This approach reduces the required calculation times by up to one order of magnitude with respect to the reference case.

2.3.5. Daylight Coefficient Methods

The concept of daylight coefficients has been originally proposed by Tregenza in [tre83] as a method to calculate indoor illuminance levels due to daylight under arbitrary sky conditions. The underlying idea is to theoretically divide the celestial hemisphere into disjoint sky patches. Afterwards the contribution to the total illuminance at a point in a building is calculated for each sky patch individually. Fig. 2-5 shows that for a point and orientation, x, a daylight coefficient, $DC_\alpha(x)$, related to the sky segment S_α is defined as the illuminance, $E_\alpha(x)$, at x caused by the sky segment S_α divided by the luminance L_α and the angular size, ΔS_α, of the sky segment.

The decisive advantage of the daylight coefficient method over all formerly mentioned methods is that the daylight coefficients for a given point in a building merely depend on the building geometry, material characteristics and the division of the surrounding sky and ground into disjoint segments. Daylight coefficients are independent of any actual celestial sky luminance distribution. Hence, the building characteristics and the surrounding sky conditions are separated. A complete set of daylight coefficients can be coupled with an arbitrary sky luminance distribution, L_α, with α =1...N, by a simple linear superposition to calculate the total illuminance E(x) at x:

$$E(x) = \sum_{\alpha=1}^{N} DC_\alpha(x) L_\alpha \Delta S_\alpha \qquad \text{(equ. 2-4)}$$

Using this simple algebraic equation, annual daylight simulations can be carried out under simulation times in the order of minutes to hours while still allowing to model short-time-step variances of the available daylight[20].

Daylight coefficient methods differ in how the celestial hemisphere is divided into disjoint sky segments and how direct sunlight and diffuse daylight are treated. Both ESP-R as well as DAYSIM use daylight coefficients for dynamic daylight simulations.

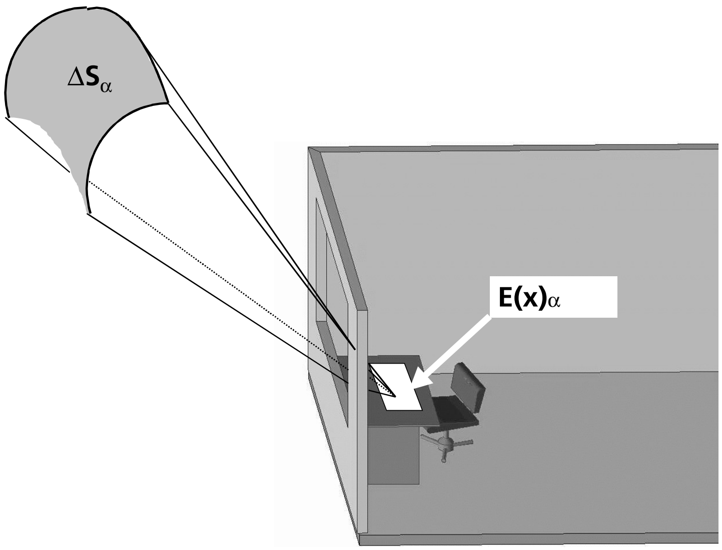

Fig. 2-5: A daylight coefficient is defined as:

$$DC_\alpha(x) = \frac{E_\alpha(x)}{L_\alpha \Delta S_\alpha}$$

where
x: point and orientation in a building
S_α: sky segment P
ΔS_α: angular size of S_α
$E_\alpha(x)$: illuminance at x due to S_α
L_α: luminance of S_α

Daylight Coefficients in ESP-R

ESP-R is a thermal building simulation tool, developed at the University of Strathclyde in Glasgow, Scotland [cla96]. It has been coupled with RADIANCE to carry out coupled lighting and thermal simulations [jan97,cla98]. In ESP-R the RADIANCE input models for the daylight calculations are generated by a conversion of the thermal building model. A circular ground plane of about the same size as the ground plan of the building is added to account for any external ground reflections. For the calculation of the daylight coefficients, the celestial hemisphere is split into 145 circular angular patches which are all modeled as *light* sources (see Appendix A.2.1). Fig. 2-6(a) shows the division of the sky according to Tregenza [tre87] with cone opening angles of 11.15 ° to avoid any double counting. To compensate for the uncovered regions of the sky, the cone angle is increased to 13.39 ° in ESP-R. This leads to an overlap and accordingly a double counting of several regions of the sky as shown in Fig. 2-6(b). Ground reflections are considered in ESP-R only indirectly via actual reflections from the circular ground plane. Rays that would hit the ground outside of this plane are discarded. The failure of ESP-R to account for these rays can lead to significant errors especially in the case of ceiling mounted sensors or regions that are mainly illuminated by multi-reflected daylight.

To calculate the 145 daylight coefficients, a new raytracing run is started for each sky segment in ESP-R, leading to a time consuming first simulation step. The same set of daylight

[20] Comparing Equations 2-2 and 2-4 reveals that the daylight coefficient approach resembles a higher order approximation of the daylight factor method. This interpretation of Equation 2-4 only holds for diffuse daylight, since L_α denotes the *total* luminance of the sky element S_a as opposed to the *diffuse* luminance, $L^{diffuse}$, in Equation 2-2.

coefficients is used for direct and diffuse daylight, i.e. the sun is modeled as an infinitely distant light source, 631[21] times its actual size, with a luminance reduced by a factor of 631.

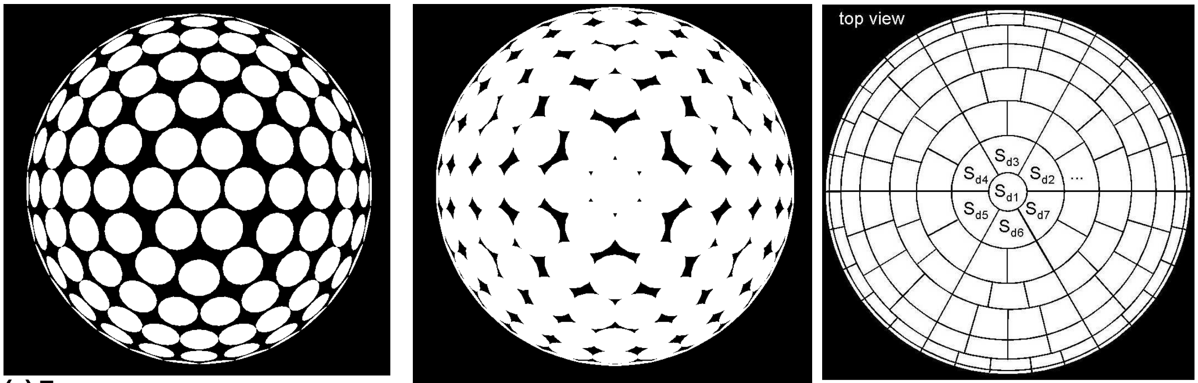

(a) Tregenza **(b) ESP-R** **(c) DAYSIM**

Fig. 2-6: **sky divisions**

(a) sky division according to Tregenza: 145 sky patches with a cone opening angle of 10.15 °. 68% of the celestial hemisphere are covered by the sky segments. (b) in ESP-R: 145 sky patches with a cone opening angle of 13.39°. The sum of the angular sizes of the sky patches adds up to 2π, but there is a substantial overlap of the single sky segments around the horizon.(c) in DAYSIM: 145 sky patches. The complete celestial hemisphere is covered and there is no overlap of the single sky segments.

Daylight Coefficients in DAYSIM

The philosophy behind the daylight coefficient calculation in DAYSIM is to reduce the number of raytracing runs necessary to calculate a complete set of daylight coefficients and still correctly model all light rays which might contribute to the total illuminance at a point. To this end, DAYSIM distinguishes between contributions from the diffuse daylight, ground reflections and direct sunlight:

$$E(x) = \underbrace{\sum_{\alpha=1}^{145} DC_{\alpha}^{diffuse}(x) L_{\alpha}^{diffuse} \Delta S_{\alpha}^{diffuse}}_{\text{diffuse daylight}} + \underbrace{\sum_{\alpha=1}^{3} DC_{\alpha}^{ground}(x) L_{\alpha}^{ground} \Delta S_{\alpha}^{ground}}_{\text{ground reflection}} + \underbrace{\sum_{\alpha=1}^{65} DC_{\alpha}^{direct}(x) L_{\alpha}^{direct} \Delta S_{\alpha}^{direct}}_{\text{direct sunlight}}$$

(equ. 2-5)

The celestial hemisphere is divided into 145 disjoint sky segments, S_{d1}, ..., S_{d145}, according to the Tregenza division for the diffuse daylight coefficients. These sky segments completely cover the celestial hemisphere so that no rays that hit the hemisphere are discarded or double counted (Fig. 2-6(c)).

To include contributions to the indoor illuminance due to external ground reflections, three additional ground daylight coefficients have been introduced for zenith angles greater than 90°. The three ground segments,S_{g1} ... S_{g3}, correspond to zenith angles from 90° to 100°, 100° to 120° and 120° to 180°. Fig. 2-7 shows the partition of the ground hemisphere into the 3 ground segments.

---

21 $631 \cong \frac{(13.39/2)^2 \pi}{(0.533/2)^2 \pi}$

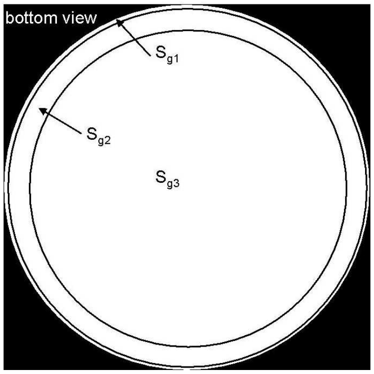

Fig. 2-7: Division of the ground hemisphere (bottom view) into three disjoint segments which correspond to the 3 ground daylight coefficients.

Contributions from direct sunlight are modeled by some 65 representative sun positions which are a subset of all possible sun positions throughout the year. Fig. 2-8 shows all annual hourly mean sun positions (dotted lines) for Freiburg, Germany, together with the 65 representative sun positions (crosses) for which direct daylight coefficients are calculated. The representative sun positions correspond to the actual sun positions on all full hours solar time for the 21st of December, February, March, April and June at which the sun is above the horizon[22]. Accordingly, the four direct daylight coefficients surrounded by the box in Fig. 2-8 correspond to the actual sun positions in Freiburg on June 21st and April/August 21st at 13.00 and 14.00 solar time. At sunrise and sunset the direct daylight coefficient correspond to the solar time with a solar altitude of 2° so that low solar altitudes can be correctly modeled. The total number of direct daylight coefficients is site dependent and varies from 61 to 65 for latitudes below 70°. Near the poles the number decreases down to 48.

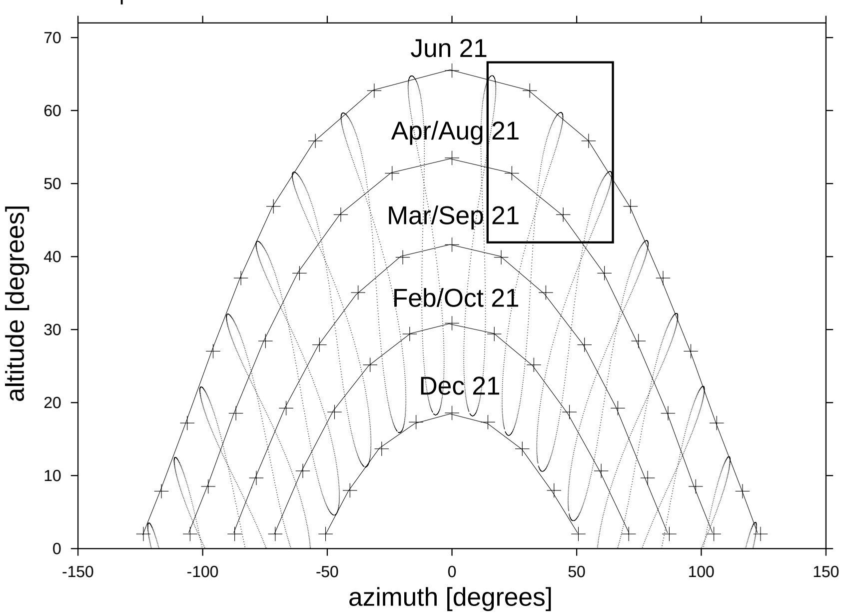

Fig. 2-8: The dotted lines mark all annual hourly mean sun positions for Freiburg, Germany (47.979° N); the crosses mark the 65 representative sun positions for which direct daylight coefficients are calculated. The box in the upper part of the figure surrounds four representative sun positions which correspond to actual sun positions at 13.00 and 14.00 solar time on June 21st and April/August 21st.

The calculation of a complete set of daylight coefficients for a given point in a building and a site on earth is the most time consuming part during a dynamic daylight simulation. To reduce this calculation time, DAYSIM calculates the daylight coefficients with an adapted version of the backward raytracer RADIANCE Version 3.1.8. Due to this adaptation all 145 diffuse, 3 ground and some 65 direct daylight coefficients can be calculated in two single raytracing runs. Details are provided in the Appendix A.2.2.

[22] These sun positions have been generically chosen, as they generate an evenly spaced grid across all possible sun positions throughout the year for median latitudes. The 21st of January/November and the 21st of May/July are not calculated since these additional direct daylight coefficients would not significantly increase the simulation accuracy whereas their calculation would increase the required simulation times by roughly 40%.

Once the daylight coefficients are available, they need to be coupled with the mean luminances of their associated sky segments for a given sky condition according to equ. 2.5. The luminances of the 145 diffuse sky segments for a particular sky condition are calculated with the Perez all weather sky model based on date and time as well as on direct normal and diffuse horizontal irradiances. The diffuse luminance, $L_\alpha^{diffuse}$, of a particular sky segment is set equal to the value of the Perez sky luminance distribution function at the center of the sky segment. This assignment procedure introduces an error as the continuous Perez sky luminance distribution is approximated by a discontinuous step function that is constant for each of the 145 sky segments. This inaccuracy can be neglected since the difference of the luminances between two neighboring sky segments is usually smaller than the absolute luminance errors caused by the underlying luminous efficacy model.

The luminances pertaining to the 3 ground daylight coefficients are modeled according to the RADIANCE program *gendaylit* [del95].

The assignment of the direct luminances, L_α^{direct} (α=1...65), for a given sky condition is not as unambiguous as for the diffuse luminances. Three assignment modes have been tested which are described in detail in chapter 4. The most straightforward assignment mode, *Nearest Neighbor*, has been used during the comparison of DAYSIM with the other methods in chapter 3. In this mode DAYSIM pretends for a given sky condition that the actual sun position corresponds to the nearest available position for which a direct daylight coefficient has been calculated. The luminance for this nearest-neighbor sun position is then set equal to the luminance of the sun while all other luminances in the third term of equ. 2-5 are set to zero. This crude assignment mode can lead to considerable errors, e.g. if a sensor point directly *sees* the actual sun position while the approximated sun position is shaded or *vice versa*. The performances of the three DAYSIM assignment modes for the direct daylight coefficients are discussed in the validation chapter 4.

Fig. 2-9 depicts the different input parameters and simulation steps of a dynamic daylight simulation with DAYSIM.

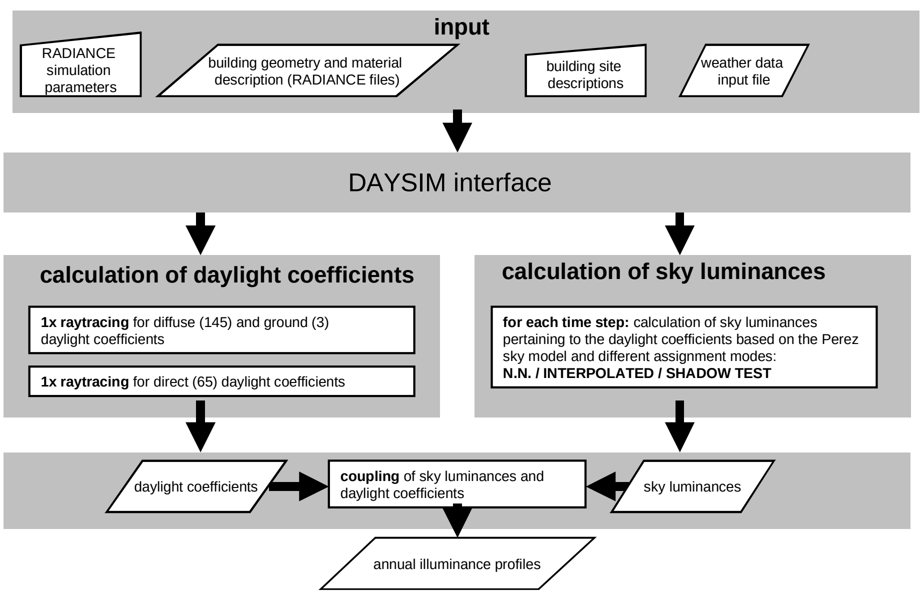

Fig. 2-9: Flow chart of the DAYSIM method[23].

[23] A similar diagram in Appendix A.2.4 shows the various subprograms of the DAYSIM simulation environment which incorporates the dynamic daylight simulation method of the same name.

Daylight Coefficients in Mardaljevic's approach

Shortly before the final submission of this thesis yet another implementation of daylight coefficients into the RADIANCE environment has been published by Mardaljevic [mar01] which is not explicitly considered in the comparison in chapter 3. The approach distinguishes between direct and indirect contributions to indoor illuminances from direct sunlight as well as diffuse daylight. Contributions from diffuse daylight and indirect contributions from the sun are all treated just like in ESP-R via a division of the celestial hemisphere into 145 sky elements. Direct contributions from the sun are considered via a division of the celestial hemisphere into 5010 patches to minimize displacements between the actual and the approximated sun positions. The bulk of simulation time is required for the calculation of the 145 indirect daylight coefficients and Mardaljevic mentions a calculation time which is roughly 145 times larger than the times for a conventional static RADIANCE simulation[24] [mar01]. Based on this information the author concludes, that the required calculation times of Mardaljevic's method and ESP-R are roughly the same.

2.4. Summary

Daylight simulations may assist the development and evaluation of a daylighting concept in the design phase of a building by providing illuminance distributions[25] due to daylight under a single or multiple sky conditions. Several RADIANCE-based dynamic daylight simulation methods have been proposed for the latter application. All existing methods exhibit weaknesses concerning either their accuracy, their required simulation times or the possibility of introducing shorter simulation time-steps. Therefore, a new RADIANCE-based dynamic daylight simulation method called DAYSIM has been developed which uses the concept of daylight coefficients. In the following chapter, the calculation results of DAYSIM are compared to conventional dynamic simulation methods.

[24] compared to a factor between 6 and 8 for DAYSIM (see Appendix A.2.3)
[25] and luminance distributions if needed

Chapter 3 Comparison of Dynamic Daylight Simulation Methods

In this chapter the performances of six dynamic daylight simulation algorithms are compared for two example office geometries. Performance indicators are calculation times, accuracy and the ability to model the short-time-step dynamics of daylight. The simulation results reveal that the accuracy of an annual daylight simulation method is not necessarily coupled with the required simulation time. The quality of a method rather depends on the underlying sky luminous efficacy model and whether it considers the hourly mean direct and diffuse illuminances for each time-step explicitly.

3.1. Methodology

The goal of this chapter is to quantify in how far the six RADIANCE-based dynamic daylight simulation algorithms which have been described in section 2.3 succeed at providing reliable simulation results for various building geometries[26]. Once again, the six methods are:

(1) Complete Year Runs
(2) Daylight Factor Method
(3) ADELINE
(4) Classified Weather Data
(5) ESP-R
(6) DAYSIM

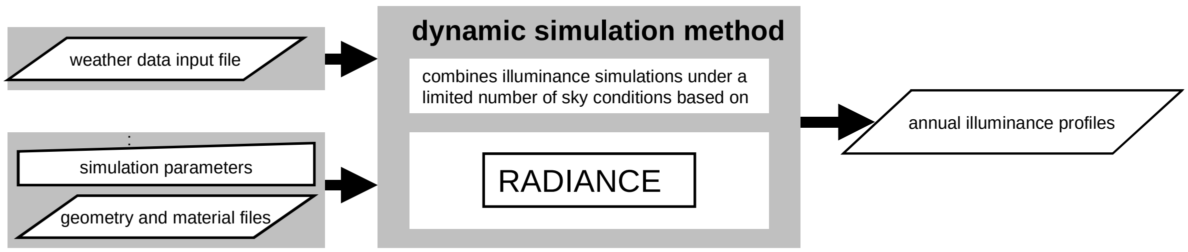

Fig. 3-1: All considered dynamic daylight simulation methods are based on RADIANCE and merely differ in how indoor illuminances under arbitrary sky conditions are estimated from simulations under a limited number of sky conditions.

Since all these simulation approaches are based on RADIANCE (Fig. 3-1), their results can be readily compared. Method (1) requires prohibitively long calculation times but the method has been included to serve as a reference case against which the other simulation results are tested. The underlying assumption, that *Complete Year Runs* produce the most reliable simulation results with respect to reality, seems to be justified to the author since

- all the other methods are based on RADIANCE and merely try to approach the simulation accuracy of a single raytracing run for a specific sky condition and since
- all the other considered methods – except for the Daylight Factor Method and ADELINE (2.3.2 and 2.3.3) – are also based on the Perez sky model. ADELINE and the Daylight Factor approach are based on the CIE sky model which is here understood as a subset of the Perez model, covering only the extremes of a dark overcast and a clear sky.

The same set of geometry, material, weather input files and simulation parameters were used for all simulations. Accordingly, differences in the simulation results are exclusively due to how the respective method extracts the development of mean hourly illuminance levels from a chosen set of sky luminance distributions (Fig. 3-1). As the focus of this chapter lies on how raytracing simulations with RADIANCE can be used for dynamic daylight simulations, simulation errors intrinsic to the raytracing or due to simplifications of the geometric model and material descriptions are neglected. Errors introduced by modeling the continuously changing external daylight conditions as discrete hourly mean Perez sky luminance distributions are also discarded[27].

All calculations have been carried out based on hourly direct horizontal and diffuse horizontal irradiance data taken form the German Test Reference Year (TRY) for Freiburg, Germany [blü86]. For the hours of sunrise and sunset the sun position at the middle of the time interval when the sun is above the horizon has been taken.

The investigated geometries, material descriptions, sensor positions and simulation parameters are described below.

[26] This chapter summarizes results from a study which has been published in *Energy and Buildings* [rei00_a].
[27] These simulation errors are addressed in chapter 5.

3.1.1. Investigated Geometries

Simulations have been carried out for a single rectangular office with a southern facade (Fig. 3-2 (a)) and a more advanced five story office building, featuring partly glazed inner walls between neighboring offices and the aisle (Fig. 3-3 (a)). Fig. 3-2(b) and 3-3(b) present floor plans of the two offices. The numbered black circular dots mark the position of sensors for which annual indoor illuminance distributions are presented further below. The sensors are situated at work plane level, i.e. 0.85 m above the floor facing upwards.

No surrounding buildings or landscape details were considered and the ground reflectance has been set to 20% in all simulations. As the same input files were used for all simulation methods, the absence of a surrounding landscape in the building models does not impede the general validity of the results in this chapter. The influence of modeling the surrounding landscape on the accuracy of a daylight simulation is addressed in chapter 4.

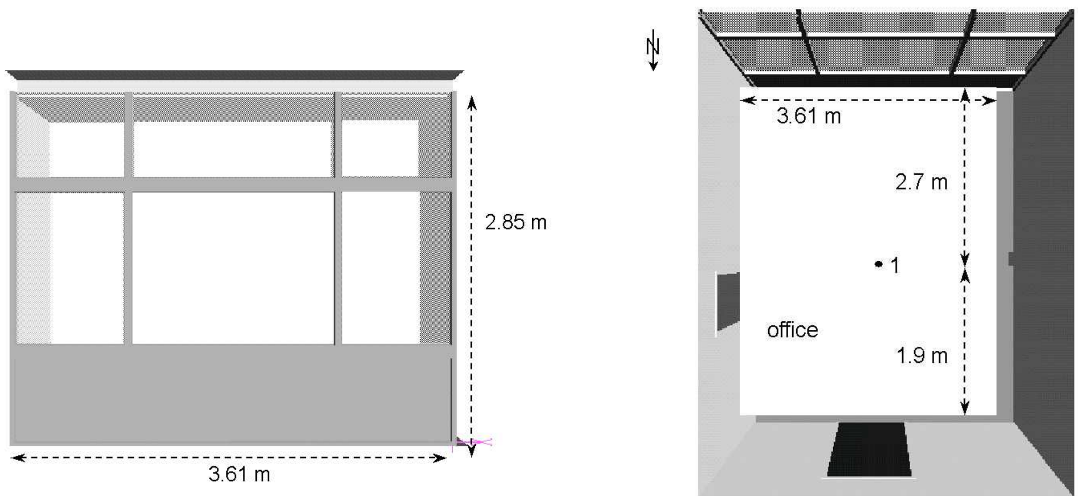

(a) (b)

Fig. 3-2: View and floor plan of the single office.

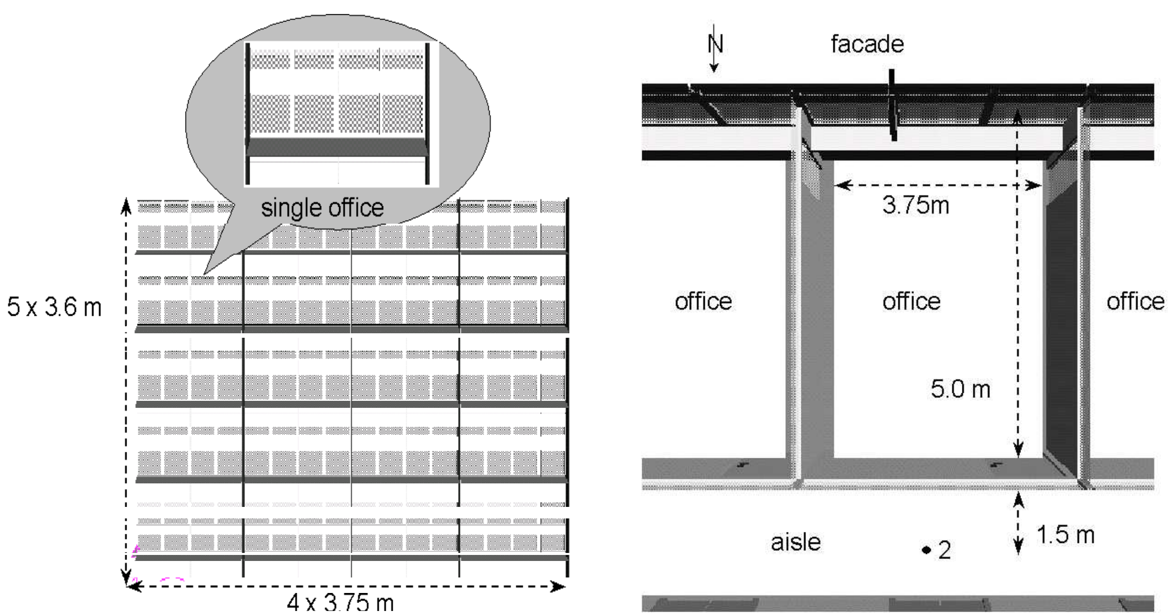

(a) (b)

Fig. 3-3: View and floor plan of the five-story office building.

The five-story office building has been added to discuss differences of how the daylight coefficient method has been integrated in ESP-R and DAYSIM, respectively. Accordingly, only simulation results for ESP-R, DAYSIM and the reference case are presented for the office building. Table 3-1 lists the utilized material surface descriptions.

Table 3-1: Material descriptions.

reflectance/visible transmittance for normal incidence [%]	single office	office building
wall	75	70
outer windows	72	72
ceiling	80	80 diffuse + 10 specular
floor	30	30
inner windows	/	80
door, furniture	75	40

3.1.2. Simulation Parameters

The same set of RADIANCE simulation parameters has been used for both office geometries and all simulation methods (Table 3-2). As discussed in Appendix A.4.1, the actual choice of RADIANCE simulation parameters decisively influences the accuracy and simulation time of the raytracing calculations.

Table 3-2: Simulation parameters (only non-default values are listed).

ambient calculation	ambient bounces	ambient division	ambient sampling	ambient accuracy	ambient resolution
	5	1500	500	0.2	64
direct calculation	direct threshold	direct sampling			
	0	0			

3.2. Results and Analysis

3.2.1. General Features

This section qualitatively describes how well methods (2) to (6) simulate indoor and outdoor illuminances with respect to Complete Year Runs for the *single-office-geometry* (Fig. 3-2 (a)). Actual simulation results for a cloudy and a clear day are presented in Appendix A.3.1.

Daylight Factor Method (2): Under overcast sky conditions, the daylight factor method coincides with the reference case for external illuminances while it constantly underestimates the internal illuminances. The first result is obvious, since an external daylight factor corresponds to unity and since the same sky luminous efficacy model as for the reference case has been used for the daylight factor calculation. The reason for the underestimation of the indoor illuminances under overcast skies is that the CIE overcast sky tends to underestimate horizontal sky luminances which in turn have a significant contribution to indoor illuminances at deeper room depths. Under sunny sky conditions the daylight factor grossly underestimates both internal and external illuminances since the daylight factor by definition only considers diffuse daylight contributions (Equ.2-2).

ADELINE (3): In the absence of direct sunlight ADELINE underestimates both indoor and outdoor illuminances except for very dark overcast skies. This clearly shows that in the absence of direct sunlight ADELINE does not consider the given hourly mean diffuse illuminance values but always relies on the same CIE overcast sky of the corresponding month. For partly cloudy sky conditions the method tends to underestimate the diffuse illuminance distribution since a mixture of a clear CIE sky without the sun and a CIE overcast sky fails to model bright overcast skies (see 2.3.3). In contrast to that, the Perez model is able to distinguish between bright and dark overcast skies (see 2.2). Under clear sky conditions, ADELINE approaches the reference case for external and internal illuminances since a clear Perez sky basically coincides with the clear CIE sky.

CLASSIFIED (4): The classified data slightly overestimates external illuminances while internal illuminances are underestimated. These errors result from the classification since every hourly mean sky condition is merely approximated by its nearest available weather class. The magnitude of the errors can be reduced by increasing the number of weather classes on the expense of longer calculation times. The results for ADELINE and CLASSIFIED show that a method only yields convincing simulation results if the diffuse and direct irradiance input data is considered for each simulation time-step explicitly.

ESP-R (5) and DAYSIM (6): For the single office, the results of ESP-R and DAYSIM are always very close to the reference case. On a cloudy day all three methods basically coincide since the only error introduced by the daylight coefficient methods is that the continuous Perez sky luminous distribution is approximated by a discontinuous function. In the presence of direct sunlight, another error source is introduced since both methods approximate the hourly mean sun position by the nearest sun position for which a daylight coefficient is available[28]. The relative root mean square errors (RMSE[29]) for diffuse sky conditions alone are 6% (ESP-R) and 3% (DAYSIM) for internal illuminances in the single office at a distance of 2.7 m from the facade (sensor #1 in Fig. 3-1(b)). The relative RMSEs amount to 19% and 16% if sky conditions with direct sunlight are considered as well.

3.2.2. Required Simulation Times

Table 3-3 shows the simulation times for all methods on a Pentium Pro 200 MHz Linux Workstation. The simulation times of 12 days and 80 days for Complete Year Runs show that this method is unfit for *day-to-day* design proposes. ADELINE and Classified have simulation times which are about an order of magnitude smaller than for the reference case. ESP-R requires roughly twice as long calculation times as DAYSIM for the single office. For the more advanced geometry, ESP-R necessitates over 7 times longer simulation times. This reveals that reducing the number of raytracing runs from 145 (ESP-R) to 2 (DAYSIM) yields a decisive performance gain.

Table 3-3: Required simulation times for the two investigated office geometries.

simulation method	simulation times single office	simulation times five-story office building
Complete Year Runs (ref. case)	12 days	80 days[30]
Daylight Factor Method	6 min	-
ADELINE	25 h	-
CLASSIFIED	20 h	-
ESP-R	3 h	2 days
DAYSIM	1.5 h	6.25 h[31]

3.2.3. Cumulative annual Illuminance Distributions

A helpful number to judge the daylight availability in an office is how many hours per year a predefined minimum illuminance level can be maintained by daylight alone. This information can be drawn from the cumulative annual indoor illuminance distribution for a given point in a building. For a specific application the chosen minimum illuminance depends on the applicable legal requirements and the individual user preferences. Proposed minimum illuminance levels for office work range from 150 lux [new94] to more than 1000 lux [ten97]. Fig. 3-4 shows the cumulative indoor illuminance distribution for the six methods for sensor #1 in the single office[32].

[28] Only the nearest neighbor assignment DAYSIM mode (see App. chapter 4) has been considered in this chapter to facilitate the comparison between DAYSIM and ESP-R.
[29] The definition of the relative MBE and RMSE are given in the Glossary.
[30] The calculation time for the Complete Year Run method would have been 80 days on a single machine but the calculations have actually been carried out in parallel on a total of 15 UNIX and Linux workstations.
[31] The simulation time of 6.25 h instead of 1 day as stated in [rei00_a] stems from the introduction of the adapted *rtrace version* as discussed in Appendix A.2.2.
[32] While the daylight autonomy (*see* glossary) is based on annual working hours, Fig. 3-3 and Table 3- 4 consider all annual hours with non-vanishing ambient daylight levels.

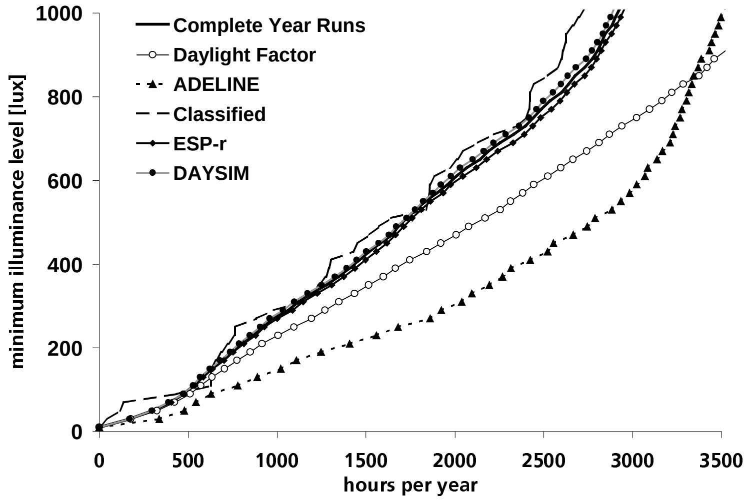

Fig. 3-4: The annual cumulative distribution of indoor illuminance levels for point 1 in the single office.

To quantify how well the different methods agree with the reference case over the course of the year, the relative RMSEs and MBEs with respect to the reference case for the cumulative illuminance distributions have been calculated. The relative RMSEs and MBEs in Table 3-4 are referring to annual hours with non-zero external illuminances at which the indoor illuminances lie below 1000 Lux.

Table 3-4: Relative RMSEs and MBEs of the cumulative annual illuminance distribution for sensor #1 for all annual illuminances ∈[1,1000] lux in the single office.

simulation method	RMSE ∈[1,1000] lux	MBE ∈[1,1000] lux
Complete Year Runs (ref. case)	-	-
Daylight Factor Method	12 %	-20
ADELINE	25 %	-48
CLASSIFIED	25 %	8
ESP-R	5 %	-2
DAYSIM	2 %	1

The cumulative distribution for the Daylight Factor Method lies below the reference case for all regions with a relative RMSE of 12% and an MBE of –20%. ADELINE grossly underestimates the cumulative distribution for illuminances up to 1500 Lux as these indoor illuminances usually appear under overcast sky conditions. CLASSIFIED approaches the reference case reasonably well in the considered illuminance range below 1000 Lux. The plot approaches the reference case in steps, due to the bundling of the single hourly mean illuminances into classes. This causes a high relative RMSE of 25%. Fig. 3-4 clearly reveals that the two daylight coefficient methods and the reference case basically coincide for the considered illuminance range. The RMSEs lie around 2% for DAYSIM and 5% for ESP-R. To gain more insight into the differences between ESP-R and DAYSIM the more advanced office geometry is investigated in the following.

3.2.4. ESP-R and DAYSIM Results for the advanced Office Geometry

The simulation results for the single office have clearly shown that the two daylight coefficient methods are the fastest and most accurate methods to predict hourly mean indoor illuminances for a straightforward office geometry. How well do the methods perform for the more advanced office building?

Fig. 3-5 presents the cumulative indoor illuminance distribution for the aisle point #2 from Fig. 3-3(b) on the fifth floor of the office building. As mentioned above, the inner walls in the building are glazed from 2m to ceiling height (3.4m) so that all daylight on the aisle first needs to penetrate through the adjacent southern offices. Table 3-5 corresponds to Table 3-4 for sensor #2.

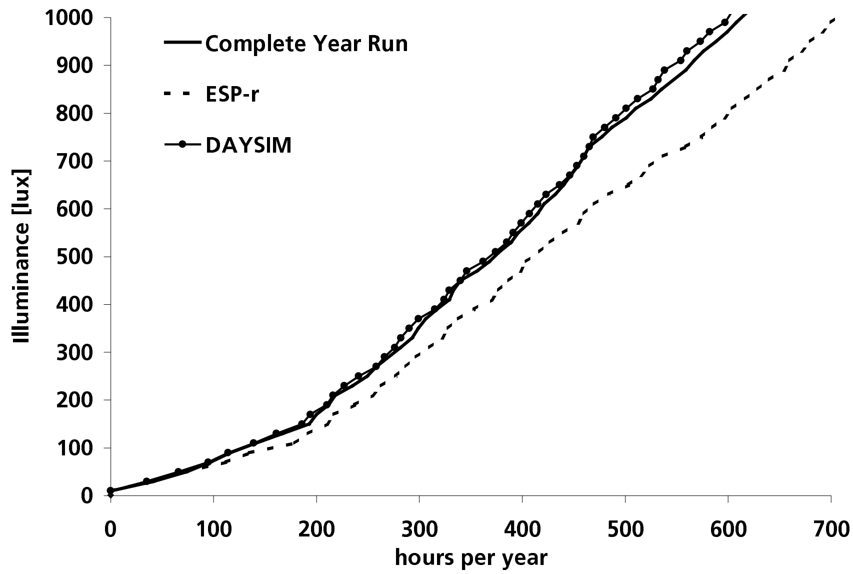

Fig. 3-5: The annual cumulative distribution of indoor illuminance levels for point 2 on the fifth floor of the office building for the reference case and the two daylight coefficient methods.

Table 3-5: Relative RMSEs and MBEs of the cumulative annual illuminance distribution for sensor #2 on the aisle for all annual illuminances ∈[1,1000] lux in the office building.

simulation method	RMSE ∈[1,1000] lux	MBE ∈[1,1000] lux
Complete Year Runs (ref. case)	-	-
ESP-R	54 %	-13 %
DAYSIM	2 %	2 %

Fig. 3-5 shows that ESP-R somewhat underestimates the indoor illuminance levels on the aisle. The relative RMSE and MBE amount to 54% and –13% as opposed to 2% and 2% for DAYSIM. Comparing how often the illuminance levels in the aisle fall below 500 Lux the reference case predicts 378 hours as opposed to 404 hours by ESP-R and 374 hours by DAYSIM.
The reasons for the systematic underestimation of the indoor illuminances by ESP-R stems from the treatment of ground reflections in ESP-R. As mentioned in section 2.3.5 ESP-R does not consider any external ground daylight reflections that lie out of the circular ground plane inserted by ESP-R into the building geometry. Therefore, the majority of rays which would hit the ground is discarded in ESP-R. For a region in a building that is mainly illuminated indirectly via multi-reflected daylight, like the example point on the aisle or like a ceiling mounted sensor, this can lead to significant simulation errors.

3.3. Discussion and Conclusion

The results from the last section revealed several aspects that should be remembered when choosing a method to simulate the annual availability of daylight in a building:

- Longer simulation times are not necessarily coupled with a higher accuracy of the simulation results.
- The utilized luminous efficacy model is crucial. The comparison of the Daylight Factor Method, ADELINE and DAYSIM for indoor illuminances below 500 lux in Fig. 3-3 shows that the luminous efficacy model – which is identical for DAYSIM and the Daylight Factor method – has a stronger impact on the reliability on the indoor illuminance values than the sky luminance distribution. I.e. the difference between DAYSIM and the Daylight Factor Method is less pronounced than the difference between the Daylight Factor Method and ADELINE which always uses the CIE overcast sky in the absence of direct sunlight. Since direct and diffuse irradiance data are widely available for a dynamic daylight simulation and since the Perez luminous efficacy model is able to model overcast skies of varying brightness, it should be given preference over the CIE model.

- An annual simulation method should consider direct and diffuse illuminance values for each time-step individually. The bundling of similar daylight situations into a few classes or the consideration of monthly mean daylight levels leads a smoothing of the actual short-time-step variances of the available daylight and hence to less reliable simulation results. On the contrary, an annual simulation tool should be able to predict the development of indoor illuminances in time-steps of several minutes. The necessary input data can be either measured or generated from hourly data (chapter 5).

These findings harmonize well with the requirements for a simulation tool, fit for daily usage, formulated in section 3.2.2 and provide a basis on which the six compared simulation methods can be evaluated:

<u>(1) Complete Year Runs:</u> The simulation times between 12 and 80 days revealed that this method will probably be restricted to academic purposes at least in the near future. For weather input data with time-steps below an hour the method is clearly apt to fail.

<u>(2) Daylight Factor Method:</u> Concerning the required calculation times the daylight factor yields satisfying results for diffuse sky conditions and simple building geometries if coupled with reliable external illuminances. A major weakness of the daylight factor is the underlying CIE overcast sky model.

<u>(3) ADELINE:</u> The relatively poor performance of ADELINE in section 3.2. can be attributed to the utilized sky model and the smoothing of the weather data discussed above. The accuracy of the simulation results could be greatly enhanced by scaling[33] the overcast sky with the actual diffuse illuminances for a given time-step, comparable to the daylight factor method.

<u>(4) CLASSIFIED:</u> The weakness of the classified data is also covered by the last aspect listed above. The cumulative distribution of the classified data shown in Fig. 3-3 has shown that the CLASSIFIED principally approaches the reference case for illuminances below 1000 Lux. The high RMSEs in Table 3-4 are caused by the step-like shape of the plot due to the classification. As has been mentioned above, the accuracy of the simulation method could be enhanced by increasing the number of classes, but since the necessary calculation times are already high compared to the daylight coefficient methods this procedure does not seem promising at this point.

<u>(5) ESP-R and (6) DAYSIM:</u> All results in section 3.2 indicated that daylight coefficient methods are the fastest and most reliable methods to model total indoor illuminance distributions. The calculation times ranged from a few minutes to several hours and shorter time-step variances of the available daylight can be simulated at hardly any time expenses. The two methods performed equally well for a simple office geometry, but a set of ground daylight coefficients should be integrated into ESP-R to account for ground reflectances which can play a significant contribution in more advanced building geometries. In its present state, DAYSIM outperforms ESP-R in the required simulation time and simulation accuracy.

At the end of the chapter, it should be stressed that any dynamic daylight situation method can only perform as well as the facade elements and blind system of the investigated building can be modeled by RADIANCE for a single given sky condition. For a movable system like venetian blinds a set of daylight coefficients has to be calculated for several intermediate blind positions between which one has to interpolate (chapter 4). On the other hand, the daylight coefficient method is able to take advantage of any future improvement of both the raytracing algorithms in RADIANCE as well as of the underlying sky luminous distribution model. A clear strength of the DAYSIM-approach is that the annual daylight availability can be automatically modeled with roughly the same effort for the planner as for a daylight factor simulation while yielding a more complete picture of the daylight situation in a building.

[33] "Scaling" in this context paraphrases the introduction of a correction factor that chances the sky luminances of the CIE overcast sky under a bright overcast sky.

3.4. Summary

The performance analysis of six dynamic daylight simulation methods in this chapter yielded that:

- longer simulation times do not necessitate a higher accuracy of the simulation results,
- the utilized luminous efficacy model is crucial and
- daylight coefficient methods are the fastest and most reliable methods to model total indoor illuminance distributions.

Chapter 4 Validation of DAYSIM Simulations

In this chapter DAYSIM simulations are validated against actually measured data. Indoor illuminances under over 10,000 sky conditions have been measured and simulated in a full-scale test office with a double glazing and external venetian blinds. The simulation results yield that indoor illuminances can be modeled with a comparable accuracy for various blind settings under arbitrary sky conditions with simulation errors stemming to roughly equal parts from the raytracing and the sky model.

4.1. Methodology

While chapter 3 yielded that the dynamic daylight simulation algorithm DAYSIM provides faster and more reliable results compared to the other investigated algorithms, this chapter validates DAYSIM simulation results with respect to actually measured data. The chapter summarizes the results of a validation study which has been published in *Energy and Buildings* [rei01_b]. The study encompassed the measurements of outdoor direct and diffuse irradiances which have been taken synchronously with indoor illuminances in a full-scale test office in 30 second intervals. The facade of the test office featured a double glazing and outer venetian blinds (Fig. 4-1(a)). The goal of the study was to reproduce measured indoor illuminances based on outside direct and diffuse irradiances under a wide range of sky conditions and under three different settings of the external venetian blinds. Over 80,000 indoor illuminances have been collected under more than 10,000 sky conditions.

The venetian blind system was chosen since it is a widely used, multi-functional device which serves as a glare protection, a barrier to unwanted solar gains and a daylighting element to redirect direct sunlight deeper into the room. Apart from its significance as a versatile daylighting element, the venetian blind system is computationally challenging as it requires the simulation of multi-reflected rays.

(a)

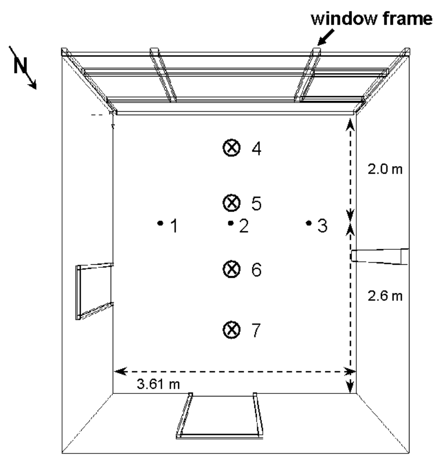

(b)

Fig. 4-1: (a) Photo of the full-scale test office with the blinds closed. (b) Sketch of the investigated test office and the sensor positions. Sensors 1 to 3 are at work plane height (85 cm) facing upwards while the remaining sensors are ceiling mounted facing downwards.

Mardaljevic has presented a validation of RADIANCE-based indoor illuminance simulations in which he used sky scanner data to describe the luminance distribution of the celestial hemisphere including the sun [mar97, mar95]. He started a new raytracing run for each investigated sky condition (Complete Year Run Method from chapter 2) and his results show how well the RADIANCE raytracing algorithm can model indoor illuminances under perfectly controlled sky conditions. Investigated facade variants encompassed a double glazing and an inner lightshelf with either a diffuse or a partly specular surface and a gray tinted solar control glazing. In contrast to Mardaljevic's work this chapter aims to validate how accurate a *dynamic* RADIANCE-based daylight simulation method can simulate indoor illuminances under arbitrary sky conditions based on widely available input parameters like direct and diffuse irradiances instead of sky scanner data of the celestial hemisphere.

It should be stressed, that the simulation results presented in the following do *not* reflect how well a RADIANCE-based daylight simulation can possibly reproduce reality but provide an estimate of how well a lighting engineer or architect can expect to predict the annual indoor illuminance distribution in a real-world project based on the building geometry, optical properties of the material surfaces and direct and diffuse irradiances. Simulation errors largely stem from shortcomings of the Perez sky luminance distribution model, the DAYSIM algorithm, the RADIANCE raytracing calculation and the accuracy of the CAD model of the test office. The author is aware that a number of simulation error sources have been avoided during the simulations which can further limit the reliability of a daylight simulation. Among them are:

- modeling errors introduced in the process of generating short-time-step irradiance data from hourly or monthly mean values if no measured values are available.[34]
- the deterioration of material surfaces with time.
- simplification errors in the CAD-model of a complex building (construction details, furniture, plants, etc.)[35]

Details of the experimental setup and the simulation inputs are given in the following.

4.1.1. Experimental Setup

All indoor illuminance measurements were taken in January 2000 at the Fraunhofer Institute for Solar Energy Systems in Freiburg, Germany. The measurements were recorded at several points in a full-scale test office in 30 second intervals with a Hagner detector SD2 in combination with a Keithley Multimeter. Each recorded value is the mean of 3 measurements taken in 10 second intervals. Fig.4-1(a) shows the full-scale test office with the outer venetian blinds closed. Room dimensions and the positions of the seven indoor illuminance sensors are shown in Fig. 4-1(b). Sensors 1 to 3 were mounted at work plane height (85 cm above the floor) facing up at a 2m distance from the facade which was facing Southwest. Sensor 8 (not shown in Fig. 4-1(b)) measures vertical illuminances perpendicular to the facade. Sensors 4 to 7 were ceiling mounted facing downwards. Outside direct normal and diffuse horizontal irradiances as well as horizontal and vertical North, South, East and West illuminances have been collected in 10 second intervals since 1997 [IDMP01]. The direct irradiances were measured with an Eppley NIP while diffuse irradiances were taken with a Kipp & Zonen CM 11 pyranometer. Both measurement devices were mounted on a 2AP tracker. Horizontal and vertical outdoor illuminances were recorded with an LMT illuminance measuring unit and a Licor LI-210SZ, respectively. The measurement errors for the indoor illuminances and the outdoor irradiances are estimated to be 5% and 10%, respectively [wie99a].

Three blind settings were investigated: blinds retracted, blinds down and slat angle in horizontal position and blinds down and slats fully closed, tilted downwards. For all three blind settings completely and partly overcast as well as sunny sky conditions were recorded and simulated.

4.1.2. Simulation Inputs

As shown in Fig. 2-9, DAYSIM requires direct and diffuse irradiances, RADIANCE simulation parameters as well as the test office geometry and material surfaces as simulation inputs. The geometry of the full-scale test room was modeled with an accuracy of ±2cm. According to [wie99a] the walls, the ceiling and the floor of the test room were treated like perfectly Lambertian surfaces. The direct hemispherical visible transmittance of the double glazing was modeled with 79%. The optical surface properties of the gray metallic outer blinds were characterized with an integrating sphere. The test office is situated on the roof of the Fraunhofer Institute for Solar Energy Systems and several initial simulation runs revealed, that the reflectivity of the roof is a crucial simulation input parameter as it nearly directly scales with the daylight that is seen by the ceiling sensors. Accordingly, the roof was added to the CAD Model of the test office and modeled as a purely Lambertian surface with a reflectivity of 5%. The remaining ground albedo was assigned a reflectivity of 20%.

During the simulation, indoor illuminances at the seven sensor positions shown in Fig.4-1(b) were modeled for over 10,000 sky conditions. Only sky conditions with outdoor horizontal illuminances above 1000 lux were considered. All simulations were carried out with the same set of RADIANCE raytracing parameters on several Pentium Pro 400 MHz Linux Workstations with

[34] This error source is addressed in chapter 5.
[35] The problem of modeling building details and surfaces with sufficient accuracy is not further addressed in this thesis even though such modeling errors can easily dominate the overall simulation errors. Modeling errors directly influence the quality of a daylight simulation and largely depend on the experience of the simulator and the availability of reliable material data bases.

256 megabyte RAM and a dual processor board. Even though DAYSIM requires additional RAM compared to a conventional *rtrace* run (see Appendix A.2.3) swapping could be avoided during all simulations.

In Table 4-1 the RADIANCE parameters used for simulating the different blind settings are listed. This choice of parameters is motivated in Appendix A.4.1.

Table 4-1: Simulation parameters for blind simulations (only non-default values are listed).

ambient calculation	ambient bounces	ambient division	ambient sampling	ambient accuracy	ambient resolution
	7	1500	100	0.1	200
direct calculation	direct threshold	direct sampling			
	0	0			

4.1.3. Assignment Modes for the Direct Daylight Coefficients in DAYSIM

As explained in chapter 2.3, DAYSIM differentiates between diffuse, ground and direct daylight contributions.

While the assignment of diffuse and ground luminances to the corresponding daylight coefficients is rather unambiguous, the assignment of the direct sunlight to the 65 site dependant direct daylight coefficients can be carried out in multiple ways. The following figure visualizes three modes which are tested in the following.

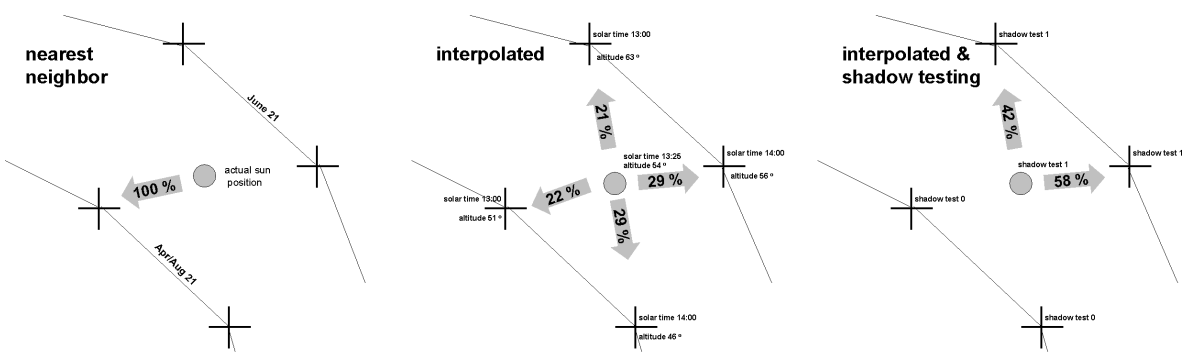

(a) NEAREST NEIGHBOR (b) INTERPOLATED (c) SHADOW TEST

Fig. 4-2: Visualization of the three investigated assignment modes of direct solar luminances to the representative sun positions. The three clippings correspond to the "box" marked in Fig. 2-8.

<u>NEAREST NEIGHBOR (N.N.):</u> the luminance from the sun, L^{sun}, for a given sky condition is completely assigned to the representative sun position which lies closest to the actual sun position in the altitude-azimuth plane, i.e. $L^{direct}_{\alpha=n.n.} = L^{sun}$. The luminances of the remaining representative sun positions are set to zero (Fig. 4-2(a)). This mode has been employed throughout chapter 3.

<u>INTERPOLATED:</u> for a given date and time the four representative sun positions which surround the actual sun position are picked (Fig. 4-2(b)). The luminance from the sun, L^{sun}, is distributed among these four daylight coefficients according to a weight which considers the time and solar altitude of the actual and the four picked representative sun positions. This twofold division is exemplified in Fig. 4-2(b): The actual sun position corresponds to 13.25 solar time on Mai 7th. The actual solar altitude is 54°. The weight assigned to the two representative sun positions at 13.00 solar time and the two sun positions at 14.00 solar time is divided according to the fraction 25:35. The two sun position pairs on June 21st and April/August 21st are weighted according to the altitude difference fraction of the actual altitude and the solar altitudes on these dates at 13.25 solar time: 60° for June 21st and 49° for April/August 21st. Accordingly, the direct illuminance assigned to the representative sun position at 13.00 solar time June 21st is

27%[36]. The weights assigned to the other three surrounding representative sun positions are shown in Fig. 4-2(b). The luminances pertaining to the 61 remaining direct daylight coefficients are set to zero.

<u>*SHADOW TEST:*</u> a shortcoming of the two above described algorithms is that in case the point of interest in the building, x, lies in direct view of the actual sun position while the position of one or several of the surrounding representative sun positions is shaded or *vice versa*, the assignment of direct luminances to these representative sun positions is not suitable to model the indoor illuminance at x for the investigated actual sun position. To avoid this problem, INTERPOLATED can be coupled with a simple shadow testing procedure: an initial shadow testing[37] notes for each representative sun position whether x lies in its direct view (direct view=1) or not (direct view=0). For a given sky condition only those surrounding representative sun positions are considered whose direct view status equals the status of the actual sun position. In Fig. 4-2(c) the 2 representative sun positions corresponding to April/August 21st cannot be seen from x opposed to the actual sun position. Therefore, the direct solar luminance is assigned to the remaining two representative sun positions. SHADOW TEST runs into problems if all surrounding representative sun positions are shaded while the actual sun position is not or vice versa. In this case a warning is generated for the considered time-step. During the validation study in chapter 4, this problem appeared in 10 out of 70679 indoor illuminance simulations for all the sky conditions, blind settings and sensor positions. If this problem should become more urgent for a particular building design, the number of representative sun positions can be enlarged at the expense of longer calculation times.

4.2. Results and Analysis

In this section simulation results are compared to measured illuminances and the performances of the three above described assignment modes of direct sunlight to the direct daylight coefficients are briefly addressed.

4.2.1. Overcast Sky Conditions

This paragraph discusses how well DAYSIM performs under overcast sky conditions under which all three direct assignment modes yield the same results. Fig. 4-3 shows the daily development of measured and simulated illuminances at sensor #2 from Fig. 4-1(b) for the three considered blind positions on cloudy days. Note how well DAYSIM reproduces measured illuminances for the whole range of 10 to 1000 lux. The simulation errors are comparable for all three facade geometries.

A more detailed investigation yields that the simulated illuminances for the retracted blinds basically coincide with the measured results, if they are corrected with the ratio of the measured to the simulated illuminances onto the facade. From this it can be inferred that for this straightforward facade geometry the simulation errors can be largely attributed to shortcomings of the sky model. This *scaling procedures* does not significantly improve the simulation results when the blinds are down. The reason for this might be, that with the blinds lowered, most daylight is reflected from the ground before it enters the test office. Therefore, the significance of the sky luminous distribution model falls [rei01_b] (see Appendix A.4.2).

A comparison of the different ceiling mounted sensors revealed that the sensor closest to the facade was modeled with the lowest accuracy for all blind settings and sky conditions. Obviously, this sensor is strongly influenced by the surrounding landscape which could not be modeled as precisely as the remaining test office.

[36] 100%* [35 min/60 min]*[(54°-49°)/(60°-49°)]

[37] A shadow testing involves the backward tracing of a single ray to test whether a point is directly illuminated by a light source.

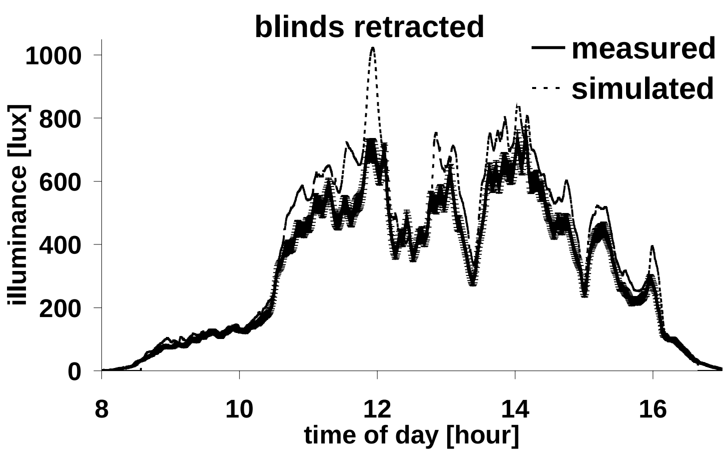

Fig. 4-3: comparison of measurements and simulations under cloudy sky conditions.

(a) blinds retracted

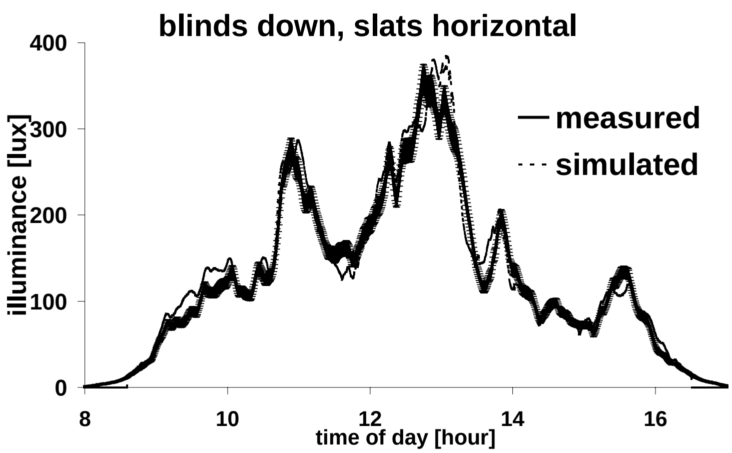

(b) blinds down, slats horizontal

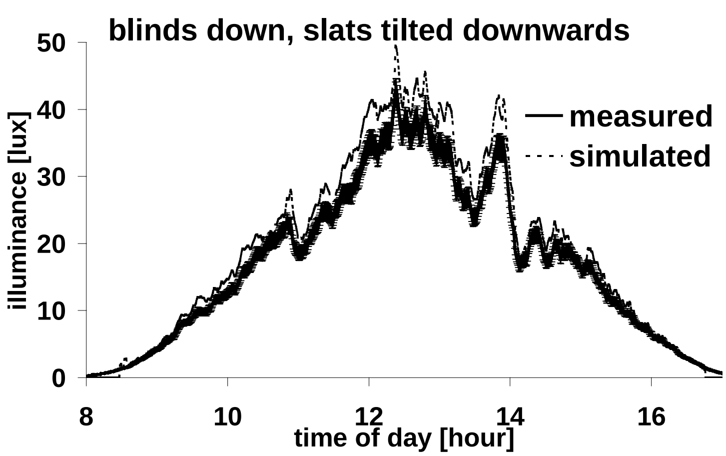

(c) blinds down, slats downwards

4.2.2. Sunny Sky Conditions

For sunny sky conditions all three assignment modes yield different results. In Fig. 4-4 measured illuminances at sensor #2 are compared to INTERPOLATED and NEAREST NEIGHBOR (N.N.) simulations for a sunny morning with the blinds retracted. While INTERPOLATED approaches the measured values very well NEAREST NEIGHBOR introduces a step-like behavior in the temporal development of the illuminances. The discontinuities appear when the nearest representative sun position changes. Fig. 4-4 suggests that the NEAREST NEIGHBOR assignment mode which is also used by ESP-R is not apt to model short-time-steps dynamics of indoor illuminances with sufficient detail. The method is discarded for the rest of this chapter.

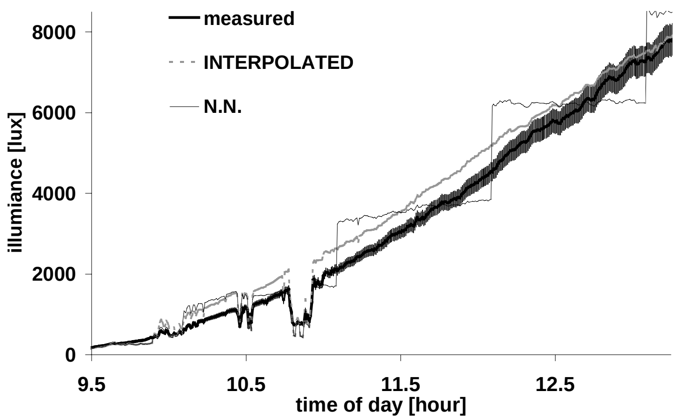

Fig. 4-4: Measured, INTERPOLATED and NEAREST NEIGHBOR (N.N.) illuminances for sensor #2 (Jan 8th 2000). The N.N. assignment mode introduces a step-like behavior in the development of the indoor illuminances.

While SHADOW TEST does not differ from INTERPOLATED for an unshaded point, Fig.4-5 pictures its advantage for the indoor sensor #2 on a sunny afternoon with the blinds closed and the slats in horizontal position. The measured illuminances exhibit sharp illuminance variations throughout the day as the sensor point move in and out of the shadows of the blind slats. SHADOW TEST reproduces these variations while INTERPOLATED fails to model them. Fig. 4-5 shows that if an investigated point is temporary subject to direct sunlight, SHADOW TEST is superior to INTERPOLATED and may help to predict the appearance of glare as well as irritating abrupt illuminance variations.

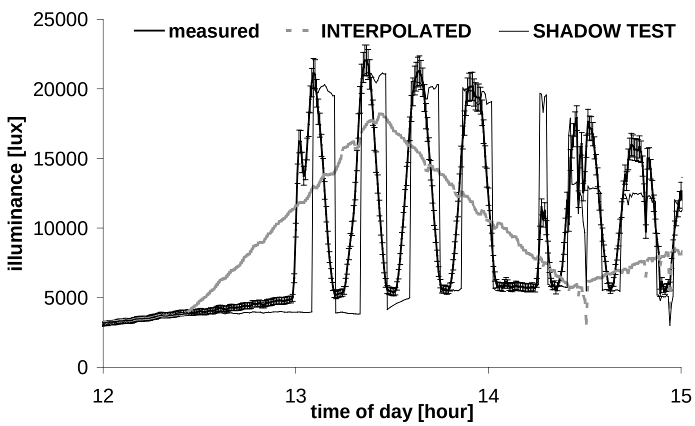

Fig. 4-5: Measured, INTERPOLATED and SHADOW TEST horizontal illuminances for sensor #2 (Jan 13th 2000). The blinds are down with slat angles horizontal. Note how SHADOW TEST simulates the pronounced illuminance variations as the sun moves in and out of direct view of the investigated point.

Fig. 4-6 provides an impression of how the two assignment modes perform under sunny sky conditions with the blinds fully closed. The bump of INTERPOLATED at 16.00 comes about as one of the representative sun positions lay in direct view of the sensor - even with the blinds fully closed. This was possible since the closed venetian blinds left about 10 centimeters of the glazing uncovered. As the sensor has never really been directly illuminated by the sun on this day, SHADOW TEST eliminates such simulation errors.

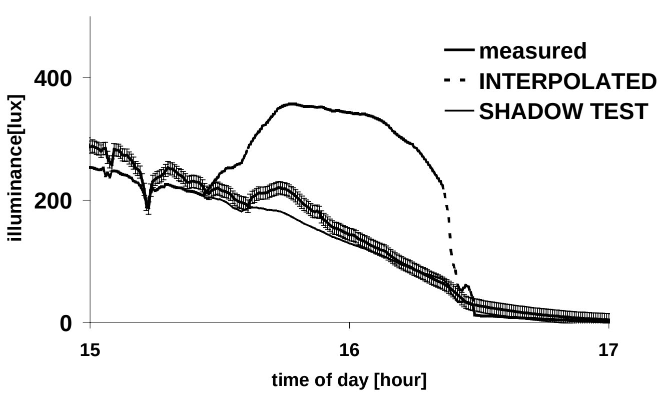

Fig. 4-6: Measured, INTERPOLATED and SHADOW TEST horizontal illuminances for sensor #2 (Jan 16th 2000). The blinds are down with the slats tilted downwards. The artifact introduced by INTERPLOATED vanishes if shadow testing is activated.

4.2.3. Arbitrary Sky Conditions

Table 4-2 summarizes relative MBEs and RMSEs for all three blind settings for all sky conditions for which indoor illuminances have been measured. The 4 ceiling and the 3 desk height sensors are listed separately and only sky conditions with outside horizontal illuminances above 1000 lux are considered. The statistical errors for SHADOW TESTING and INTERPOLATED are identical for all ceiling sensors as these sensors are never in direct view of the sun.

For the retracted blinds, the MBEs and RMSEs tend to be higher for the ceiling than for the desk sensors. As mentioned above, the difficulty with the ceiling sensors is that they are strongly influenced by details of the surrounding landscape which usually cannot be modeled with any detail[38]. The MBEs and RMSEs are similar for both assignment modes.

When the blinds are lowered, SHADOW TESTING exhibits lowers simulation errors than INTERPOLATED as explained in the proceeding section. Nevertheless, the advantages of SHADOW TESTING do not seem to significantly improve the statistical accuracy of the simulation with respect to the measured data. Differences between both methods might be more pronounced if e.g. the artificial lighting demand for an automated lighting control system is predicted based on simulated illuminances. In chapter 5 it will be shown that a failure to model short-time-steps variations of indoor illuminances – be they due to modeling artifacts or due to too large simulation time-steps – can impede the simulation accuracy of a daylight simulation.

Table 4-2: Relative RMSEs and MBEs for the three investigated assignment modes.

		INTERPOLATED		**SHADOW TEST**	
		MBE [%]	RMSE [%]	MBE [%]	RMSE [%]
blinds retracted	**ceiling**	17	30	17	30
	ground	8	24	6	22
blinds closed, slats horizontal	**ceiling**	20	31	20	31
	ground	7	28	5	25
blind closed, slats tilted downwards	**ceiling**	-6	26	-6	26
	ground	2	33	-6	24

Appendix A.4.2 provide some insight into how the total simulation errors from Table 4-2 can be divided into errors due to the raytracing and to the sky model.

4.2.4.How representative are the measured Data?

Indoor and outdoor illuminance measurements have only been collected for two weeks in January 2000 in Freiburg, Germany. Therefore, a pressing question is whether the results can be generalized for a whole year. As explained above, the simulation errors stem from the raytracing calculation as well as from the underlying sky model. While the former error does principally not change for various sky conditions, the latter can change as overcast and clear skies can generally be modeled more accurately than intermediate sky conditions.

A careful analysis has been carried out to test how accurately the recorded sky conditions in the two-week measurement interval can be modeled compared to all appearing sky conditions throughout a year. In Table 4-3 simulation errors of horizontal and vertical outside illuminances based on direct and diffuse irradiances are listed for the two weeks and (in brackets) the complete year of 1998 in one minute time-steps. As SHADOW TEST yields identical results as INTERPOLATED for outside horizontal illuminances and nearly identical results (±1%) for outside vertical illuminances, both assignment modes are listed together.

[38] As closed-looped automated control systems for an artificial lighting system often feature ceiling-mounted photosensors, the modeling accuracy of the energy performance of such systems is similarly affected.

Table 4-3: Relative MBE and relative RMSE of simulated illuminances for an unshaded point facing up and in the 4 main sky directions. The values are based on the 10,097 sky conditions with measured outside horizontal illuminances above 1000 lux for which indoor illuminances have been collected. The values in brackets are based on measured values for the whole year of 1998 (250,196 values).

	INTERPOLATED/Shadow Testing	
	rel. MBE [%] (whole year)	rel. RMSE [%] (whole year)
horizontal	-6 (-7)	10 (12)
North	4 (-1)	17 (19)
South	5 (3)	24 (21)
West	6 (-1)	21 (20)
East	7 (0)	23 (21)

The table reveals that the MBEs and RMSEs for global horizontal illuminances for the whole year and for the two weeks are nearly identical (< 2%), showing that the Perez sky luminous efficacy model yields slightly too low values for the Freiburg climate all year around (negative MBE). The annual RMSEs for the vertical sky directions tend to lie below the values for the two weeks. Only Northern illuminances are slightly better simulated for the two weeks than for 1998. The main differences between the two data sets are the MBEs for the vertical illuminances which vanish for the whole year while they lie between 4% and 7% for the two weeks. These results imply that the sky conditions which have been collected during the two weeks can be modeled with an accuracy which is representative for all sky conditions throughout the year. From this information it can be further inferred, that – at least for retracted blinds – the results from sections 4.2.1 to 4.2.3 can be generalized for arbitrary sky conditions throughout the year.

4.2.5. Error Analysis for the Daylight Autonomy

While the relative MBE and RSME are standard statistical measures to express how well a simulation method approaches a reference case, it is difficult to infer from these quantities how well more instructional characteristics of a building design like the daylight autonomy can be modeled by DAYSIM.

Fig. 4-7 plots measured and simulated daylight autonomies for sensor #2 in the test office for different minimum illuminance levels[39]. The underlying time interval are all hours between 7 a.m. and 6 p.m. during the two weeks when indoor illuminances were collected. The daylight autonomies are rather low, as the blinds were lowered during two thirds of the considered time interval, independent of the surrounding sky conditions. The figure clearly shows that simulated and measured daylight autonomies never differ by more than 2 percentage points even though all three blind positions are considered to roughly equal parts. As it has been shown in the proceeding section that the sky conditions in the measurement interval are rather challenging to model compared to all appearing sky conditions of the year, it can be inferred that DAYSIM is able to model annual daylight autonomies with a comparable accuracy – if the status of the venetian blinds is known throughout the year.

[39] The error bars for the measured values correspond to a 5% error of the Hagner SD2 illuminance detectors.

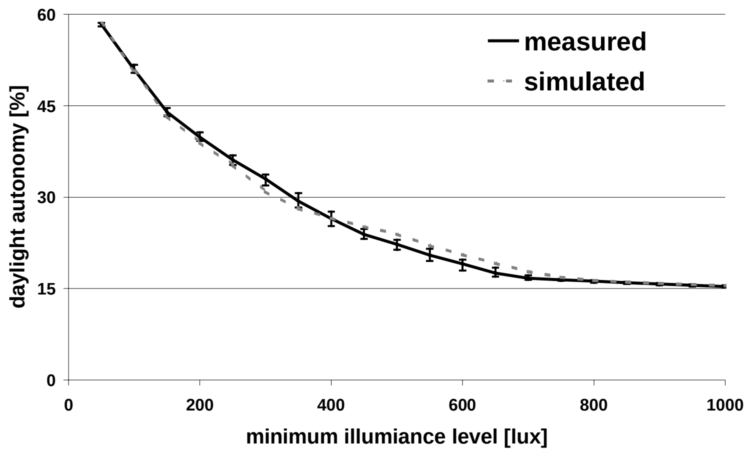

Fig. 4-7: Measured and simulated (SHADOW TEST) daylight autonomy for the 2 week measurement period for a point at 2m distance from the facade.

4.3. Discussion and Conclusion

Section 4.2 covered the impact of different assignment modes, blind settings, sky conditions, sensor positions and the surrounding landscape on the simulation accuracy of DAYSIM simulations.

<u>assignment modes:</u> NEAREST NEIGHBOR introduces discontinuities in the temporal development of indoor illuminances and is therefore not as suitable to model the short-time-step dynamics of indoor illuminances as the other two assignment modes. In most real-world design projects INTERPOLATED will be the assignment mode of choice as it quickly yields indoor illuminance profiles which are reliable under the majority of possible sky conditions. SHADOW TEST should only be employed when needed as it involves additional calculation times[40]. It should be used if the point of interest is only temporarily subject to direct solar illumination and if the appearance of glare is investigated.

<u>accuracies of indoor illuminances:</u> it has been found that the accuracy of SHADOW TEST only slightly depends on the actual blind setting or sky condition. For the desk sensors the magnitude of the MBEs and RMSEs stayed below 6% and 26% for all blind settings. The ceiling sensors - especially the one near the facade - tend to be harder to simulate as the surrounding landscape can usually not be modeled with the necessary detail.

<u>details of the surrounding landscape:</u> the quality of daylight simulation results decisively depends on whether details of the surrounding landscape are adequately modeled. In this study, modeling the ground in direct vicinity of the facade of the test office proofed to be crucial for the accuracy of the simulation results especially for ceiling mounted sensors. The necessity to carefully model the surrounding landscape is common to dynamic and static daylight simulations.

<u>sky model and raytracing errors:</u> in this study the simulation errors were caused to roughly equal parts by errors of the sky model and the combined effect of the daylight coefficient method, the raytracing algorithm and the CAD model. When the venetian blinds were lowered, the weight of the latter rose together with the model complexity. At the same time, the significance of the sky luminance distribution model dropped since a growing percentage of the incoming daylight was reflected from the surrounding ground before entering the test office.

<u>daylight autonomy:</u> section 4.2.5 suggests that the annual daylight autonomy for an office featuring external venetian blinds can principally be predicted with an accuracy of a few percentage points. The remaining limiting factor for such precise predictions of the daylight autonomy in a real building are uncertainties of the temporal status of the shading and glare protection devices.

[40] A shadow testing procedure has to be carried out for each considered sunny sky condition.

All these findings indicate that dynamic, RADIANCE-based daylight simulation methods which use the concept of daylight coefficients are able to efficiently and accurately model complicated daylighting elements such as the considered venetian blind system.

4.4. Summary

The validation study of the RADIANCE-based dynamic daylight simulation method DAYSIM yielded that

- the short-time-step dynamics of indoor illuminances can be modeled with comparable accuracy for different settings of the external venetian blinds
- the daylight autonomy for a two-week measurement interval could be simulated with an accuracy below 2 percentage points
- the INTERPOLATED assignment mode provides fast and reliable simulation results for most applications. SHADOW TESTING should be only employed in case the appearance of direct glare is under investigation as the mode increases the required simulation times

Chapter 5 Simulating short-time-step indoor Illuminances

This chapter addresses the feasibility and benefit of modeling the annual daylight availability and artificial lighting demand in a building based on simulated 1-min instead of 1-hour irradiance input data. A stochastic model based on Skartveit and Olseth has been adapted for dynamic daylight simulations and implemented into the DAYSIM environment. Simulation results for five sites on earth show that the accuracy of annual daylight simulations can be significantly enhanced without any additional work for the planner.

5.1. Introduction

The preceding chapter concluded that DAYSIM is capable of modeling the development of indoor illuminances in time-steps as low as 30 seconds based on direct and diffuse irradiances. Unfortunately, current simulation practices are usually limited to the usage of hourly mean irradiances as data series with a higher time resolution are only available for a very limited number of sites on earth.

Fig. 5-1 visualizes how the time resolution influences the estimated daylight availability in a building. Shown are hourly and 1-min[41] means of the global horizontal irradiance on the 17th of May 1998 in Freiburg, Germany. Both data sets are based on 10 second measurements. The day exhibited clear sky conditions in the morning which changed to intermediate after about 9 a.m.. The figure shows that simulation results of the daylight autonomy and the artificial lighting demand can depend on the underlying time-step interval. Given that an ambient global horizontal illuminance of 400 W/m^2 corresponds to the minimum indoor illuminance at a particular work place, 1-hour means would yield sufficient daylight levels from 8 a.m. to 4 p.m. whereas 1-minute data would detect periods of insufficient daylight throughout the day. If, on the other hand, 800 W/m^2 corresponded to the minimum threshold, the 1-min time series would yield a higher daylight autonomy than the 1-hour time series. Obviously, shorter simulation time-steps have an effect on daylight simulation results.

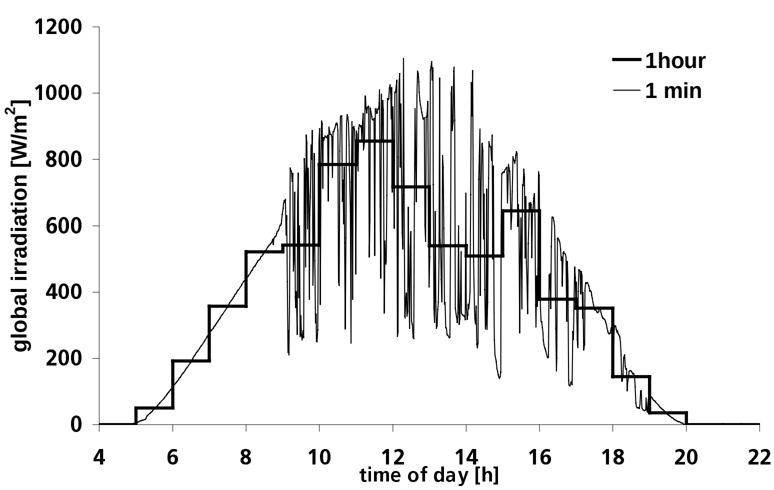

Fig. 5-1: Time development of the global horizontal irradiance in Freiburg, Germany, on the 17th of May 1998. The 1-hour and 1-min means are based on 10-sec measurements.

To fully exploit the power of a dynamic simulation tool like DAYSIM, a model which generates short-term irradiance time series from hourly mean values has been implemented into the DAYSIM simulation environment. The model incorporates randomness and is based on a model which has been developed by Skartveit and Olseth [ska92] in the early nineties. The adaptation of the model for daylight simulations and its validation for five sites on earth have been the content of a masters thesis at the Albert-Ludwigs-Universität in Freiburg, Germany [wal01]. Details of the model and an analysis of the results have been submitted for publication in *Solar Energy* [wal01_a]. This chapter merely provides a qualitative description of the model (5.2) and presents daylight simulation results for five sites on earth and three artificial lighting control strategies (5.3). To the author's knowledge no previous work has explicitly addressed the influence of the time-step interval on the accuracy of dynamic daylight simulations. Delaunay investigated the influence of the sampling interval on the resulting stored averages for direct and diffuse irradiances and found that for partly cloudy skies with fast moving clouds the direct irradiance has to be sampled below 10 seconds to gain an averaging error due to the sampling below 2% [Del94]. Goller found that in Freiburg, Germany, the periods of direct sunshine are in

[41] The shortest time-step which is considered in the following are 1 minute time-steps. This lower threshold has been chosen as the model has been originally developed based on measured 1-minute data series, to avoid large input and output files and as the author believes that no significant additional insight can be gained from further increasing the time resolution.

5% of all cases shorter than 1 minute and in 15% shorter than 15 minutes and concluded that time-steps in the order of minutes need to be considered to adequately evaluate the performance of a daylighting element [Gol00].

5.2. A model for simulating short-time-step Irradiances

In this section the basic steps of the adapted stochastic model of Skartveit and Olseth are described and exemplified for the global horizontal irradiance on the 17th of May 1998 in Freiburg, Germany (Fig. 5.1). The original model had been developed to improve simulations of energy gains of *non-linear* solar energy systems [ska92]. While the core of the model has been left untouched, a number of adaptations were carried out to facilitate the handling of the model and to improve its accuracy for daylight simulations. The former aspect mainly necessitated a reduction of the number of required input parameters whereas the latter concentrated on enhancing the model accuracy at the extremes of a day as well as improving the modeling of higher and lower thresholds of intrahour irradiances under certain sky conditions[42] [wal01_a]. The following gray box explains the 4 model steps for a day which exhibited several different sky conditions.

Generating short-term irradiances

Step (0) Model Input: the goal of the model is to reproduce measured 1-min global horizontal irradiances. Model input are hourly mean global irradiances. The example day corresponds to Fig. 5-1.

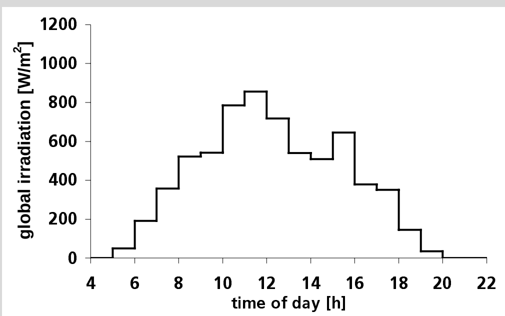

Step (1) Transformation to relative quantities: the global horizontal irradiance can range from 0 up to 1500 W/m^2. A clear sky model simulates irradiances under a clear sky based on the position of the sun as well as model dependant parameters which quantify the amount of scattering of solar radiation in the atmosphere. In step (1) the ESRA clear sky model [Rig00] is used to transform global irradiances into global clearness indices[43] in order to get rid of daily and seasonal variations of the solar irradiance. The ESRA clear sky model only requires the Linke turbidity factor to describe influences of the atmosphere. On a perfectly clear day the index would correspond to unity throughout the day. On a dark overcast sky the clearness index lies around 0.2 throughout the day. The figure below shows the hourly mean global clearness indices for the example day.

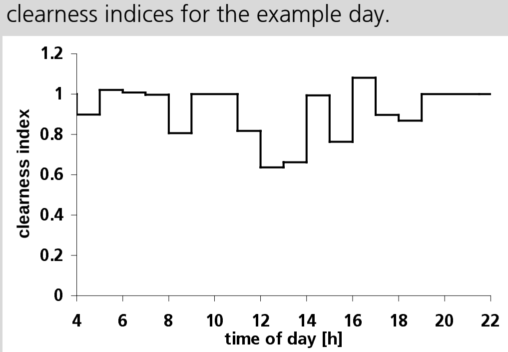

[42] If annual energy gains of a PV or solar collector system are investigated, modeling errors of solar irradiances are negligible at the extremes of a day. On the other hand, such errors become important if the daylight situation in a building is considered as a temporary illuminance surplus cannot outweigh a subsequent underpinning of the minimum illuminance threshold.

[43] The clearness index, K, corresponds to the ratio of the input hourly mean global irradiance to the theoretical clear sky global irradiance. In the absence of daylight K corresponds to unity.

Step (2) Computation of 1-min irradiances: For each hour the model estimates sixty 1-min irradiance values in two steps:

(a) In a first step the intrahour standard deviation of the ith hour, σ_i, is picked from a probability distribution. The shape of the probability distribution for a considered hour has been fitted by Skartveit and Olseth for irradiance data from Atlanta and San Antonio, USA, as well as Geneva and Payerne, Switzerland, [ska92] and is a function of the clearness indices of the considered hour, K_i, as well as of the two neighboring hours, K_{i-1} and K_{i+1}. The shape of the probability distribution for σ_i is determined by two terms: according to the first term a low or high K_i tends to results in a low intrahour standard deviation, σ_i, whereas an intermediate K_i around 0.5 (intermediate sky conditions) favors a high σ_i [44]. The second term depends on the variability between K_i, K_{i-1} and $K_{i+1}$and a high *interhour* variability yields a high *intrahour* standard deviation.

(b) In a second step the picked intrahour standard deviation from the above described stochastic procedure is used to parameterize a second probability distribution. The resulting probability distributions for 7 to 8 a.m. (clear sky) and 2 to 3 p.m. (intermediate sky) on the example day are depicted below. For the clear sky condition the clearness index was 0.97 and the estimated standard deviation 0.05. The resulting probability density of the clearness indices is unimodal and peaked around 1. For the intermediate sky conditions the probability density is bimodal, i. e. it changes between times with and without direct sunlight.

7 a. m. to 8 a.m.

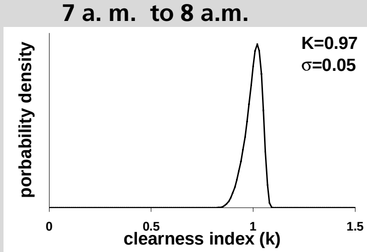

2 p. m. to 3 p.m.

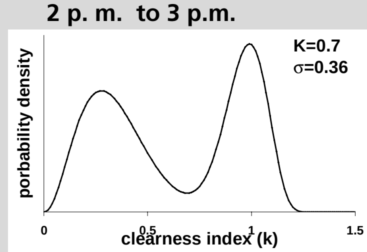

From the probability density function of the clearness index for each hour of the day sixty 1-minute irradiances are picked randomly. The following two graphs show exemplary realizations from the above two probability densities in ascending order. The picked values clearly reflect the shape of their underlying probability density functions.

7 a. m. to 8 a.m.

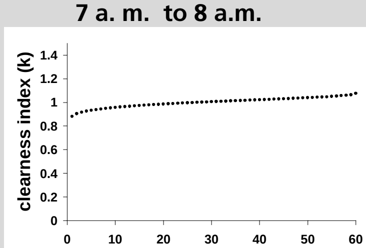

2 p. m. to 3 p.m.

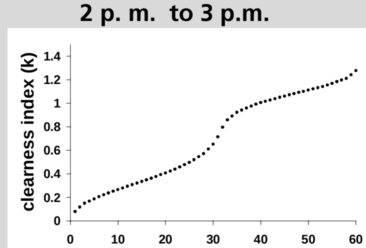

Step (3) Ordering the 1-min irradiances: The sixty 1-min irradiances from step (2) are ordered within the hour with an autoregressive model. The model is based on a lag one autocorrelation function which requires a single parameter, the autocorrelation coefficient. A high autocorrelation coefficient indicates persistence between succeeding values. Two possible time sequences are shown below.

7 a. m. to 8 a.m.

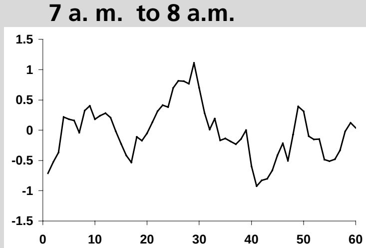

2 p. m. to 3 p.m.

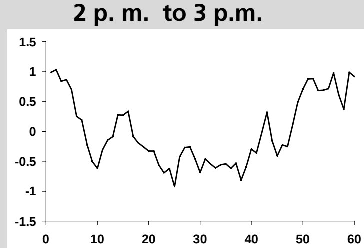

The two time series are combined with the sixty 1-min irradiances from step (2) and yield the following time series of the clearness index.

[44] During intermediate sky conditions the clearness index tends to scatter between successive bright and dark sky conditions.

7 a. m. to 8 a.m.

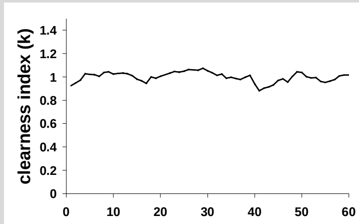

2 p. m. to 3 p.m.

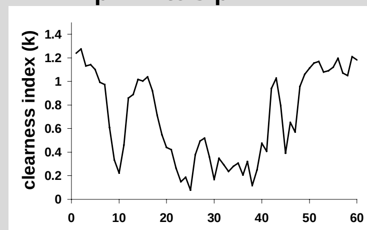

All 1-hour time series are grouped together to yield the development of the clearness index during the example day.

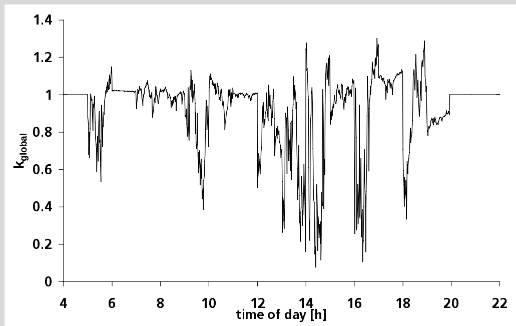

Step (4) Transformation to absolute quantities: The modeled clearness indices are transformed back into global horizontal irradiances based on the ESAR clear sky model.

Simulated 1-min global irradiances

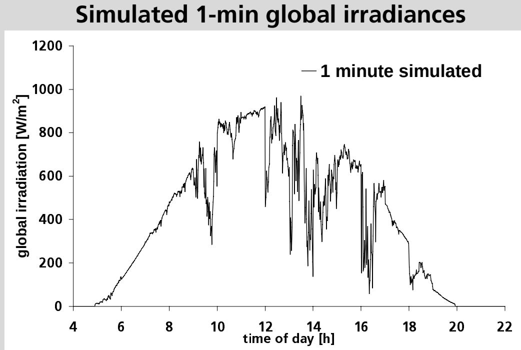

measured 1-min global irradiances

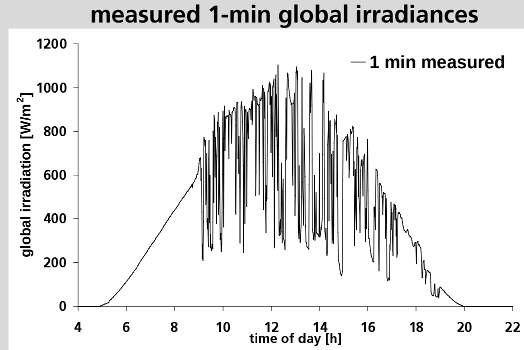

A comparison of the simulated and measured 1-min irradiances on the example day shows that the model is able to distinguish between clear and intermediate skies. The amount of intrahour variations are less pronounced by the model than in reality. This is not surprising, as the model is stochastic and while differences between measured and simulated values may be substantial for a single day, they tend to vanish if a greater number of hours is considered (see section 5.3).

5.2.1. Implementation into DAYSIM

The adapted stochastic model which has been described above has been implemented into the DAYSIM simulation environment so that short-time-step indoor illuminances can be modeled from 1 hour irradiance data series. The DAYSIM subprogram written by Oliver Walkenhorst has been termed *genshortterm* (Fig. A.2.4-1). The program requires about 90 seconds on a Pentium Pro 200 MHz Linux Workstation to generate an annual 1-min time series of direct and diffuse irradiances and the user of DAYSIM simply needs to set the desired simulation time-steps (usually 1 or 5 minutes). The only required input parameters are the site coordinates and the elevation of the input weather data station. Monthly mean Linke turbidity factors are either automatically estimated from the input data or can be explicitly given. The resulting time series of global irradiances is used to estimate direct and diffuse irradiances with the help of the Reindl model[45] [rei90].

[45] The Reindl model yields direct and diffuse irradiances based on global irradiances. *genshortterm* normalizes the resulting time series of direct and diffuse irradiances with the help of the hourly mean direct and diffuse input irradiances.

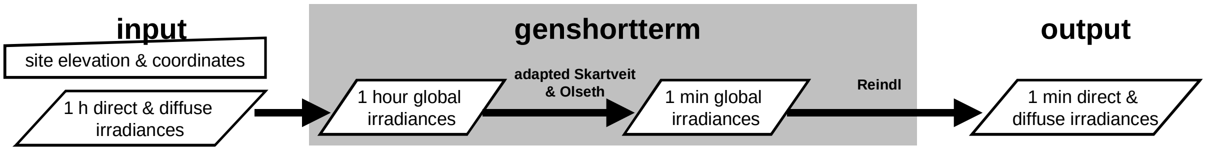

Fig. 5-2: flow chart of the implementation of the adapted Skartveit model into DAYSIM.

5.3. Application of the Model

In this section dynamic daylight simulation results are presented which are based on hourly mean as well as measured and simulated 1-min irradiance data. The comparison of these input data series must not be understood as a physically sound validation of the model but it merely aims to provide the reader with a feeling of

- how strong the simulation time-step influences the results of a dynamic daylight simulation and
- in how far simulated 1-min time series enhance the simulation accuracy.

5.3.1. Methodology

Annual times series of direct and diffuse 1-min irradiances have been investigated for 5 sites on earth (Fig. 5-3). For these sites daylight autonomies and annual artificial lighting demands for three lighting strategies have been calculated for sensor #2 in Fig. 4-1. The sensor represents the work place of an office worker in a private office with a southern facade. The occupancy profile of the user corresponds to the simulated occupancy profile of the user in room #4 in chapter 7 (see Appendix A.7.1 and section 8.1). The daylight autonomy has been calculated for a minimum illuminance threshold of 500 lux based on all the times of the year when the work place is occupied, i.e. 1752 hours for the considered private office.

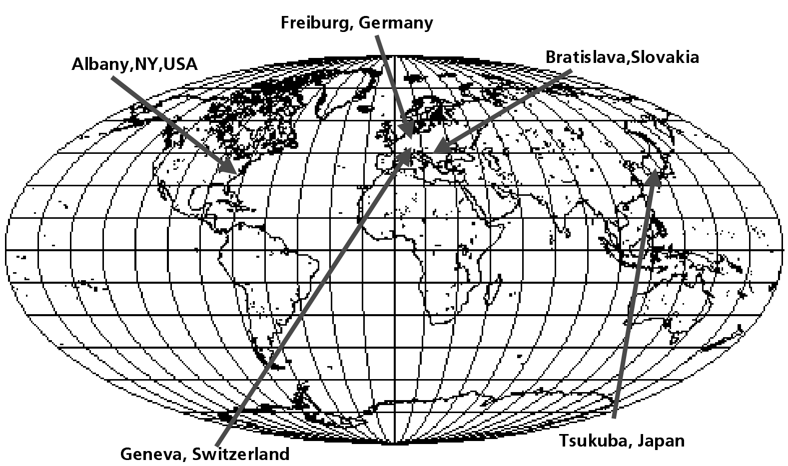

Fig. 5-3: geographical position of the investigated five sites.

	latitude	longitude
Freiburg	47.98	-7.83
Bratislava	48.17	-17.08
Tsukuba	36.15	-140.05
Geneva	46.33	-6.02
Albany	42.70	73.85

Three artificial lighting strategies have been considered which cover a range of currently available lighting control options including manual control, dimming and occupancy sensors. The three example strategies do not lay claim to represent current lighting design practices and the author discourages a comparison of absolute predicted energy demands for the different strategies. The aim of the present chapter is only to quantify the influence of the underlying irradiance data series on the predicted electric energy demand for artificial lighting. The installed power of the lighting system has been modeled to be 15 W/m^2 for all three variants:

manual control: this variant corresponds to an undimmed artificial lighting system which is manually operated by a single user who operates the lighting system in accordance with the available daylight. Model details are provided in chapter 8.

facade sensor: this variant corresponds to an undimmed, automated lighting system which is activated on weekdays between 8 a.m. and 6 p.m.. When activated, the lighting in the office is switched via a vertical sensor in the southern facade. The lighting is switched on when indoor illuminances fall below a threshold of 500 lux and switched off once the threshold illuminance has been maintained for more than 15 minutes by daylight alone. This inertia of the system has been added to reduce the number of distracting, automated switching events.

closed loop: the last variant corresponds to an ideally dimmed, automated lighting system which is combined with an occupancy sensor. The lighting is activated when occupancy is detected and deactivated after a 20-minutes delay time[46]. When activated, the system complements (tops up) the available daylight in the building until 500 lux are provided at the work place. The relationship between the dimmed lighting output and the corresponding electrical power demand of the system has been taken from [kno98] and is depicted in Fig. 5-4.

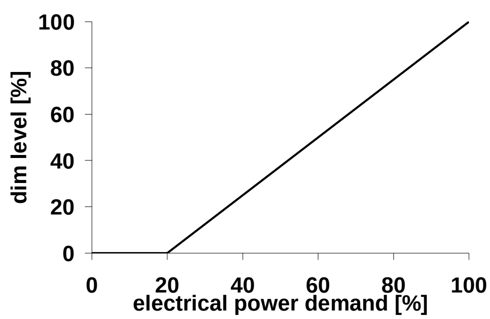

Fig. 5-4: relation between electrical power demand and dim level of the considered *closed loop* lighting system.

5.3.2. Results and Analysis

Fig. 5-5 shows simulated daylight autonomies and the annual electric energy demands for artificial lighting for the three control strategies based on hourly means as well as measured and simulated 1-min values for Bratislava, Slovakia. As two complete 1-min annual data sets of direct and diffuse irradiances have been available for Bratislava two neighboring columns of the same color correspond to simulation results for 1998 and 1999.

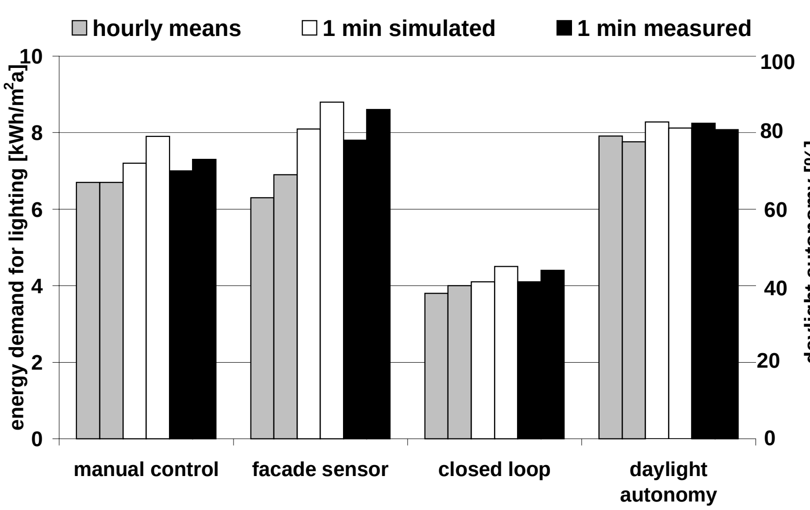

Fig. 5-5: Artificial lighting demand for the three control strategies and daylight autonomies for sensor #2 for Bratislava, Slovakia. The Facade orientation is South. Two neighboring columns of the same color correspond to the irradiance data sets for the years 1998 and 1999.

daylight autonomy: All six daylight autonomies lie between 78% and 83%. This shows that this quantity does neither significantly depend on the underlying time-step interval nor on the chosen year. All three data sets yield that the daylight availability was higher in 1998 than 1999.

closed loop: measured and simulated 1-min data series basically coincide while the 1-hour data underestimates the electric energy demand by up to 9%. The high differences between simulation results for the electric energy demand compared to simulation results for the daylight autonomy come about as the investigated sensor point #2 represents a comparably bright work place so that the times when the artificial lighting is switched on are relatively rare. Therefore,

[46] According to Pigg, actually build-in delay times in occupancy sensors range between 6 and 21 minutes [pig96].

the simulation results critically depend on how well a considered irradiance data series reproduces indoor illuminances during the few times of insufficient daylight.

facade sensor: While the simulated 1-min data series still outperforms the 1-hour data series, simulation results for the two 1-min data series lie not as close together as for *closed loop*. The simulated 1-min data slightly overestimated the measured 1–min data. As elaborated in [wal01a], the reason for this overestimation is that the adapted Skartveit and Olseth model still yields too many single low 1-min irradiances within an hour. While a single low outliner within an hour has a negligible impact on the *closed loop* lighting status, it leads to a 15 minutes switching of the lighting system in the case of *facade sensor*.

manual control: The largest differences between the three data series appear for *manual control*. Both 1-hour as well as simulated 1-min lie above and below the reference measured 1-min electric energy demands.

Fig. 5-6 corresponds to Fig. 5-5 for the other 4 considered sites on earth. The daylight autonomies for the simulated and the measured 1-min data series never differ by more than one percentage point. The difference between 1-hour and 1-min measured data ranges from 1 percentage point for Tsukuba to nearly 5 percentage points for Geneva.

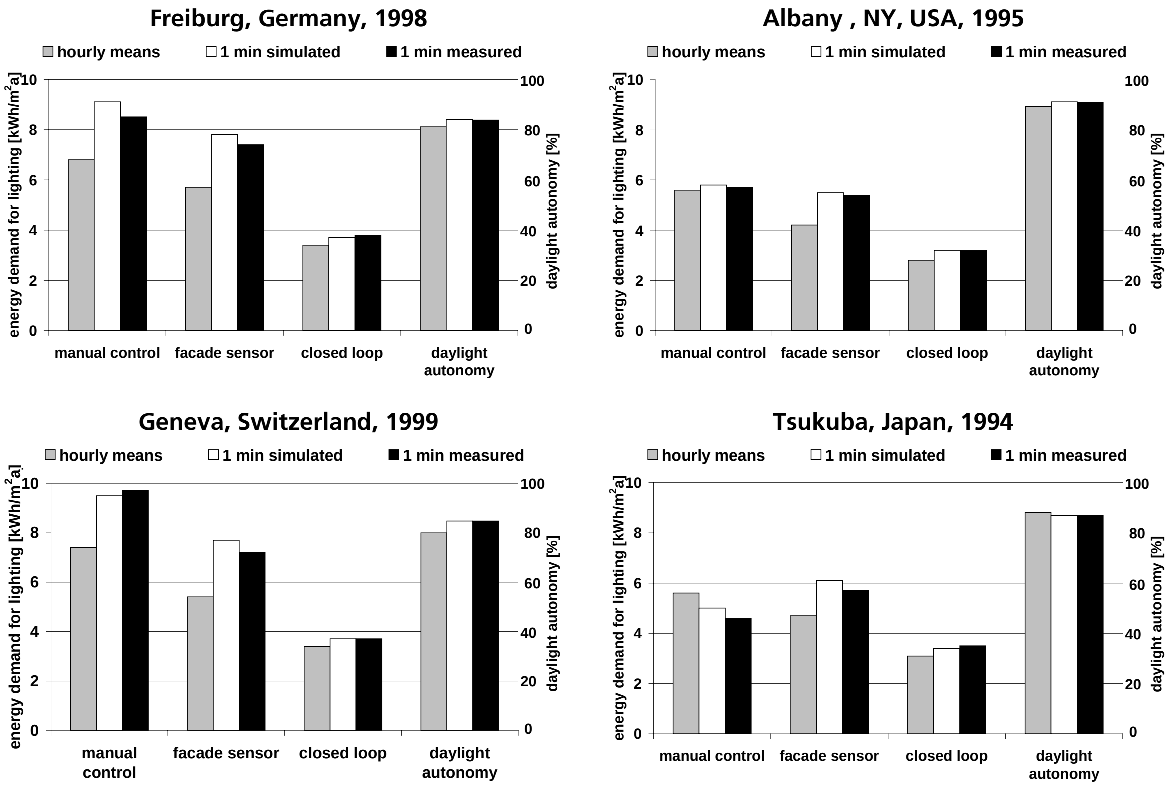

Fig. 5-6: Electric energy demands for artificial lighting for the three control strategies and daylight autonomies for sensor #2 for 4 sites on earth. The Facade orientation is South.

As for Bratislava, the differences between the electric energy demands for artificial lighting are more pronounced than between daylight autonomies. Table 5-1 lists the relative RMSEs of the predicted artificial lighting demands based on 1-hour and 1-min simulated data series with respect to the measured 1-min series for all 5 weather stations explicitly. All values in the table are means of the three lighting strategies. While the relative RMSEs of the simulated short-time-step irradiances lie around 2-3% for all considered climates, they amount up to 12% if hourly means are used. This reveals that simulated short-time-step data series yield more reliable results than hourly means for different lighting systems and different climates and sites on earth.

Table 5-1: Relative RMSEs of the 1-hour and 1-min times series compared to 1-min measured times series for the five investigated sites. The values are means of the three investigated lighting control strategies.

rel. RMSE [%]	Bratislava	Freiburg	Albany	Geneva	Tsukuba
1-hour	8	11	9	12	8
1-min simulated	2	3	1	2	2

5.4. Discussion and Conclusion

The following conclusions can be drawn from the last section.

influence of short-time-steps: the underlying time-step interval of annual daylight simulations influences the resulting daylight autonomies and predicted energy demands for artificial lighting. For a daylight-oriented work place a quantity which scales with the available daylight, e.g. the daylight autonomy, tends to be slightly overestimated, if 1 hour instead of 1-min data series are used. As a consequence, the artificial lighting demand is usually underestimated if the short-time-step dynamics of daylight are neglected.

influence of different years: simulation results for 1998 and 1999 in Bratislava show that the daylight autonomy for a daylight-oriented work place does not significantly vary for different years. Natural variations of the daylight autonomy lie around 2 percentage points for all three considered data series. As 2 percentage points have also been identified in chapter 4 to be a lower limit of the combined errors of the dynamic daylight simulation algorithm, the building description and the modeling of the surrounding sky conditions, natural variations of the daylight autonomy seem to be negligible.

The artificial lighting demands for different years vary by up to 10%. Whereas the daylight autonomy is a uniquely defined, physical quantity which solely depends on annual illuminance profiles, artificial lighting profiles further depend on user occupancy, individual behavioral patterns and how well an automated or manual lighting system functions in a real building[47]. The combined effect of these diverse factors is considerably larger than the impact of irradiance data sets for different years (see chapter 8).

model quality: section 5.3 revealed that the adapted Skartveit and Olseth model significantly enhances annual daylight simulation results for a range of climatic zones on earth. Due to the reduced number of required input parameters, the model can be used by a planner with hardly any additional effort and therefore constitutes a useful and *easy-to-use* extension to dynamic daylight simulation methods.

influence of lighting control strategies: Fig. 5-5 and 5-6 showed that the control strategy of an artificial lighting system has a decisive impact on the energy demand. To assist a planner in deciding what lighting strategy is most suited for a building, the artificial lighting demand for each considered variant should be compared to a reference case. This reference artificial lighting system should be undimmed and manually operated as such a system is cheap and common. As the simulation differences between 1-hour and 1-min measured data series are pronounced for manual control strategies, the adapted Skartveit and Olseth model is a necessary requirement for carrying out meaningful comparisons between automated and manual artificial lighting control strategies.

[47] Love carried out a field study on the actual performance of lighting systems with photoelectric controls in three office buildings in Calgary [lov95]. He found that the actual energy savings of the investigated systems were low, as they were either not properly commissioned, grouped together too many offices with different daylight availabilities or were installed in offices with a low daylight potential due an unfavorable building design.

5.5. Summary

The investigation of the influence of the time-step interval on annual dynamic daylight simulations yields that

- short-time-step simulation intervals in the order of 1 minute are a necessary condition for reliable calculations of the manual and automated electric energy demands for artificial lighting and that
- the adapted stochastic Skartveit and Olseth model can significantly enhance the simulation accuracy of artificial lighting usage without any additional effort for the simulator.

Part B Modeling Manual Lighting Control

In part A it has been shown that annual indoor illluminance levels can be principally predicted with a high accuracy if building geometry, optical surface properties and the status of the electric lighting system and venetian blinds as well as the sky luminous distribution are known throughout the year. As the former two quantities are available for a catalogue of materials and daylighting devices, the remaining simulation errors largely stem from uncertainties of which manual control strategies are practiced in office buildings. Part B is concerned with this topic. Based on results from past studies a monitoring procedure has been developed to further exploit the behavioral patterns of office building occupants. The procedure has been applied in 10 offices in a near Stuttgart, Germany, from March until December 2000. The analysis of the monitoring data yields already well-established as well as new quantitative correlations between external stimuli and the setting of the artificial lighting and blinds. These behavioral patterns have been combined with the dynamic daylight simulation method from part A and a stochastic user occupancy model. The resulting *manual lighting control model* predicts the annual electric energy demand for artificial lighting in an office.

Chapter 6 Monitoring of User Behavior

A literature review of past studies on manual control strategies for artificial lighting systems and venetian blinds is presented. Based on the results of these studies a new experimental procedure is proposed and thoroughly discussed.

6.1. Introduction

So far, most building models tend to "treat people like fixed metabolic heat generators passively experiencing the indoor environment" [new94]. These models neglect the fact that office users do actually influence their immediate working environment by operating the artificial lighting system and/or the shading and glare protection device. The exact nature of this *user-building interaction* may significantly influence the incoming solar gains and therefore the thermal and visual comfort conditions as well as cooling and heating loads. The influence is pronounced in buildings with large architectural glazings.

Chapters 6 to 8 aim to gain more insight into the degree and kind of manual control strategies of external blinds and artificial lighting systems which are practiced in office buildings. The first part of this chapter provides a review of past experimental studies. Based on the results of these studies a new monitoring procedure has been designed and applied in an office building in Southern Germany with private and two-person offices (6.3). An analysis of the results from the pilot study is presented in chapter 7. In chapter 8 the results are implemented into a *manual lighting control model*.

6.2. Previous Research

Studies which investigate the behavioral pattern underlying manual lighting and shading control strategies try to quantify the likes or dislikes of people towards a given thermal and visual comfort situation. They usually involve the participation of test subjects whose behavior is monitored in the field or observed in the laboratory. The *objective* of monitoring user behavior is to

- collect objective and quantifiable data based on when and how users manipulate their immediate environment - including the blind system and artificial lighting
- identify various external, measurable stimuli/variables and their interdependencies which contribute to personal comfort,
- search if user manipulations are related in a systematic fashion to such external variables
- establish quantitative correlations between a stimulus and the resulting user behavior: What are accepted/required luminance and illluminance distributions? How and when do people operate their lighting system/shading device to achieve a desired working condition? Is there an underlying principal of how people manually operate their blinds or artificial lighting?

Apart from the above mentioned goal of improving existing building simulation tools, user behavior studies are carried out under the assumption that a better understanding of individual user preferences leads to innovative products. The latter yields higher user acceptances, which may in turn lead to an improved task performance or other benefits to the organization, i.e. a payoff for the purchaser who buys the advanced product [vei96]. Apart from such economic considerations, a growing interest in user preferences stems from the observation that the success of an energy saving strategy depends on the appreciation and the cooperation of the user.

There is a wide consensus that people influence their immediate environment if they are exposed to climatic conditions which lie out of their personal comfort range [bak99]. Table 6-1 lists some of the stimuli that have been proposed to influence visual and thermal comfort and therefore the setting of shading devices and the artificial lighting.

thermal comfort [fan82]	- temperature distribution (ambient, operative and radiant) - humidity - air speed
visual comfort [sic99,Poh98,vei96]	- illuminance levels and uniformity - luminance distribution within the view of the spectator - readability of a screen and the presence of veiling reflections - color temperature
personal variables [vei96]	- occupancy profile - metabolic rate - clothing insulation - missing privacy / a feeling of loneliness

Table 6-1: External stimuli that may contribute to individual comfort and therefore influence the manual setting of lighting and blinds.

Some of these variables like occupancy, ambient temperature and external illuminances are independent input variables which define the boundary conditions under which a building has to operate. Other variables like indoor illuminance levels and cooling loads or indoor temperatures depend on these independent variables and are closely entangled with the employed control strategy. To be able to understand the various actions and reactions between these dependant variables, it is necessary to gain an understanding of the purposes and underlying motivations which people follow when they operate artificial lighting and shading devices. The following paragraphs list some mechanisms, which have been identified to provoke the manipulation of these systems.

Artificial lighting is generally used to provide a suitable indoor luminance distributions to enable a user to perform a specific task, i.e. to satisfy the users' visual needs. The required illuminance levels vary with the user's task, age, degree of fatigue and cultural background [lov98]. Apart from this principal task of electric lighting, the act of switching on the lighting can also be interpreted as a signal that the occupant is "at work and has not left for the day"[48]. Research results on chosen preferences for artificial lighting levels indicate that individuals choose a wide range of illuminance distributions at the work place. Veitch and Newsham reported chosen desk plane illuminance levels in cubicle offices without daylight which provided between 83 lux and 725 lux desktop illuminances although most subjects chose lighting levels between 400 and 600 lux. This result supports current design recommendations [vei01, IESNA93, CIBSE93, DIN 5035]. In contrast to this, a Dutch study reported measured user preferences for lighting levels well above 1000 lux (see 6.2.1) [beg97].

Blinds serve diverse purposes. They often act as a combined heat and glare protection device to maintain adequate visual and thermal comfort conditions under sunny ambient sky conditions and/or to reduce the cooling loads if the building is actively cooled [ino98, rub78]. Blinds are very flexible elements that often allow the user to maintain visual contact with the outside even when direct sunlight is incident on the facade. Usually the goal of a blind system is to admit sufficient daylight to a building's interior at all times in order to avoid artificial lighting. Unfortunately, this goal is sometimes not accomplished due to an unfavorable building layout or low solar altitudes that provoke glare if the blinds are not fully closed. Apart form managing incoming solar gains, blinds are employed to provide visual shelter for the users: Even though the view to the outside is a "highly prized benefit", windows near the ground tend to provoke a need for privacy with people feeling observed [mar67, rub78]. The need for privacy is pronounced if ambient daylight levels fall below indoor illuminance levels.

In the past, diverse correlations of the external stimuli from Table 6-1 with the status of blinds and lighting systems have been observed, quantified and explained based on the behavioral mechanisms listed above. The following sections summarize the results of some of these studies.

6.2.1. Manual Control of Artificial Lighting

The first studies on manual switching patterns of artificial lighting systems have been carried out in English offices and schools by Hunt at the Building Research Establishment in the late seventies [hun79,hun80]. Hunt used time-lapse photography, recording pictures in 8-minute intervals to measure lighting status and user occupancy. The measurement periods covered half a daylight availability cycle (Jan.-Jun. or Jul.-Dec.). The ambient sky conditions were synchronously recorded in the form of hourly mean diffuse and global irradiances. Hunt established a strong correlation between the times of switching of electric lighting systems and the extremes of a period of occupation. His major findings are summarized in the following [hun79]:

(H1) all lights in a room are switched on or off simultaneously
(H2) switching mainly takes place when entering or vacating a space
(H3) the *switch-on probability* on arrival for artificial lighting exhibits a strong correlation with minimum daylight illuminances in the working area. This correlation is depicted in Fig. 6-1.

[48] Private communication of the author with Professor Inoue from the Scientific University of Tokyo, Japan

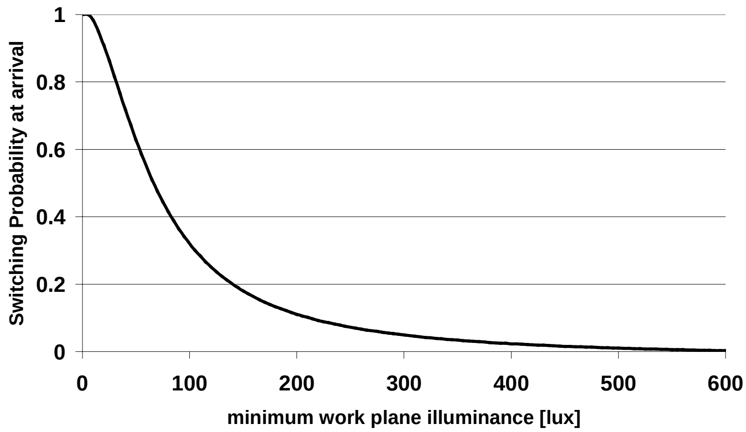

Fig.: 6-1: Hunt derived a strong correlation between switch on probabilities upon arrival and the minimum indoor illuminance level on the work plane. He gained the following quantitative relation:

$$y = a + c/\{1+\exp[-b(x-m)]\}$$

with

y = switching probability
$x = \log_{10}$(min. work plane ill.)
a = -0.0175
b = -4.0835
c = 1.0361
m = 1.8223

In a later paper Hunt linked the formula from Fig. 6-1 with cumulative external annual illuminance levels to predict annual artificial lighting use in offices. He suggested that the *switch-on* criterion is the same during the day as at the beginning of a period of occupation and that people

(H4) switch on their lighting when entering in the morning
(H5) switch the light off during the day when leaving a space for lunch and
(H6) switch the light on after lunch, if the daylight levels fall below the ones in the morning.

The general validity of Hunt's conclusions are still widely acknowledged today and have recently found their way into the coupled lighting and thermal simulation program ESP-R.

Love investigated manual switching behavior in private offices with southern and northern facade orientations in Calgary, Canada [lov98]. In a first study he recorded the artificial lighting usage in southern offices and the six observed subjects could be assigned to two behavioral patterns:

(L1) people who switch the lights for the duration of the working day and keep it on even in times of temporarily absence
(L2) people who use electric lighting only when indoor illuminance levels due to daylight are low

In Love's study the former behavior was exhibited by 5 out of 6 observed subjects in southern offices. Love concluded that the switching behavior is as much dependent on the individual as on the daylight availability. He also suggested that unsuitable glare protection devices might have been the reason for the indifference of most monitored subjects towards daylight. Accordingly, in a second study Love chose offices with a northern orientation, which are less susceptible to glare. He explicitly picked two subjects who used electric lighting selectively and collected occupancy, lighting status and desktop illuminances in 4-minute time-steps for about 4 months. The shading devices in the investigated two offices were retracted throughout the whole measurement period. During the analysis of the data Love defined a *switching judgement* as the moment when a subject entered the room for more than 15 minutes after a temporarily absence of at least 20 minutes. Like Hunt, Love grouped these judgements into cases in which the light was switched on or not and derived a probability function similar to Hunt's (Fig. 6-1) for both subjects. Only the absolute minimum illuminances slightly varied compared to Hunts data and between both subjects. Love attributed subject-specific differences to age differences and the need of one subject for spectacles. Quantitative differences to Hunt were assigned to cultural differences, an insufficient sampling size as well as measurement errors[49]. Although Love's findings support Hunt's results, they cannot be interpreted as a final validation of Hunt's theory as only 2 subjects were investigated in Love's second study.

[49] The minimum work plane illuminance is a somewhat arbitrary quantity.

Pigg *et al.* investigated how people interacted with automated lighting control devices in 63 private offices in a university building in Wisconsin, USA[50] [pig96]. User occupancy and lighting status were recorded for an 11-month period and complemented by walk-through observations and two surveys. While all investigated offices featured occupancy sensors, the sensor was disconnected from the artificial lighting in about one fourth of the offices, so that differences in manual switching patterns with and without occupancy sensors could be resolved. One focus of the study was to quantify how often and under what conditions people turn off their lighting when leaving the office. Fig. 6-2 shows Pigg's results and establishes that

(P1) the length of absence from an office strongly relates with the switch-off probability of the artificial lighting system and
(P2) the presence of an occupancy sensor influences the behavioral patterns of some people. On the average, people in private offices with occupancy control are only half as likely to turn off their lights upon temporarily departure than people without sensors (Fig. 6-2).

Pigg's survey yielded that a number of subjects did consciously choose not to manipulate their lighting any more due to the occupancy sensor. Due to the build-in delay times of the occupancy sensor, this *adapted* user behavior actually reduced energy savings of the occupancy sensors by 30%.

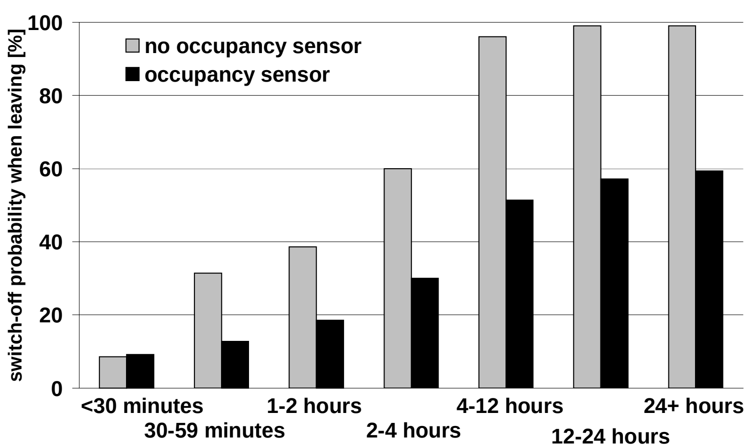

Fig. 6-2: Manual switch-off probability of the artificial lighting in private offices for lighting systems with and without occupancy sensors [pig96].

Upon arrival, the lighting was manually switched on in 95% of all cases. Only in 10% of all occupied times was the lighting not activated. Pigg further notes that on an individual level half of the observed subjects had their lights off for less than 5% of the occupied times and that no occupant spent more than 40% of the time in the office with the overhead lights off. Pigg's measurement setup did not allow to establish a correlation between indoor daylight illuminances and the times of deactivated artificial lighting.

Maniccia *et al.* collected 8 weeks of data on the manual switching patterns in 58 private offices in Boulder, Colorado, USA [man98]. They collected user occupancy and the dimming and switching status of the artificial lighting together with the status of an internal venetian blind system. The focus of the study was to understand the influence of manual dimming and switching controls on occupant behavior and energy use. Their results show that 74% of the observed subjects dimmed their lighting and that some occupants sometimes worked with their lighting off. This indicates that the majority of subjects used their artificial lighting in some relationship to prevailing daylight conditions. Concerning the blind usage, most blind adjustments appeared in southern and western offices as people used their blinds mainly to occlude direct sunlight. The data was collected from December to March and the number of blind adjustments fell as time progressed due to seasonal variations of daily solar altitudes. Overall, blinds were operated three times more often than the lighting system.

[50] Private offices were chosen as people are more likely to manage the lights when they perceive ownership over a space.

Begemann, Tenner *et al.* from *Philips Lighting* observed how a total of 170 subjects manually adjusted the dim level and color temperature of their artificial lighting system in Eindhoven, The Netherlands, during one-day observation periods in private test-bed offices [beg97]. The investigated lighting system could provide horizontal lighting levels up to 2000 lux at the work plane and was either automatically switched off each hour [beg94] or slowly dimmed down [ten98] after a manual reset to provoke reactions from the subjects. The experiments were carried out in 4 test offices with Northern facades. To complement the one-day experimental data, two test-offices were permanently monitored and occupied by two middle-aged males over an extended period which included summer and winter seasons.

While the essence of Hunt's and Love's results is that increasing daylight levels reduces the need for additional electric lighting for user type (L2), the Dutch researchers found that in their test bed subjects chose an average of 800 lux artificial lighting *independent* of the prevailing daylight levels. When the blinds were retracted under clear and intermediate sky conditions, the chosen artificial lighting levels even increased up to 2000 lux as indoor daylight levels increased over 2500 lux. These user preferences resulted in average work plane illuminances of around 1900 lux (daylight + artificial lighting) which lie significantly above current lighting design guidelines. Begemann *et al.*'s analysis of the two long-term data sets revealed that there is a large range of individual preferences and that individual behavior is consistent. In fact, the two monitored users exhibited drastically different behavioral patterns adding on the average 300 lux and 1200 lux artificial lighting to the available daylight.

Begemann *et al.'s results* are in contrast to various other related field studies. Veitch and Newsham investigated "the effects of individual control over lighting on performance and satisfaction" [vei01]. They allowed a total of 94 persons to set two dimmable lighting fixtures and a task light in cubicle offices according to their preferences. They found that all chosen desktop illuminances lay below 725 lux and that over 60% of participants chose values below 500 lux. Over 80% of the subjects stated that office lighting was important to them, that they preferred to work in an office with a window with a blind or curtain and that they wanted to have individual control over their lighting. All participants spontaneously chose luminance conditions well within current energy codes [IESNA93, CIBSE93, DIN 5035] and expressed a high satisfaction with the lighting system.

So where do the high illuminances which were generally favored by their test subjects in Begemann's study come from? The Dutch researchers interpreted their results with a need of their participants for *biological stimulation*, i.e. high illuminances on the human eye which influence the cardiac wake-sleep rhythm (see chapter 2.1) [beg97]. According to Begemann, current lighting practices, which usually provide below 1000 lux lighting levels, merely meet the *visual* needs of users to perform a task. They quote a medical study from Jung and Holick [jun94] which claims that biological effects of light entering the human eye mainly appear at relatively high illuminances: "lighting levels below 1000 lux are biological darkness". As a permanent deprivation of biological stimulation can lead to health problems ranging from minor sleep and performance difficulties to depression (*ill lighting syndrome*), Begemann *et al.* concluded that "higher artificial lighting levels at the work place might act as a preventive medicine against these widely spread symptoms" [beg97]. Love questioned some of Begemann's results [lov98]. He suspected that the high artificial lighting levels were actually chosen to reduce the large spatial brightness gradient within the test-bed offices due to the absence of blinds[51]. Another point of discussion is whether biological interpretation – in case it really is a valid interpretation of Begemann's results – should be provided via electric lighting as a preventive medicine, or whether the related health issues should not be addressed by adequately daylit office environments or short walks outside over lunch.

Whereas all previously mentioned studies concentrated on physical stimuli and their relation to manual switching patterns, Boyce investigated how far social constraints influence the setting of

[51] Apparently, the investigated subjects in Begemann's study even asked whether the blinds could be lowered to reduce the brightness of the windows [lov97].

artificial light in open office environments [boy80]. Boyce recorded the switching patterns in two open offices which hosted between 30 and 40 people each in a commercial building in England. The experiments lasted 2 weeks (1 in summer and 1 in winter) and involved the collection of the occupancy and lighting status based on half hourly personal visits. Desktop illuminances were measured indirectly in comparable open offices on other floors. Boyce provided a histogram of desktop illuminances at switch on and off events, but as the measurement period was very short, no quantitative correlations as in Fig. 6-1 could be established. Nevertheless, Boyce's switch on data is in qualitative agreement with Hunt's results as the number of switch on events increased with decreasing illuminance levels. To gain some knowledge about individual switching behavior, Boyce observed the subjects during the data collection and found the following behavioral patterns:

(B1) individuals who dislike artificial lighting and turn it off for themselves if possible
(B2) group leaders who turn off the lighting if they think it appropriate for their group
(B3) people who turn off all lighting when the room is vacated

Finding (B1) implies that it is energetically advantageous if people can switch the lighting within the space over which they have a feeling of possession, i.e. the zoning of artificial lighting systems encourages that lighting is switched off during the day[52]. Individuals who fall under category (B1) probably correspond to Love's user type (L2). (B3) corresponds to Hunt's model of artificial lighting switching (H5) [hun80]. Boyce further observed that even though switching is a matter of personal initiative the observed users exhibited consistent switching patterns throughout the measurement period.

Jennings measured the energy saving potential of various lighting control strategies in private offices with facade orientations in all four major sky directions in San Francisco, U.S.A., over a 7-month period[53] [jen99]. She collected ambient diffuse and global irradiances in 5-min intervals together with one-minute data of user occupancy, the status of the artificial lighting switches and the momentary artificial lighting power used. A total of about 3500 occupied working days were recorded for 35 perimeter offices. All investigated offices featured manually operated venetian blinds. Even though the paper concentrated on energy savings due to occupancy and dimming control systems, the data also revealed that in only 8 out of 35 offices the total lighting periods were lower than cumulated total work place occupancies. This implies that only 8 occupants at least sometimes switched off their lighting due to sufficient daylight levels, i.e. they belonged to Love's behavioral pattern (L2). Apparently, all other subjects left their lighting on independently of the prevailing daylight situation in accordance with the user behavioral class (L1). Like Boyce, Love and Begemann, Jennings states that lighting control is highly individual. For the investigated offices occupancy sensors yielded about 20% energy savings compared to manual switching alone. These savings were caused by intermittent vacancies throughout the day. According to Jennings, an additional saving of up to 30% total could be realized by a combination of an occupancy sensor with a properly commissioned, dimmed artificial lighting system. Obviously the effectiveness of occupancy and dimming lighting control strategies depends on the occupancy profile of the subjects. Jennings further found – again in agreement with Boyce and Begemann – that individual behavioral pattern were consistently used by individuals.

Summing up, it is important to note that despite the variety of interpretations of manual switching patterns there is an overall consensus that switching behavior is *individual but not arbitrary*. This observed consistency of individual control patterns is the basis for the development of user behavioral models which would otherwise be meaningless.

[52] This is compatible with the theory of adaptive comfort, i.e. people influence their immediate environment if ownership is perceived (see chapter 1).
[53] The solar transmittance of the windows varied from 88% for the north facade to 40% for east, west and south facades.

6.2.2. Manual Control of Blinds

Only a very limited number of studies concerning the manual operation of glare protection and shading devices has been carried out so far.

In a classical study Rubin investigated manual switching patterns in private offices with northern or southern facade orientations [rub78]. Rubin used photography analysis to collect the status of internal, manually operated venetian blinds in several office buildings at the National Bureau of Standards in Maryland, U.S.A.. The investigated offices were private or two-occupant offices. The main focus of the study was to test whether different blinds positions are the result of a conscious decision on the part of the window occupant or whether they merely represent the effect of extraneous variables like the maintenance personnel. Are there any design-related variables which influence the use of window blinds? Rubin was mainly interested in the influence of window orientation, quality of view and seasonal changes. To gain some insight into these questions Rubin first recorded the blind positions in all offices and subsequently fully closed or opened the blinds to provoke reactions from an ensemble of users. An ensemble consisted of some 700 windows. Blind positions were taken at least 4 times in the week preceding the induced blind manipulation and three times a day on 3 weekdays in the following week. Climatic conditions were approximated by attributes like *clear and sunny* or *hazy and humid*. Rubin differentiated between 5 window coverage positions and 2 slat angles, horizontal and closed. The rating of the photographs was carried out independently by two people. Rubin's results are summed up in the following:

(R1) Blind occlusion is higher in southern than in northern offices as people tend to use their blinds to block direct sunlight.
(R2) People consciously set their blinds in a certain position. As only 50 out of 700 windows were adjusted more than once after the manipulation, the blind position of choice seems to be a result of weighing positive and negative effects over a period as long as weeks or months whereas diurnal blind operations are rare.
(R3) People are more likely to accept that their blinds are extraneously opened than closed.

Rubin could not establish inter-seasonal or daily changes in how blinds are set, i.e. the recorded blind positions seemed to be independent of sky condition, season and time of day.

Rea analyzed blind positions on three facade orientations in a high-rise office building in Ottawa, Canada, on a cloudy and a sunny day [rea84]. External photos were taken in the morning at midday and in the afternoon. The study concentrated on the influence of window orientation, time of day, prevailing sky conditions and the interactions between these external variables on blind positions. 10 different blind heights were considered whereas the slat angles could not be determined due to the unfavorable angle under which the photos were taken. As a consequence, a single variable called "blind occlusion" was used to describe the average window occlusion by the blinds for a given facade orientation. The analysis revealed a strong correlation between shading status, window orientation and sky condition. Blind occlusion was positively correlated with incident irradiance even though Rea found no adjustment of blinds throughout the day. Rea's findings support Rubin's result (R1) that occupants manipulate their blinds to reduce penetration of solar radiation. Whether solar heat or daylight reduction were the driving forces for the blind manipulations could no be resolved from Rea's results. As people refrained from changing the blinds throughout the day, Rea concluded – again in agreement with Rubin (R2) – that they have a long term perception of solar irradiances. This inertia of people to react towards changing sky conditions might resemble the tendency of people to only operate their electric lighting once or twice a day upon arrival or departure.

Inoue *et al.* took photos of offices facades of four high-rises in Tokyo, Japan, to extract the manual control of venetian blinds [ino88]. Synchronously with the photos, direct and diffuse irradiances were collected. The total measurement period was one to three weeks for each high-rise and the measurement interval was one hour. All investigated office buildings were fully air-conditioned and occupancy was assumed in an office for the whole working day, if the blinds were operated at least once. This procedure excluded cases when users passively experienced their environment without feeling the need to act. The major findings of Inoue's study are:

(I1) Beyond a threshold direct solar radiation onto a facade of about 50 Wm^{-2} blind occlusion is proportional to the depth of sunlight penetration into a room. Inoue also established a quantitative correlation between the percentage of blinds closed and the amount of solar radiation incident on a facade. Both relationships are depicted in Fig. 6-3. The relation between blind operation and incident illumination on the facade is not linear but follows an arc, showing that even at times when the incoming solar irradiance decreases the number of blinds closed can still rise.

Blinds are usually not fully reopened again as irradiance decreases presumably because the visual connection to outside conditions is lost due to closed blinds.

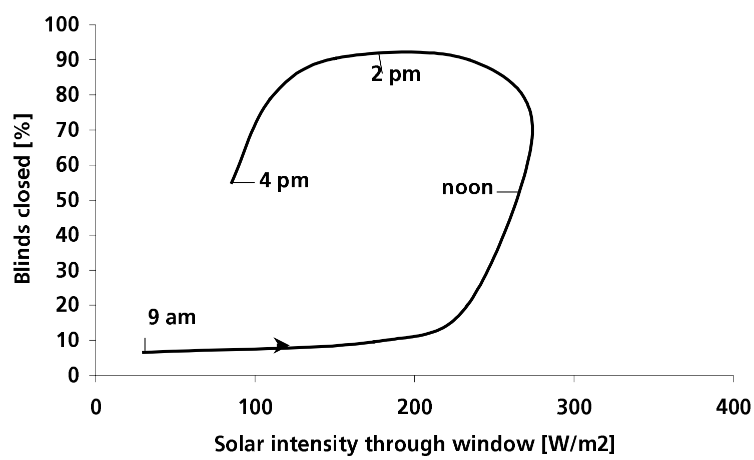

Fig.: 6-3:
(a) Relationship of vertical solar radiation in a room and the percentage of blinds closed in a SSW facing facade in Tokyo, Japan [ino88, new94].

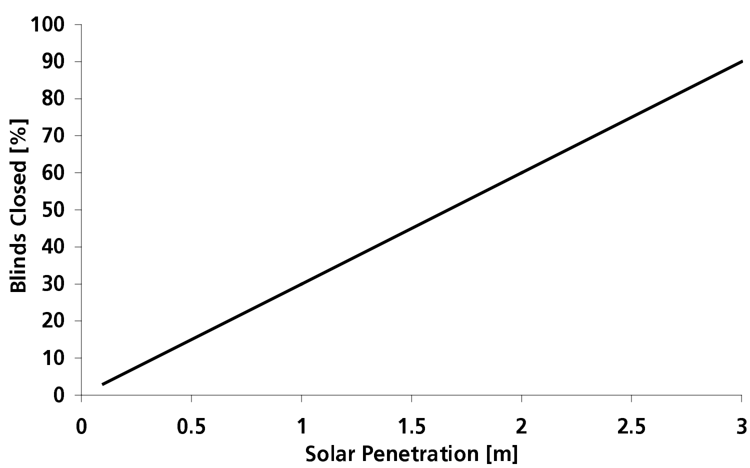

(b) Relationship of direct solar penetration in a room and the percentage of blinds closed SSW facing facade in Tokyo, Japan [ino88, new94].

Based on user questionnaires, Inoue further established that people prefer spaces near a window and that occupants only react when a situation becomes intolerable. The latter finding might explain the aforementioned tendencies of occupants in other studies to only consider long term irradiance levels while short-time-step dynamics are largely ignored.

Lindsay *et al.* investigated venetian blind use in five different office buildings in England. Both private and open plan offices were considered [lin93]. In one building, blind positions were recorded twice a day over a period of 4 months using time lapse photography. Ambient temperatures and the type of sky condition (clear/overcast) were also collected during each recording. In a second building blind positions were recorded by a video camera together with user occupancy in 2-hour-time-steps from 8 a.m. to 4 p.m.. In a third, forth and fifth study blind positions as well as direct and diffuse irradiances were collected in 1-hour-time-steps from May to September on a southern facade with 54 window, from January to June on a southwestern facade with over 100 windows and from August to November on a southern facade with 105 windows. Both blind occlusion as well as the slat angels were collected. Based on the resulting extensive data set Lindsay found that regular blind manipulation did occur in a number of investigated offices and that the individual blind manipulation rates for different windows in the same facade ranged from never (0%) to daily (100%) with an average around 40%. In agreement with Inoue's results, blinds were operated in response to the amount of sunshine and the position of the sun with respect to facade. People tended to manually lower the blinds during the days as direct sunlight penetrated onto their facade whereas they mainly retracted them at the end of the working day or early in the morning. The correlation between hours of direct sunlight onto a facade and a rising of the overall blind occlusion in the facade was significant in all buildings. On the other hand, the rate by which blind occlusion rose with direct sunlight varied by up to an order of magnitude for different buildings. The reason for this was, that the building with the weakest correlation had a continuously high average blind occlusion above 70%. As a consequence, the impact of direct sunlight was less pronounced in this building as the majority of blinds were always lowered. Lindsay speculated, that the reason for the permanently high blind occlusion was that the building tended to be overheated.

Despite this finding in a particular building, Lindsay further suggested that the general motivation for people to use blinds is to avoid glare rather than to prevent overheating. This assumption is supported by Inoue's conclusion (I1) which states that direct sunlight as low as 50 Wm^{-2}, which corresponds to relatively low solar gains, does already trigger increased blind occlusions.

Pigg also monitored blind usage in the study mentioned in 6.2.1 and found that 36% of the users never operated their blinds. His data further confirms (R1) that blind occlusion is significantly lower in northern that in southern offices [pig96]. In Pigg's survey 37% of the subjects stated that they used blinds to reduce glare on their computer screen.

Bülow-Hübe investigated preferred settings of an awning and an external venetian blind system for 50 subjects in two test offices in Lund, Sweden [bül00]. During the experiment she let the subjects adjust the shading devices and the dimmable artificial lighting while ambient sky conditions, indoor illuminances and vertical luminances were recorded. The subjects also filled out a questionnaire so that some insight into the underlying motivation could be gained. The results show that both investigated shading devices were frequently used throughout the day to control glare. The artificial lighting was operated by 30% of the subjects. Unfortunately, the data did not allow to correlate the need for shading devices to measurable factors such as illuminance or sky luminances. According to Bülow-Hübe, possible reasons for this shortcoming were too few subjects, large individual spread and insufficient measurement points. Nevertheless, she found that the existence of sunlight patches in the room tends to trigger the use of shading devices. From the survey she also concluded that individual control over a person's environment is preferred to having no control.

Vine *et al.* compared occupant response and satisfaction of 14 subjects who experienced 3 hours in a private test office under three different modes of operation of an integrated venetian blind and artificial lighting system [vin98]. The investigated interior blinds were not retractable and only the slat angle could be adjusted. Vine detected a preference of most subjects for higher illuminances than the default level of 510 lux on their work plane. He could not resolve whether these user preference could be attributed to visual or biological needs like the ones Begemann referred to in his studies. Vine's conclusion is that the investigated integrated artificial lighting and venetian blinds system exhibits a high user acceptance but that a larger user sampling and longer measurement periods are necessary for a further-going evaluation of the system.

Summing up, all above mentioned studies on blind usage seem to indicate that blinds are consciously used in offices to block direct sunlight. Glare protection seems to be the major driving force, followed by the avoidance of excessive heat gains. Accordingly, blind occlusion is generally higher in offices with southern than with northern facade orientations. Inoue and Lindsay found that the rate of blind manipulation is lower on western than on southern facades. The reason for this might be that the former are more susceptible to glare so that blinds are more prone to be lowered all the time [lin93]. In buildings which are susceptible to overheating in the summer the function of blinds as a heat barriers seems to gain importance. In such buildings the blind occlusion tends to be high throughout the day. The main discrepancy between past studies is that in some studies users operated their blinds on a daily basis whereas others readjusted their blinds once every few weeks or months.

A limitation of all past long-term field studies on blind usage is that user occupancy has not been recorded [rub78, rea84, ino88], or was not explicitly considered during the analysis of the data [lin93]. This might have partly hidden the mechanisms which trigger individuals to operate their blinds, i.e. it is never clear whether a given sky condition was really tolerated by the users or whether the investigated offices were not occupied.

6.3. Presentation of a Pilot Study

Based on the above summarized results a monitoring procedure was designed and applied to validate and possibly refine previous findings. The procedure was designed to meet the following requirements:

<u>generate complete data sets:</u> To develop a manual lighting control model, it is necessary to collect a *complete* data set – in the sense of the last paragraph of the proceeding section – which covers user occupancy, indoor illuminance levels as well as ambient climatic conditions and the status of the blinds and artificial lighting.

<u>collect long-term data:</u> several of the above mentioned studies have shown that a great number of manual control events needs to be collected if one wants to establish quantitative correlations between external stimuli and manual control events. Therefore, a long-term data collection setup was designed to collect data for several seasons.

<u>collect unbiased data:</u> a conceptual problem of evaluating user preferences or acceptances in the laboratory is that the observed subjects might exhibit exaggerated responses to a visual sensation which is not necessarily representative for behavioral patterns that are observed in the field. To avoid such problems, users have been monitored in their regular working environment. Great care was taken to install the measurement equipment in an unobtrusive way (see Appendix 6.1). The author expects that the office workers adjusted to the monitoring setup due to the long-term data collection and that the novelty aspect of being monitored vanished within due time.

<u>identify interrelations between artificial lighting and venetian blind settings:</u> While Pigg qualitatively measured that people tend to operate their blinds more regularly than their artificial lighting, the author is not aware of any study which explicitly addressed possible interrelations between the setting of the blinds and the artificial lighting. What is the status of the blinds when the lighting is activated? Do people rather adjust their blinds or their lighting?

Details of the investigated building and the experimental setup are provided in the following.

6.3.1. Building Description

Fig. 6.4 shows the investigated building, which is situated in Weilheim near Stuttgart, Germany. It has a net heated floor area of 1000 m^2. The building has been occupied since the early spring of 2000 and hosts the land surveying company *Lamparter GbR.* It consists of two rows of offices with 10 office on each side facing SSW and NNE. Only the southern offices were considered in this study. As no active air-conditioning system has been installed the offices rely on a careful management of incoming solar gains in the cooling period. Another distinct feature of the building is the high quality thermal envelope and triple window glazings with wooden frames.

The building is part of the German SolarBau:MONITOR Projects and is described in detail in [vos01]. In addition to the monitoring of user behavior which is described in this thesis, the Fachhochschule Stuttgart has carried out a thorough investigation of the energy performance of the innovative building climatisation concept.

Fig. 6-4: Photo of the monitored Lamparter building[54]. (architects: Meier-Weinbrenner-Single, Nürtingen, Germany, Photo © K. Voss)

Fig. 6-5 provides a sketch of the daylighting concept. The artificial lighting and the external venetian blinds are connected to an EIB (European Installation Bus) building control system. The artificial lighting is provided by two purely indirect dimmable luminaires, each with 2x58 W lamps. At full capacity, this system yields up to 350 lux on the work plane[55]. This comparatively low desk top illuminances are a consequence of the chosen lighting system in the offices[56] and probably contributed to the fact that the measured annual electric energy demand for lighting in 2001 was only 7.2 kW/m^{2}a [mül01]. This lighting system alone cannot accommodate the preferred desktop illuminance range from 80 lux to 800 lux which has been measured by [vei01] and needs to be complemented by daylight which is not always avaialble. As a consequence, the satisfaction of the users with the installed lighting system might be impeded[57].

While the artificial lighting system is manually switched on and off, lighting levels are automatically dimmed via a ceiling mounted illuminance sensor which is connected to a closed-loop control system. The external two-component[58] blinds system (Fig. 6-6(a)) acts as a combined heat and glare protection device and is supported by an external lightshelf which often shades the occupants from direct sunlight and redirects daylight deeper into the room. The blinds are operated both automatically and manually. Manual blind control is possible at all times, and any manual blind manipulation disables the automated blind control for 2 hours. When active, the automated control system fully lowers/retracts the blinds if the illuminance onto the SSW facade exceeds/falls below 28,000 lux. When the blinds are automatically lowered, they are moved into the *daylighting blind position* shown in Fig. 6-6 (a) which reflects most of the unwanted solar gains while admitting sufficient daylight into the room to principally allow the user to work without additional electric lighting. The electric blind motors require roughly 2.5 minutes to move the blinds from fully retracted into the daylighting position. This automated blind control algorithm has been chosen to avoid overheating in times of temporarily absence[59]. All 10 offices are private or two-occupant offices. Details are provided in Table 6-2.

[54] For further photos of the building, please refer to: http://www.solarbau.de/monitor/doku/proj07/mainproj.htm
[55] measured in March 2000
[56] The lighting power density per net floor area is only 11.6 Wm^{-2}.
[57] In the field study of the Lamparter building it was only investigated how people *cope* with their regular working environment and what behavioral patterns guide manual lighting control. No information was collected on user preferences and acceptance levels, or whether the users would have chosen higher levels if given the opportunity.
[58] *Two component* signifies that the blind slats can be adjusted independently above and below 2 m height.
[59] As no active climatisation system is available, a careful solar gains control is vital at all times.

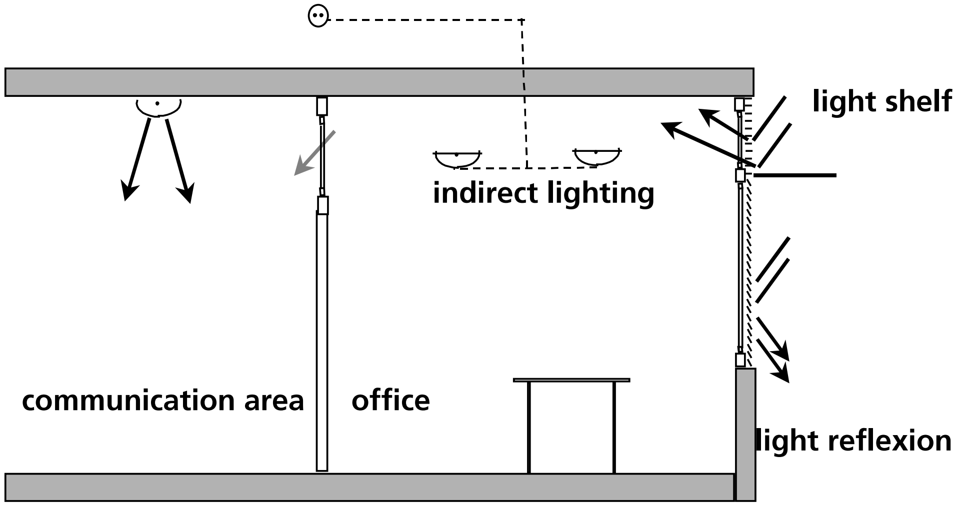

Fig. 6-5: Daylighting concept in the offices.

Table 6-2: Detail of the investigated subjects.

room	1	2	3	4	5	6	7	8	9	10
occupied by	2 female	1 female	2 male	1 male	1 male	2 female	2 male	1 male	1 female	1 male

(a) external view (b) interior view

Fig. 6-6: photos of the utilized two-component semi-automated external venetian blind system in the Lamparter building in *daylighting position* (Photos © K. Voss).

6.3.2. Experimental Setup

A number of external and internal variables as well as the shading status of the electric lighting and the venetian blinds were collected. Table 6-3 lists all physical quantities which were recorded by the monitoring setup. For the interested reader, further details are described in Appendix A.6.1.

quantity	[units]	measurement interval [min]
work place occupancy	[0/1]	15[60]
work plane illuminances	[lux]	15
indoor temperatures	[°C]	15
ambient temperature	[°C]	5
global horizontal irradiance	[W/m^2]	5
diffuse horizontal irradiance	[W/m^2]	5
vertical illuminance in facade	[lux]	5[61]
status of artificial lighting	[0/1]	5
status of external blinds[62]	[1...15]	5

Table 6-3: List of collected variables.

6.3.3. Discussion of the Procedure

This paragraph addresses several limitations of the experimental procedure:

unrepresentative building design: One might argue that the results from this procedure are not applicable to arbitrary buildings as the indoor daylight availability of the investigated building is extraordinary high. As user-friendly working environments combined with an energy conscious building design constitute the general focus of this work and as the Lamparter building exhibits no "spectacular" design features, it seemed appropriate to the author to chose a building with an innovative but cost effective daylighting concept. The selected building also proved to be a good choice as the occupants were very cooperative throughout the measurement period. Another bonus of the building was that all offices are private or two-person offices[63].

users feel intimidated by the video surveillance setup: as the status of the venetian blinds was determined via a video surveillance camera, the observed office workers might have felt intimidated by the presence of the camera. This in turn might have influenced the behavioral patterns of the office workers. The author addressed this issue during an information session which took place before the data collection started. In order to divert the occupants' attention from the behavioral aspects of the study, technical details of the experimental setup were explained to the occupants with an emphasis on the measurements of the energy flows within the building. A few sample photos of the surveillance camera were also shown to the occupants to reassure them that the photos are of insufficient quality to invade their privacy.

limited number of subjects: As only 10 offices have been monitored, the applicability of the resulting behavioral patterns is intrinsically limited. Obviously, the preliminary manual lighting control model which is proposed in chapter 8 will need to be validated in further experiments.

6.4. Summary

The development of models which describe the manual control strategies of artificial lighting and venetian blinds is still at an early stage although a number of studies have been carried out over the past two decades world-wide. These studies found that individuals consistently follow the same manual lighting control strategy. The observed control strategies for artificial lighting can be generally classified into two behavioral classes: People who constantly keep their lights switched on and people who operate their lighting with respect to indoor daylight levels. Concerning the manual control of blinds, there exists an overall consent that people consciously

[60] To get 5-minute time-steps from 15-minute averages, the average value was assigned to all three 5-minute intervals. For indoor temperature and occupancy, this straightforward procedure seemed justified to the author. The original reason for choosing different measurement intervals was the limited storage capacity of the stand-alone hobo data loggers which would otherwise have required a readout cycle of 9 days instead of a month.

[61] The illuminance data from the HOBO only served as a reference value to test weather HOBO data and the remaining data sets were synchronized.

[62] see Appendix A.7.1.

[63] In open plan office environments individual preference sometimes have to give way to hierarchical considerations [boy80].

set their blinds and tend to avoid direct sunlight. There is no general agreement on the how often blinds are usually operated. The proposed new experimental procedure aims to

- identify possible interrelations between the setting of artificial lighting and venetian blinds
- provide long-term, complete and unbiased data based on which a preliminary manual lighting control model can be developed

Table 6-4 summarizes the main findings from past studies which have been discussed in this chapter.

Table 6-4: Overview of findings from previous studies.

artificial lighting		**ref**
(H1)	all lights in a room are switched on or off simultaneously	[hun79]
(H2)	switching mainly takes place when entering or vacating a space	[hun79]
(H3,4,6)	the *switch-on probability* on arrival for artificial lighting exhibits a strong correlation with minimum daylight illuminances in the working area. People tend to switch on their lighting according to this probability function when entering in the morning and after lunch	[hun80]
(H5, B3)	people tend to turn off all lighting when the room is vacated, e.g. for lunch	[hun80, boy90]
(P1)	the length of absence from an office strongly relates with the manual switch-off probability of the artificial lighting system	[pig96]
(P2)	the presence of an occupancy sensor influences the behavioral patterns of some people. On the average, people in private offices with occupancy control are only half as likely to turn off their lights upon temporarily departure than people without sensors	[pig96]
(B1)	certain individuals dislike artificial lighting and turn it off for themselves if possible	[boy80]
(B2)	some group leaders tend to turn off the lighting if they think it appropriate for their group	[boy80]
(L1,2)	people usually pertain to either of the following two behavioral classes: They switch the lights on for the duration of the working day and keep it on even in times of temporarily absence or they use electric lighting only when indoor illuminance levels due to daylight are low	[lov98]

blinds		**ref**
(R1)	blind occlusion is higher in southern than in northern offices as people tend to use their blinds to block direct sunlight	[rub78]
(R2)	people consciously set their blinds in a certain position. The blind position of choice seems to be a result of weighing positive and negative effects over a period as long as weeks or months whereas diurnal blind operations are rare	[rub78]
(R3)	people are more susceptible to accept that their blinds are extraneously opened than closed	[rub78]
(I1)	beyond a threshold direct solar radiation onto a facade of about 50 Wm^{-2} blind occlusion is proportional to the depth of sunlight penetration into a room. The relation between blind operation and incident illumination on the facade is not linear but follows an arc, showing that even at times when the incoming solar irradiance decreases the number of blinds closed can still rise	[ino88]

Chapter 7 Results and Analysis of Monitoring Data

This chapter presents and analyzes the results of the monitoring setup which has been described in the previous chapter. Section 7.1. presents an overview of the data which has been collected from March to December 2000. In the following sections the manual control of the artificial lighting system (7.2), of the semi-automated venetian blinds system (7.3) and finally the interaction between both systems (7.4) are described and discussed (7.5).

7.1. Description of Monitoring Data

The overall experimental setup as described in Appendix A.6.1 has been collecting data from March 22nd to December 3rd 2000 corresponding to a total of 257 days. Table 7-1 lists the number of days that the four single data acquisition systems have successfully collected data.

setup	collected quantities	# of data collection days
HOBO & occupancy sensor	work place occupancy	248[64]
	work plane illuminances	
	indoor temperatures	
weather station	ambient temperature	142
	global horizontal irradiance	
	diffuse horizontal irradiance	
	vertical illuminance in facade	
EIB system	status of artificial lighting	243
video surveillance system	status of external blinds	243

Table 7-1: Overview of the collected data.

HOBO & occupancy sensor: The HOBO data acquisition system proved to run reliably. Unfortunately, the signal from the integrated illuminance sensors was of lower quality than originally expected due to the low sensor quality (rel. error of 20%) and the measurement position: the desk plane was unfavorable for long-term monitoring as occupants tended to forget the sensors –which is *per se* desirable – and placed working material on top of them. As indoor illuminances had been identified in the past to be a crucial quantity to trigger user action, dynamical daylight simulations were carried out instead based on measured direct and diffuse irradiances[65]. The monitoring data from the occupancy sensors were largely consistent with the data from the EIB system, i.e. switching events tended to lie at the extremes of a period of occupation[66].

weather station: Unfortunately, the weather station had initial problems so that data was only sporadically collected until the end of July. Afterwards it ran quite stable.

EIB system: the EIB system ran very stable throughout the whole measurement period except for a two-week-period during which the data collection was accidentally turned off.

video surveillance system: The video surveillance camera was triggered by the EIB system and worked reliably after sender and receiver were installed in a way that the transmission was not impeded by any metal parts within the building.

7.2. Manual Control of Artificial Lighting

The investigated artificial lighting system was a dimmed closed-loop system, which aimed to provide a fixed desk plane illuminance of around 400 lux. The users could only control whether the lighting system was activated or not. Fig. 7-1 shows the ratio of the accumulated times when the lighting was activated to the total times of occupancy for all 10 offices. The offices were numbered according to Fig. 7-2.

[64] One of the HOBOs was not properly re-launched after one readout. Therefore, only 221 days of data are available for this sensor.
[65] To enhance the quality of the daylight simulations, simulation results were scaled with the ratio of measured to simulated vertical illuminances onto the facade [rei01_b].
[66] During the data analysis false occupancy signals were discarded at nighttime if the artificial lighting was switched off.

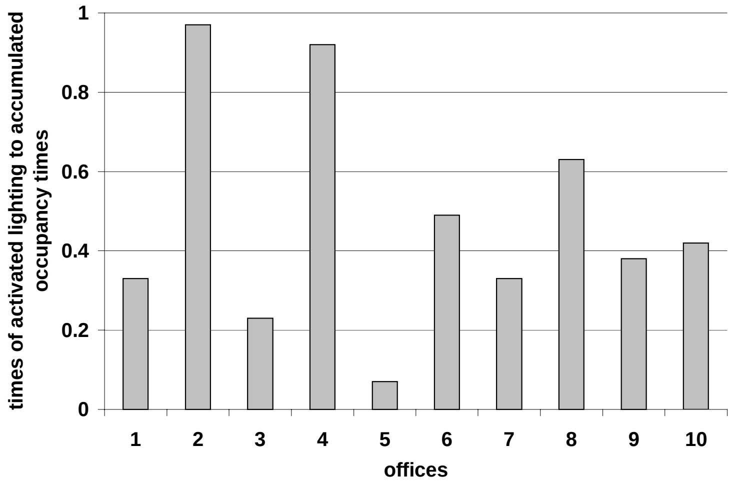

Fig. 7-1: Ratio of the times when the dimmed artificial lighting was activated to the accumulated occupancy times in the 10 offices.

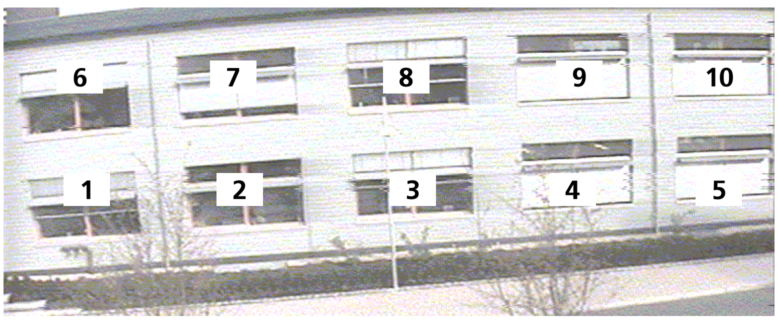

Fig. 7-2: Numbering of the 10 offices.

All ratios in Fig. 7-1 lie below unity which reveals that all the users worked at least some times without the lighting being switched on. In contrast to this, in Jennings' study only 8 out of 35 occupants in private offices had their lighting activated less often then they were at their work place, i.e. they also had to "sometimes occupy their offices without switching on overhead lights" [jen99]. Offices 2 and 4 exhibit considerably higher ratios than the other offices. These high ratios could either result from different occupancy profiles and/or different underlying behavioral patterns of the users of these offices compared to the other offices. Appendix A.8.1 shows measured *weekday occupancy probabilities* of all offices. These occupancy profiles indicate the occupancy probability at a work place for different times on a weekday. The figures reveal that offices 2 and 4 do not exhibit markedly different occupancy profiles compared to the other offices. Accordingly, Fig. 7.1 hints that the manual control strategy practiced in offices 2 and 4 differed from the ones employed in the remaining offices. These differences are further elaborated in section 7.2.1.

According to Hunt (H1), artificial lighting is mainly switched on at the beginning of a period of occupation. To verify this hypothesis, all *switch-on events* in the 10 investigated offices were grouped together into the following three classes:

<u>switch-on at arrival:</u> the lighting was switched on at the beginning of a period of occupation.

<u>intermediate switch-on</u>: after an office had been occupied for at least 15 minutes the artificial lighting was activated.

<u>no occupancy:</u> a switch-on event was detected by the EIB system but the occupancy sensor did not detect user occupancy at the work place. This situation arose either from a fault occupancy signal or if an occupant worked out of direct view from the VDT work place.

Fig. 7-3 depicts both, the relative appearance of these three switch-on events (a) as well as the cumulated times that the lighting remained switched on after these events (b). Switch-on events were only considered if the lighting was switched on or off for at least 15 minutes. The figure shows that the majority of switch-on events took place at the beginning of a period of occupation (88%) and that the pertaining lighting times accounted for 86% off all activated lighting times[67]. The remaining times mainly stem from intermediate switch-on events whereas *no occupancy* events appeared in a negligible number of cases. Accordingly, only arrival and intermediate switch-on events are further investigated in the following sections.

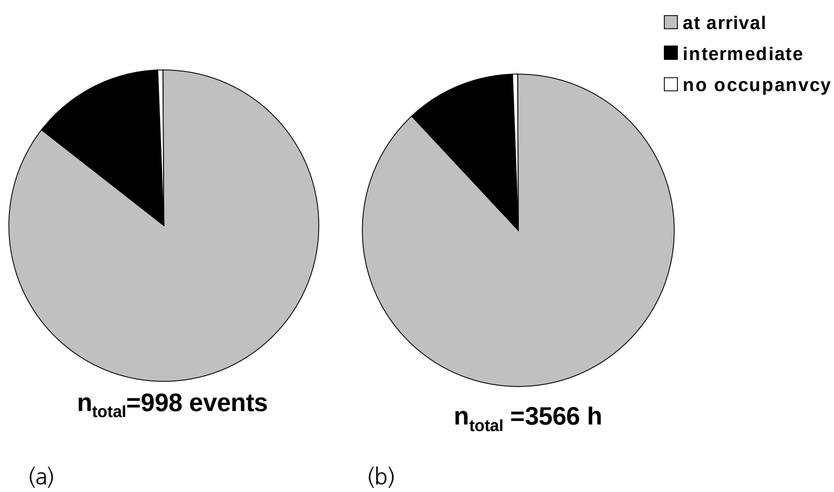

Fig. 7-3: Relative appearance of the three switch-on situations: *at arrival*, *intermediate* and *no occupancy* in all 10 offices. (a) compares the number of switch-on events while (b) compares the cumulated switch-on times following the three different event types (data from Mar 22nd to Dec 3rd 2000).

7.2.1. Switch-on upon Arrival

Fig. 7.4 shows Hunt's switch-on probability correlations with respect to minimum indoor illuminances on the desk plane for all 10 investigated offices separately. The correlations were calculated according to Hunt [hun79] as follows:

(1) an arrival event was defined as the instant following at least 20 minutes of absence and preceding more than 15 minutes of occupancy. This definition of an arrival was taken from Love [lov98].
(2) all arrivals were grouped by their pertaining minimum desk plane illuminances and bundled into groups of 30[68, 69].
(3) for each group the switch-on probability was calculated and the resulting data were fitted to Hunt's probability function (Fig. 6-1). The resulting fitting parameters for the 10 offices are listed in Table 7.1.

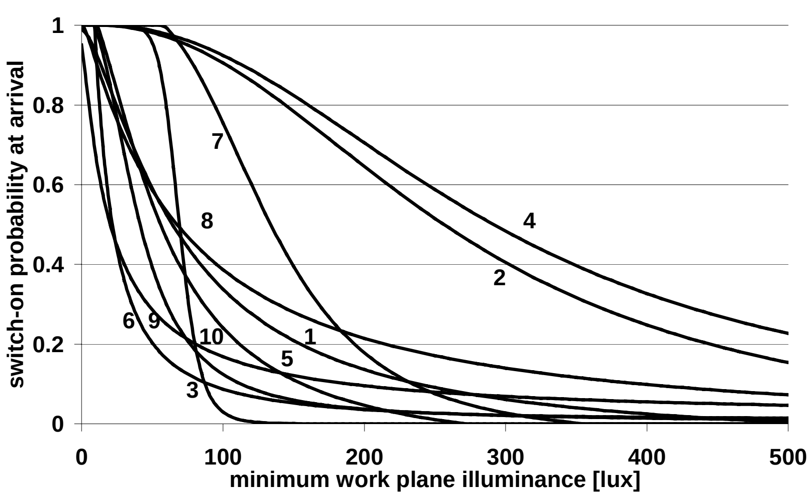

Fig. 7.4: Individual switch-on probabilities as a function of work plane illuminance in all offices (data from Mar 22nd to Dec 3rd 2000).

[67] The reason for this high proportion of arrival switch-on events is that in the afternoon when daylight levels were falling the users tended to combine the activation of the lighting with a brief absence from their work place.
[68] As motivated above, the indoor illuminance distribution in the offices was gained from dynamic daylight simulations using measured direct and diffuse irradiances. As the measurement setup could not sufficiently well resolve the position of the slat angels of the blinds only *arrival-events* were considered for which the blinds were fully retracted.
[69] Hunt grouped 9 events together but it was found that the resulting data points were smoother if 30 points were grouped together instead.

Table 7.1: Fitting parameters in the offices.

parameter	1	2	3	4	5	6	7	8	9	10
a	-0.06	-0.03	0.00	0.10	0.01	0.00	-0.01	-0.03	0.01	-0.05
b	-3.27	-5.42	-21.78	-6.72	-2.38	-3.02	-2.41	-2.50	-5.20	-6.50
c	1.05	1.04	1.00	0.90	0.98	1.88	1.01	1.05	1.02	1.15
m	1.85	2.42	1.84	2.41	1.30	1.00	1.68	1.84	1.60	1.96
median [lux]	262	369	65	410	95	38	219	277	58	112
# of data values	7	8	7	14	19	12	15	11	12	9
correlation coefficient [%]	94	98	98	92	96	97	94	95	95	92

Fig. 7.4 reveals that the switching behavior in all offices qualitatively[70] follows Hunt's correlation function even though the individual spread is enormous, ranging from a median as low as 38 lux in office 6 to 410 lux in office 4. The switching behavior which is practiced in offices 2 and 4 considerably differs from the ones in the other eight offices. While the latter control their lighting in relation to daylight levels (Love user type 2), the users in offices 2 and 4 basically always switch their lighting if indoor daylight illuminances lie below 400 lux. As 400 lux are the maximum output of the dimmed artificial lighting system, the system should ideally provide no artificial lighting above this level. Therefore, office workers 2 and 4 seem to pertain to Love's user type 1, i.e. they always switch on the artificial lighting independent of indoor daylight levels. Obviously, their switch-on behavior caused the higher lighting times which have been mentioned in the previous section.

How do the data found in this study compare to Hunt's original correlation which has been collected over two decades before in open plan offices in a different country? Fig. 7-5 compares Hunt's original function to the data for all 10 Lamparter offices. It is striking to see how similar the two curves are. The reason for this similarity is that averaging over several users smoothes out individual peculiarities. Therefore, the average switching patterns found in the two studies actually lie closer together than individual user curves in Fig. 7-4. Fig. 7-5 suggests that Hunt's original function accurately describes how a group of individuals activates their artificial lighting system upon arrival.

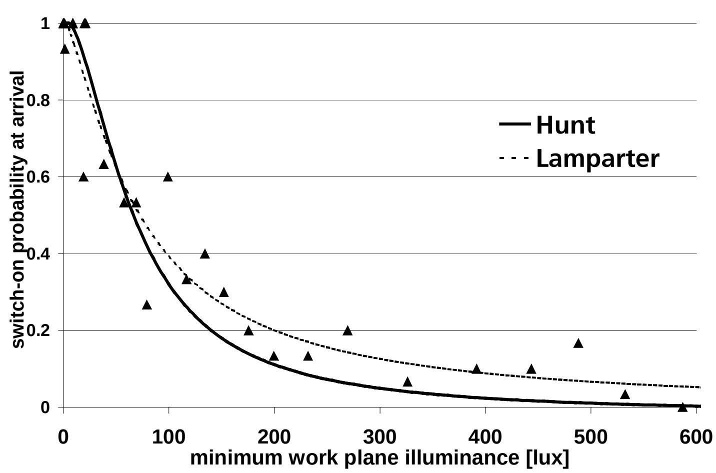

Fig. 7-5: Comparison of the switch on probabilities upon arrival found by Hunt [hun79] and in the present study (data from Mar 22nd to Dec 3rd 2000). The triangles correspond to measured switch-on probabilities.

$y= a + c/\{1+\exp[-b(x-m)]\}$

with y= switching probability
$x= \log_{10}$(min. work plane ill.)

a_{Lam}= -0.00238 a_{Hunt}= -0.0175
b_{Lam}= -3.0965 b_{Hunt}= -4.0835
c_{Lam}= 1.0157 c_{Hunt}= 1.0361
m_{Lam}=1.8536 m_{Hunt}= 1.8223
$median_{Lam}$=195 lux $median_{Hunt}$=121 lux
correlation coefficient = 97%

7.2.2. "intermediate" Switch-on

This section investigates *intermediate* switch-on events which followed a previous work place occupancy of more than 15 minutes. Fig. 7-6 shows the frequency distribution of all monitored

[70] Pearson's correlation coefficient lies above 92% for 10 offices. This is not too surprising, as the number of probability data points lies in the order of magnitude of the number of Hunt's fitting parameters. The main purpose of Fig. 7-4 and Table 7-2 is to illustrate that the spread between different users is large.

intermediate switch-on events grouped by their pertaining minimum desk top illuminances[71]. *Intermediate* switch-on events were more common at lower than at higher illuminances.

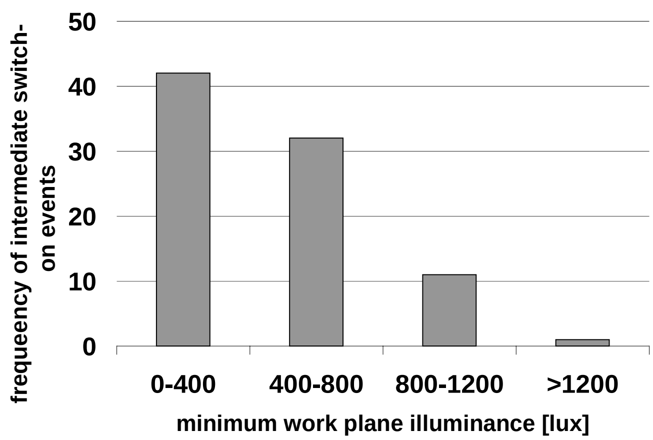

Fig. 7-6: Histogram of intermediate switch-on events ordered by their pertaining minimum indoor illuminances.

Based on this finding, an *intermediate* switch-on probability correlation function comparable to Hunt's arrival probability was calculated, following essentially the same procedure as in the proceeding section to fit the data. A difference between intermediate and arrival events is that while an arrival is a well defined point in time, an intermediate event takes place within a time period. Therefore, the time-step-intervals based on which a switch-on probability is defined can be freely chosen. In Fig. 7-7 the shortest available time-step-interval –namely 5 minutes– was used to calculate an intermediate switch-on probability correlation. I.e. every time-step at which a work place had been occupied for at least 15 minutes and the lighting was switched off was recorded as an event. As a consequence the number of considered events was a lot larger than for the arrival events and during the binning 200 instead of 30 events were grouped together to yield one probability value.

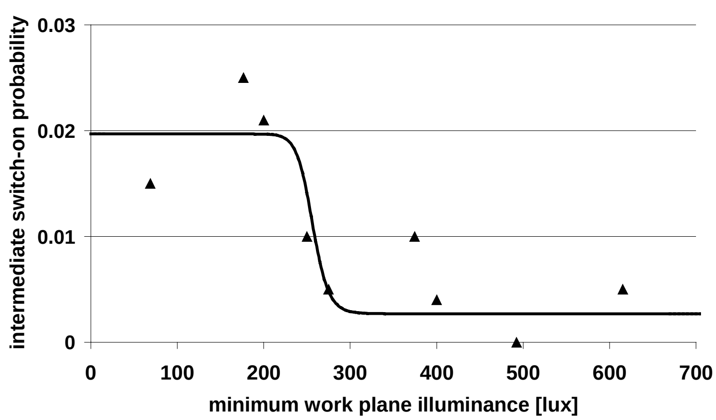

Fig. 7-7: Intermediate switch-on probability for all 10 offices based on 5-minute-time-step-intervals.

$y = a + c/\{1+\exp[-b(x-m)]\}$ for $x>0$
$y=1$ $x=0$
with y = switching probability
$x = \log_{10}$(min. work plane ill.)
$a_{intermediate} = 0.0027$
$b_{intermediate} = -64.19$
$c_{intermediate} = 0.017$
$m_{intermediate} = 2.41$
$median_{intermediate} = 241$ lux
correlation coefficient = 85%

The resulting probability function exhibits a step-like behavior. Below about 240 lux minimum desktop illuminance the probability of a switch on event lies around 2%. Above this values the probability drops to about 0.5% without further decreasing for higher illuminances. While this curve might reflect a trend, it should be remembered, that it is based on a very limited number of events. Absolute values should be treated with care.

On a qualitative level the curve suggests that intermediate switch-on behavior does not correlate as strongly with indoor illuminances as during an arrival. It is therefore probable, that parameters which have not been considered in this study – like the type of office work being performed or the alertness of the users – might be more suitable to predict intermediate switch-on events.

[71] As in the previous section only events were considered during which the blinds were fully retracted.

7.2.3. Switch-off

In this section *switch-off events* are briefly addressed. As Hunt and Pigg established a strong correlation between switch-off events and departure times, Pigg's switch off probabilities upon departure are compared to the values in the Lamparter building in Fig. 7-8. The Lamparter probabilities lie continuously below Pigg's results and a closer analysis of all switch-off events yields that only 60% took place during departure. The remaining events took place upon arrival after a temporarily absence, during user presence or even when no user occupancy was monitored.

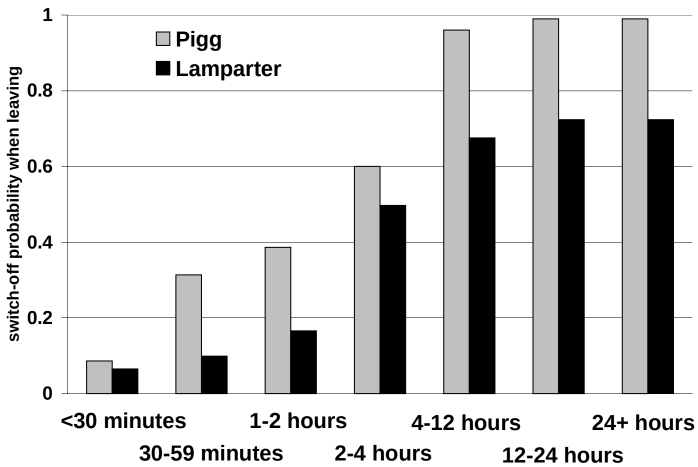

Fig. 7-8: Comparison of Pigg's switch off probabilities for different times of user absence with the results from the Lamparter building.

The low proportion of switch-off during *departure* compared to all s*witch-off events* as well as the low switch-off probabilities found in Fig. 7-8 were caused by the investigated, dimmed and purely indirect lighting system: As all artificial lighting reaches the desk plane via reflections from the ceiling, the occupants easily become unaware that the artificial lighting is activated at all. This is desirable as long as the occupant is present and daylight and artificial lighting provide an even spatial illuminance distribution. On the other hand, the occupants may sometimes fail to notice that the artificial lighting system is activated when they leave.

This undesirable situation causes unnecessary usage of electrical energy and is characteristic for a dimmed and purely indirect lighting system. It can be avoided by either coupling the lighting system with an occupancy sensor or letting it automatically switch off once the dimming levels has stayed below a threshold value for a certain time span.

7.3. Manual Control of Blinds

As explained in Appendix A.6.1.4, a picture of the investigated office facade was collected whenever the status of any of the venetian blinds in the 10 offices was changed either manually or automatically. During the subsequent analysis of the photos, the setting of the blinds was manually extracted from each picture. The position of the blind system was characterized by a set of 15 different blind positions, which are shown in Appendix 7.1. To allow a comparison of the results from this study with literature data, these 15 positions were also grouped into 4 discrete classes according to their *blind occlusion*[72].

A total of 6393 blind changes were recorded during the 174 weekdays from March 22nd to December 3rd 2000, resulting in an average of 5 blind manipulations per day and office. Fig. 7-9 shows that this high manipulation rate was mainly caused by the semi-automated blind control system as 3012 blind manipulations were carried out by the control system which were followed by 1413 *user corrections*. A manual blind manipulation was interpreted to be a

[72] The blind occlusion corresponds to the percentage of the window which is covered by the blinds. It is independent of the slat angle of the blinds [rea84].

correction of the control algorithm if carried out within 15 minutes after an automated blind readjustment. This means that over 45% of all automated blind adjustments were corrected by the users! The remaining 1973 manual blind manipulations were termed *independent blind adjustments*. Only a third of all blind manipulations can be attributed to the last category.

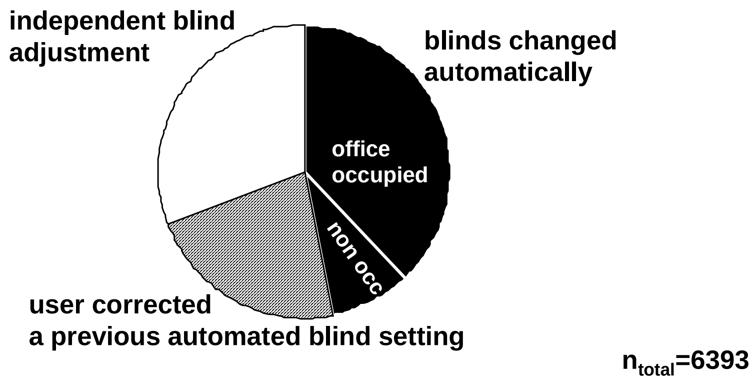

Fig. 7-9: Relative appearance of the different blind manipulation types in all 10 offices. In about two thirds of all blind manipulations the blinds were either changed automatically or the users corrected an automated previous change. Only 30% of all manipulations were independent, i.e. *not* directly triggered by the blind control system.

Whereas automated blind manipulations can be predicted based on simulated facade illuminances, manual blind manipulations depend on individual user behavior and therefore constitute the main interest of this study. Manual manipulations were grouped into four types which are listed in Table 7-2.

Table 7-2: Manual blind manipulation types.

blind manipulation type	description
corrected up	the user partly or fully retracted the blinds within 15 minutes after the blinds had been automatically lowered
corrected down	the user partly or fully lowered the blinds within 15 minutes after the blinds had been automatically retracted
independent up	the user decided to partly or fully retract the blinds without any obvious connection to the blind control system
independent down	the user decided to partly or fully lower the blinds without any obvious connection to the blind control system

A fundamental difference between independent and corrected manual manipulations is that the latter are triggered by the control system which forces a new visual and thermal comfort situation onto the user while the former arises as the user's tolerance level has been reached through natural dynamics of ambient sky conditions. The following four paragraphs analyze the appearance of the four manual manipulation types in Table 7-2.

7.3.1. corrected up

Corrected up was the most common event type and has been recorded 1263 times. Usually, the office workers tended to manually retract the blinds in the morning, after the automated blind system had automatically lowered them due to rising illuminances onto the facade. Fig. 7-10 shows the *solar penetration depth* for the 612 events for which the facade illuminance was available[73]. The solar penetration is defined as the distance from the facade that direct sunlight can penetrate into an office [ino88]. It is a very suggestive parameter as it considers the position of the sun with respect to the facade as well as the facade geometry and shading due to surrounding buildings. Fig. 7-10 shows that there was a strong tendency of the occupants of the Lamparter building to re-open the blinds at low solar penetrations. The reason for this behavior might be that the occupants preferred to maintain visual contact with the outside despite high

[73] As the weather station only temporarily collected data during the summer months, ambient daylight conditions are only available for less than 50% of all recorded manual blind manipulations.

solar gains onto the facade. This interpretation supports Lindsay's hypothesis that blind manipulation is rather triggered by visual than thermal considerations [lin93].

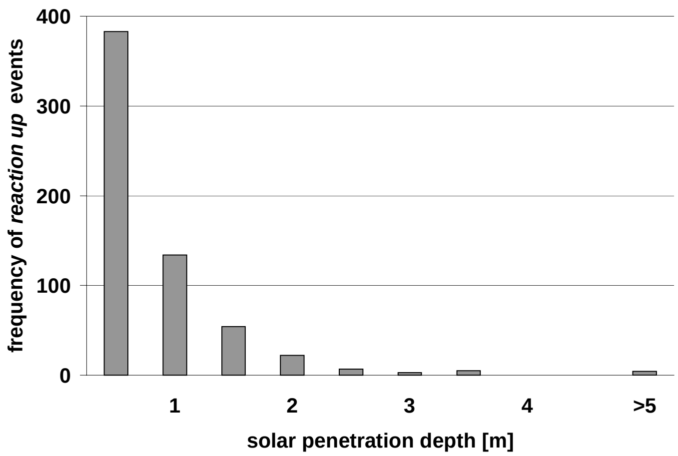

Fig. 7-10: Frequency distribution of *corrected up* events in all 10 offices for different solar penetration depths.

7.3.2. corrected down

Corrected down was the rarest manual blind manipulation type which was only recorded 169 times. The relative appearance of correction up (1263) and correction down (169) events supports Rubin's hypothesis (R3) that people are more susceptible to accept that their blinds are extraneously opened than closed. Qualitatively, *corrected-down events* tended to take place at low solar altitudes when a weak afternoon sun (Ill_{facade}<28,000 lux) caused glare.

7.3.3. independent up and down

A total of 1023 independent up and 950 independent down blind manipulations were recorded during the monitoring period. For 441 up and 370 down events ambient sky conditions were simultaneously collected. These events are analyzed in Fig. 7-11. The figure shows the frequency distribution of the solar penetration depths (a) and facade illuminances (b) for both manipulation types. While there is no remarkable difference between the distributions of the solar penetration depths, Fig. 7-11 (b) shows that blinds were closed on the average at facade illuminance of 49,000 lux and opened at 25,000 lux – a substantial difference. A possible interpretation for this behavior is that the blinds were manually opened at low ambient sky conditions to enhance the daylight availability in the work places while they tended to be closed to avoid excessive solar gains[74].

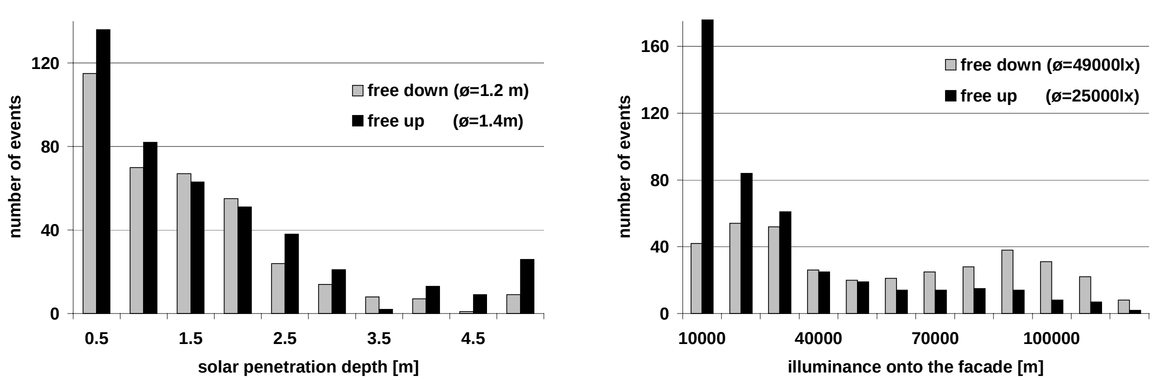

(a) (b)

Fig. 7-11: Frequency distribution of the solar penetration depths (a) and facade illuminances (b) for all independent *up* and *down* blind manipulations.

[74] This does not imply that glare was not also an issue for closing the blinds but one should bear in mind that all independent down manipulations in Fig. 7-12(b) with facade illuminances above 28,000 lux took place after a blind correction event so that the blind system was temporarily disabled.

Unfortunately, the collected data is too superficial to further confirm how representative the values from Fig. 7-13 are to describe manual blind control. One should remember, that only one building type and facade orientation were considered and that the investigated semi-automated blind control system determined the status of the blinds most of the times, i.e. a passive acceptance of automated blind changes is *not* an indicator that the office workers would have carried out the same adjustment themselves.

7.3.4. mean blind occlusion

Fig. 7-12 exploits the correlation between the solar penetration depth and the mean blind occlusion in all 10 offices for all occupied times. The dots (triangles) correspond to times when the direct solar irradiance was above (below) 50 Wm^{-2}. The data confirms Inoue's hypothesis (R1) that direct sunlight needs to lie above some 50 Wm^{-2} to cause glare and trigger people to lower their blinds.

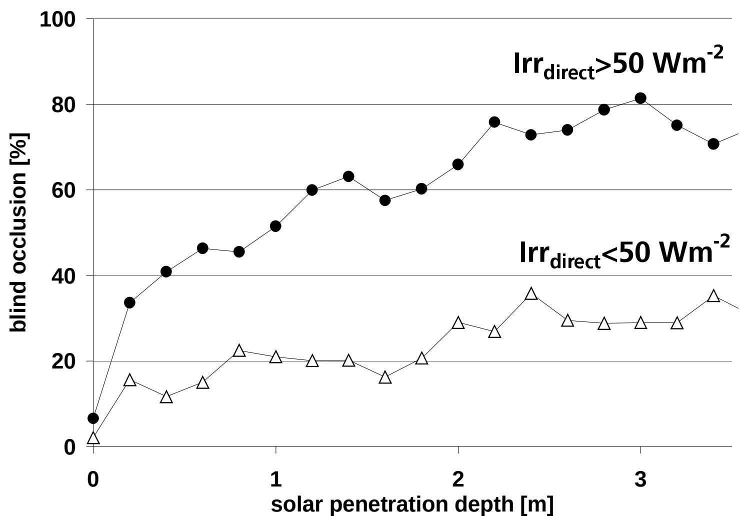

Fig. 7-12: Mean blind occlusion for different solar penetration depths for all the investigated offices for all occupied times. The dots (triangles) correspond to times with direct solar irradiances above (below) 50 Wm^{-2}.

Fig. 7-13 shows the same data as Fig. 7-12 for all the occupied times when the direct irradiance from the sun was above 50 Wm^{-2}. The solid line corresponds to Inoue's original fit of a SSW facing office facade in Tokyo, Japan, whereas the dashed line is a parabolic fit of the measured Lamparter data.

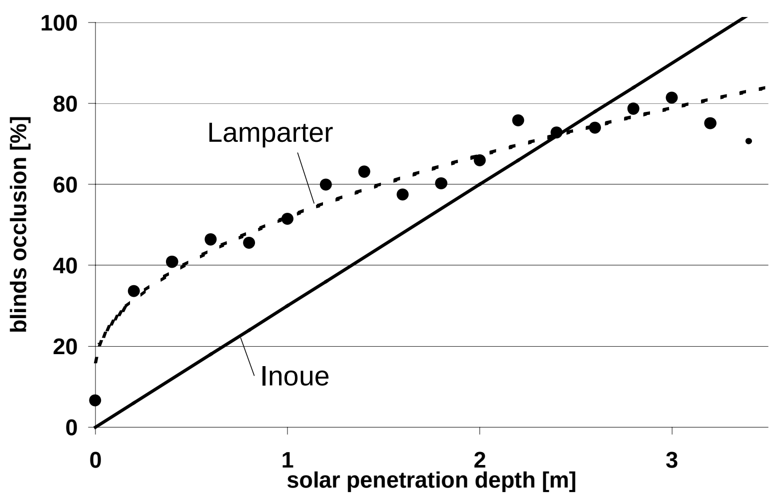

Fig. 7-13: Mean blind occlusion for different solar penetration depths for all investigated offices for the occupied times when the direct solar irradiance was above 50 Wm^{-2}. The straight line corresponds to Inoue's fit whereas the parabolic graph is fitted to the Lamparter data. The parabolic fit corresponds to $y = 15 + \sqrt{-0.116 + 1359x}$ with y= blind occlusion [%] and x= solar penetration depth [m].

The Lamparter data principally reproduces Inoue's fit which is based on high-rises in Tokyo, Japan, even though some differences exist. The main discrepancy between the two fits are found at low solar penetrations as the measured mean blind occlusion jumps from 5% for zero solar penetration depth to over 30% for very low solar penetration depths. This indicates that the blinds in the Lamparter building were usually partly closed a soon as direct sunlight hit the work place. For higher solar penetration depths the blinds were gradually further closed. This behavior is very well reproduced by the parabolic fit. A possible reason why this detail was not found by Inoue is that he had to assume that an office was continuously occupied on a day on which any blind manipulation occurred whereas the Lamparter data only considers times when the offices were really occupied. Despite this enhanced accuracy of the Lamparter data set, one cannot conclude that the parabolic fit in Fig. 7-13 is generally a better fit for the correlation between blind occlusion and solar penetration depth as the measured data may merely be a consequence of the investigated, semi-automated blind system and the investigated individuals[75].

7.3.5. indoor Temperature Distributions

The investigated blind control algorithm was originally chosen to avoid overheating in the building. Fig. 7-14 shows the cumulative temperature distributions in the 10 offices based on weekdays between 8 a.m. and 5 p.m. A cumulative temperature distribution provides the hours per considered time period that indoor temperatures lie below a certain threshold. As indoor temperatures below 26 C° are usually considered to be adequate thermal comfort conditions, the figure shows that this upper threshold was maintained in all offices throughout most of the monitoring period.

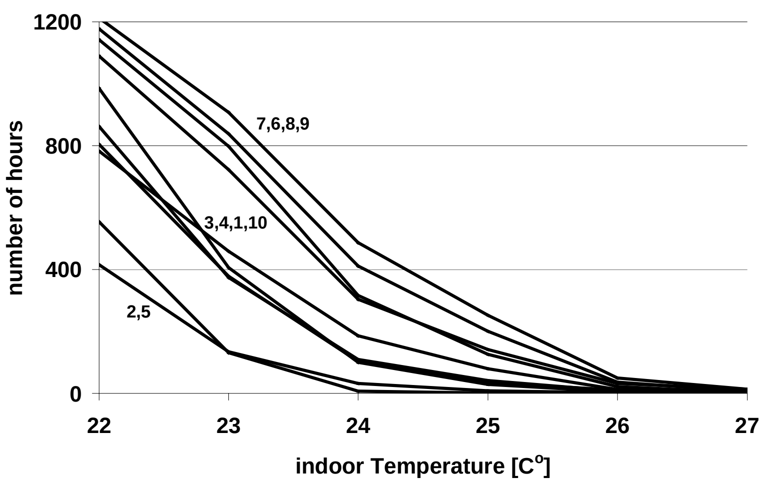

Fig. 7-14: Cumulative temperature distribution in the single offices based on weekdays from 8 a.m. to 5 p.m..

The reason for the relatively small temperature differences between individual offices is probably caused by the fact that the monitoring period did not exhibit any extended heat periods and that the automated system evened out temperature differences between the offices during user absence. Therefore, Lindsay's speculation that – while visual comfort tends to be people's immediate concern – heat management gains momentum in overheated buildings can neither be supported nor negated by the collected data.

7.4. Interaction: Blinds - Artificial Lighting

The combination of the semi-automated, 2-component venetian blind system with the external light-shelf had been originally chosen to provide the offices with glarefree daylight under a wide range of sunny and overcast sky conditions. Fig. 7-15 shows the position of the blinds for the times when the artificial lighting was activated. Three different blind positions are identified:

blinds up: these corresponds to times when the blinds were fully retracted

[75] It is possible that the high blind occlusion at low solar penetration depth found in this study were merely accepted automated blind manipulations which the users would not have carried out themselves. Another explanation of Inoue's linear fit might be that the users in the investigated high-rises in Tokyo were positioned at different distances from the facade so that the statistics "washed out" this detail.

privacy: it was considered that a user closed the blinds due to privacy concerns, if the blinds were closed while the ambient horizontal illuminance was below 1000 lux

blinds not fully retracted: all situations which did not fall under the previous two

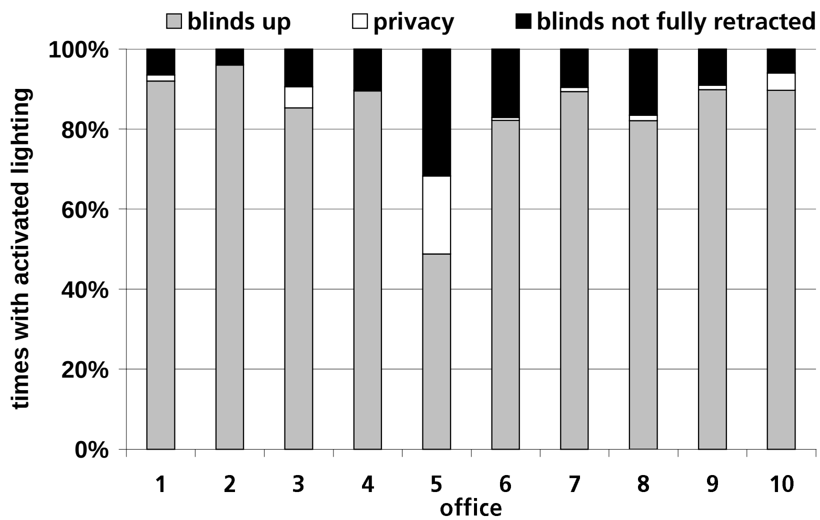

Fig. 7-15: Status of the venetian blinds during hours when the offices were occupied and the lighting was activated.

With the exception of office 5, the blinds were fully retracted in over 80% of the times when artificial lighting was switched on. This finding reveals that the utilized daylighting strategy generally succeeded at shifting artificial lighting use to the times when ambient daylight levels were low. The figure further implies that the investigated facade design often provided an adequate interior daylight distributions without the need for further artificial lighting. This convincing performance of the daylighting concept was supported by two circumstances:

(i) the investigated, artificial lighting system provided a fixed desk plane illuminance of up to 400 lux. Therefore, the users could only increase their work plane illuminance beyond this level by adjusting the blinds. With 400 lux being a rather low illuminance level, this explains why the blinds were generally the preferred device to regulate the indoor illuminance situation.

(ii) the semi-automated blind system ensured that the blinds were retracted whenever ambient daylight levels were low. As a consequence, the black columns in Fig. 7-14 result from a conscious decision of the office workers to either manually lower the blinds when ambient daylight levels were low or to activate the artificial lighting when the blinds were down. Both situations tended to take place at low solar altitudes which required the blinds to be fully closed.

7.5. Discussion and Conclusion

The analysis of the monitoring data confirmed several results from past studies on the manual control of artificial lighting and blinds:

switch-on of artificial lighting: the monitored switching patterns in the offices support Hunt's switch-on upon arrival probability function which accounted for over 80% of all monitored switch-on events. While a quantitative comparison of Hunt's function with the results from this study shows that *groups* of individuals follow very similar behavioral patterns independent of the considered office type, *individual* behavior exhibited a much wider spread. Median switch-on probabilities in identical offices actually differed by over an order of magnitude.

The collected data allowed to assign all individuals to either Love's user types (L1) or (L2). From a practitioner's point of view the frequency distribution of these two basic user types in a building is an important quantity as it determines the overall energy performance of a daylighting concept[76]. In Jennings' study only 8 out of 35 occupants worked at least sometimes with their artificial lighting turned off (L2). Pigg also quotes that the majority of people activated their lighting in over 95% of the times of occupancy and in Love's study 5 out of 6 subjects in southern offices tended to switch their lighting independent of ambient daylight levels. In contrast to the behavioral distribution found in these three studies, 80% of the investigated occupants of the Lamparter building considered ambient daylight in their artificial lighting control.

These numbers – although not conclusive yet – suggest that different building designs favor a certain behavioral response, i.e. that user behavior is polarized in different buildings towards either L1 or L2. To gain a more settled understanding of which design features might cause such behavioral trends, future research should concentrate on collecting a much larger data set from a number of office buildings.

intermediate switch-on: intermediate switch-on events accounted for roughly 20% of all switch-on events. The correlation between these events to desk plane illuminances was weaker than for arrival events so that it is probable, they were mainly triggered by quantities which have not been monitored.

switch-off events: the analysis of the switch-off events yielded that a dimmed, indirect lighting system should be coupled with either an occupancy sensor or an automated switch-off automatism at continuously low dimming levels. If neither technical improvement is implemented, the probability function from Fig. 7-8 should be used to model how people manually switch off their dimmed, indirect lighting system.

blind control: the investigated semi-automated blind control system directly accounted for over 60% of all blind manipulations. It is therefore difficult to extract from the collected data how people would operate a purely manual blind system. Rubin's findings that people consciously chose their blind positions (R2) and that they are more susceptible to accept that their blinds are extraneously opened than closed (R3) were clearly reproduced by the data. It seems that people generally dislike their blinds to be closed due to rising solar gains if solar penetration depths are low. The only circumstances under which blinds tend to be (partly) closed is to block glare from direct sunlight above 50 Wm^{-2} (I1 and R1) or to avoid substantial solar gains in the order of 50,000 lux onto the facade. This indicates that in the investigated building visual concerns were people's primarily consideration when they interfered with the blind system. This is not surprising as the blind control algorithm was mainly designed to prevent overheating.

The measured blind manipulation rate of around 5 changes per day was considerable higher than the ones observed by Rubin (R3), Rea and Lindsay but it can be largely attributed to the automated blind control system. Unfortunately, it remains unclear whether people generally manipulate their blinds on an hourly, daily or even seasonal basis.

To reduce the number of blind corrections in the investigated building it seems advisable to add a second threshold as to when the blind are automatically closed, e.g. 28,000 lux for retracting the blinds and 50,000 lux for lowering the blinds. Another improvement of the blind control algorithm might be to automatically lower the blinds into a position that maintains direct contact with the outside.

blind and artificial lighting use: in the investigated building blinds were the device of choice to change the illuminance distribution in the offices, mainly due to the fact that the artificial lighting systems was designed to function as a backup for daylighting. The facade design usually admitted sufficient daylight into the offices even when the blinds were down.

facade orientation: the results found in the Lamparter building and in the literature suggest that the mean blind occlusion in a facade correlates with the solar penetration depth. As the concept of the solar penetration depth (>50 Wm^{-2}) can be applied to eastern, southern and western facades the correlations from section 7.3.4 can be principally applied for all of these facade

[76] It is important to realize that the product of the number of users in a building with the average energy demand of a user with mean switching characteristics does not necessary equal the sum of the energy demands of all individual users.

orientations. Unfortunately, there has been no sky luminance threshold identified so far, that could be employed to predict when blinds tend to be closed in northern facades.

While most results are of a rather qualitative nature, the fact that some correlations have been monitored before in other buildings suggests that these behavioral patterns exhibit a more general validity – especially if groups of individuals are considered. These behavioral patterns form the basis of the preliminary lighting control model which is developed in the following chapter.

7.6. Summary

The analysis from the monitoring data from the Lamparter building yields that

- *groups* of people tend to activate their artificial lighting in agreement with Hunt's probability function although there is an immense spread between individual control levels
- different buildings seem to favor different behavioral patterns
- people consciously manipulate their blinds. They tend to avoid direct sunlight above $50Wm^{-2}$ and incoming solar gains above 50,000lux and rather accept that their blinds are automatically opened than closed
- unfortunately, it remains unclear how regular people would interact with a purely manually operated blind system.

Chapter 8 Development of a Manual Lighting Control Model

In this chapter a manual lighting control model termed *LIGHTSWITCH 2001* is proposed. Model inputs are user occupancy, indoor daylight illuminances and user-dependant *switching probabilities*. The basic approach of the model is as follows: In section 8.1 an existing stochastic model from Newsham [new95] to describe user occupancy in offices is validated and refined based on measured occupancy profiles. The resulting occupancy model is combined with dynamic daylight simulations and several behavioral patterns to determine artificial lighting use in offices. An example application of the model is presented in section 8.3 followed by a discussion of the model's validity and limitations in section 8.4.

8.1. Modeling User Occupancy

User occupancy at the work place is an important and independent input variable which uniquely defines the times when *manual lighting control* – i.e. blinds or artificial lighting manipulation – can take place. As this chapter aims to present a manual lighting control model, a stochastic occupancy model is developed which is based on an existing model by Newsham *et al.* [new95]. The original model in described in 8.1.1 and some technical modifications are explained in 8.1.2.

8.1.1. LIGHTSWITCH

Newsham's original stochastic model to predict user occupancy profiles at the work place was termed LIGHTSWITCH [95new]. In LIGHTSWITCH, the day is divided into discrete 5-minute-intervals and for each time-step one or two random numbers are generated and coupled with either one of the following probability functions:

arrival: this probability function applies before the user has arrived at work. If the random number which is generated for a given time-step lies above the arrival probability of the time-step (Fig. 8-1(a)), then the user "arrives".

departure: once the user has arrived, the first random number of each time step determines whether the user "leaves" for the day or not. If the first random number lies above the departure probability of the time-step (Fig. 8-1(b)), the user "leaves".

temporary absence: if the user does not leave for the day, the second random number determines whether the occupant has temporarily left the work place. Either of the two probability functions in Fig. 8-1(c) applies depending on whether the occupant is already absent or not. The peak of the two probability functions at noon corresponds to lunch break.

The arrival probability function in Fig. 8-1 was determined from the observed data from 240 employees in an office building whose network logon had been recorded for 18 days whereas the temporary absence functions stem from personal visits at a second site. All functions were chosen to reproduce behavior typical of real buildings.

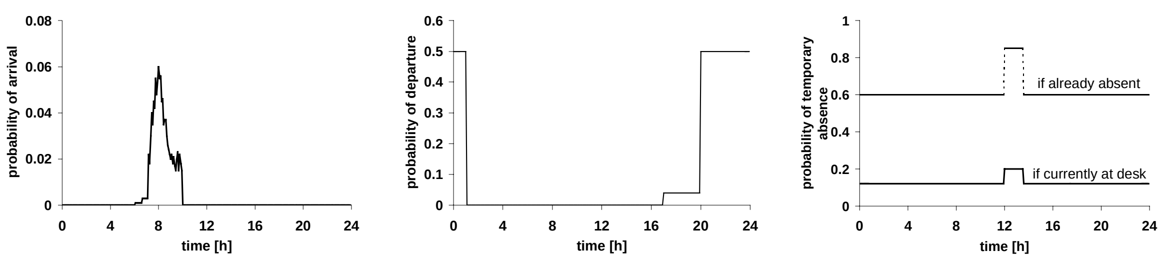

(a) (b) (c)

Fig. 8-1: Newsham's probability profiles for arrival (a), departure (b) and temporary absence (c).

8.1.2. Model Modifications

An initial attempt was to use the original LIGHTSWITCH model to reproduce the measured occupancy profiles in the Lamparter building. For each office the arrival and departure times were determined for all monitored weekdays. The resulting arrival frequency profiles were normalized by the number of investigated weekdays whereas the departure profiles were normalized to unity[77]. Temporary absence probabilities were calculated by considering the

[77] An arrival probability function which is normalized to a value below unity reflects the fact that on some weekdays office workers do not arrive at their work place for various reasons. On the other hand, the departure probability needs to be normalized to unity as any arrival is necessarily followed by a departure.

probability that a person would leave or stay absent at a particular time of day based on all monitored weekdays. The resulting simulated occupancy profiles did not satisfyingly match the monitored occupancy data for two reasons:

(1) *the distribution of simulated arrival and departure times did not resemble the measured times.* The reason for this is that carrying out a random process for each time-step explicitly yields too low probabilities if the arrival probability, which has been described above, is used. This is elaborated in the following gray box.

Consider a 12-day measurement period during which the occupant arrives at a different 5-minute time slots between 7 and 8 a.m. each day. The resulting arrival probability function is a constant 1/12th from 7 to 8 a.m. and zero for all other times, i.e. the probability that the occupant arrives at 6.30 (sixth time-step) is 1/12th.

According to the original LIGHTSWITCH model a random process is carried out for each times step individually and the probability that the occupant arrives at 6.30 equals the product of five single events where the occupant does not arrive (probability =11/12th) and 1 event when the occupant does arrive (probability=1/12th):

$$\underbrace{\left(\frac{11}{12}\right)}_{7^{00}} \bullet \underbrace{\left(\frac{11}{12}\right)}_{7^{05}} \bullet \underbrace{\left(\frac{11}{12}\right)}_{7^{10}} \bullet \underbrace{\left(\frac{11}{12}\right)}_{7^{15}} \bullet \underbrace{\left(\frac{11}{12}\right)}_{7^{20}} \bullet \underbrace{\left(\frac{11}{12}\right)}_{7^{25}} \bullet \underbrace{\left(\frac{1}{12}\right)}_{7^{30}} \cong 0.64 \bullet \left(\frac{1}{12}\right) < \left(\frac{1}{12}\right)$$

equ. 8-1

To avoid such probability inconsistencies the probability functions from Fig. 8-1 are transformed into cumulated probability functions.

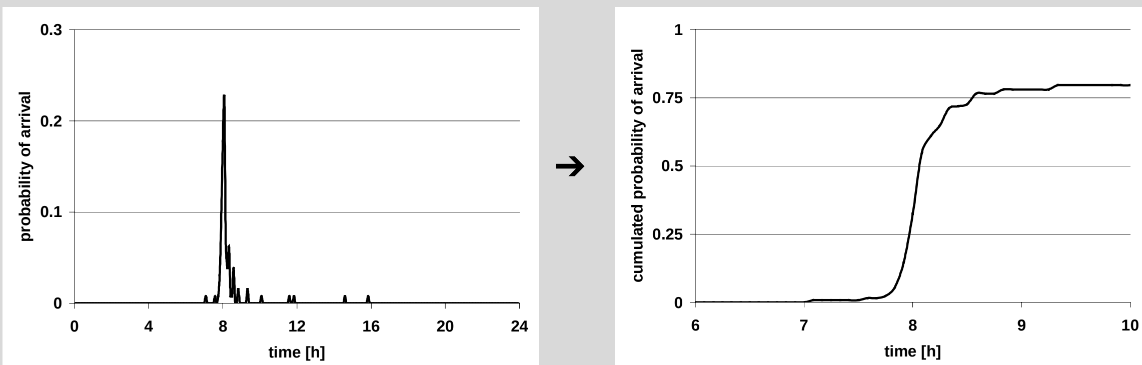

To get the arrival time for a given weekday, a single random number [0,1] is generated. In the following example the random number picked is 0.55 which corresponds to an arrival time of 8.10 a.m.[78].

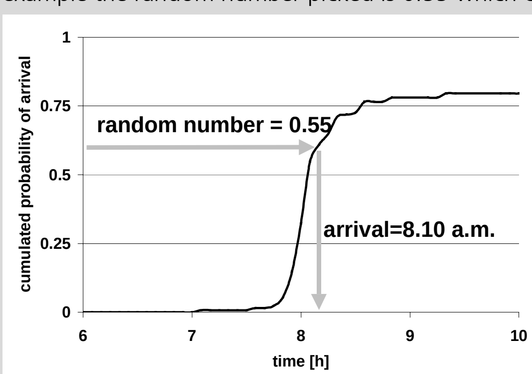

Similarly, the departure, as well as start and length of the temporarily absences throughout the day are picked through consecutive random processes.

(2) *the temporary absence probabilities form the original model failed to reproduce the absence peak at lunch time*. To correctly account for these temporary absences each weekday is instead divided into three phases: morning, lunch and afternoon. For each phase the starting times and lengths of all monitored absences are recorded and transformed into probability functions. Fig. 8-2 shows example probability functions for morning, lunch and evening starting times (a) and break lengths (b) for office 4. Fig. 8-2(b) shows that the average

[78] If the random number were above 0.8, the occupant would stay absent that day.

morning and afternoon break in office 4 usually lasted between 30 and 50 minutes whereas lunch lasted between 60 and 90 minutes.

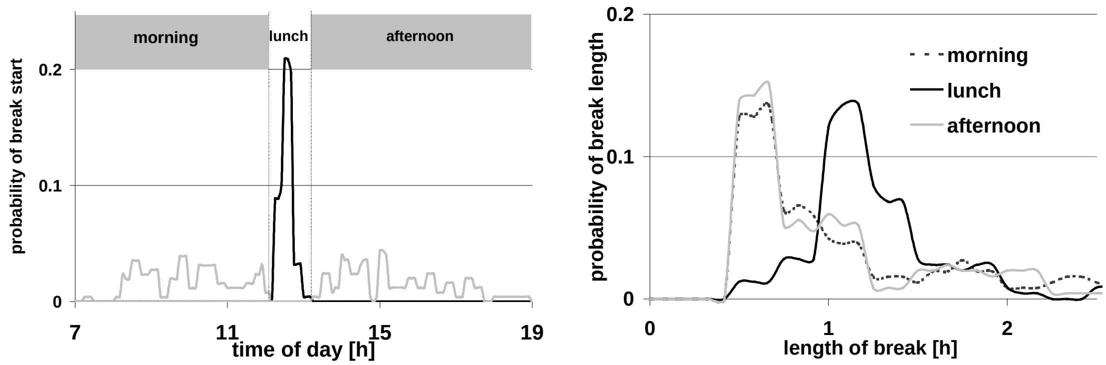

(a) (b)

Fig. 8-2: Probability functions for the Lamparter office 4 for morning, lunch and evening starting times (a) and lengths (b).

In Fig. 8-3 the resulting simulated *relative occupancy probability on a weekday* from the modified LIGHTSWITCH occupancy model is compared to the measured relative occupancy profile in office 4 of the Lamparter building. The relative occupancy probability corresponds to the probability that a workplace is occupied at a certain time between Monday to Friday. The figure shows that the simulated occupancy profile satisfyingly reproduces the individual occupancy profile in the considered office. A Kolmogorof-Smirnof test of the measured and simulated data yields a P-value of 35%. In Appendix A.8.1. the results are shown for the remaining 9 offices. The modified LIGHTSWITCH occupancy model will be used in the following as an input for the *preliminary manual lighting control algorithm*.

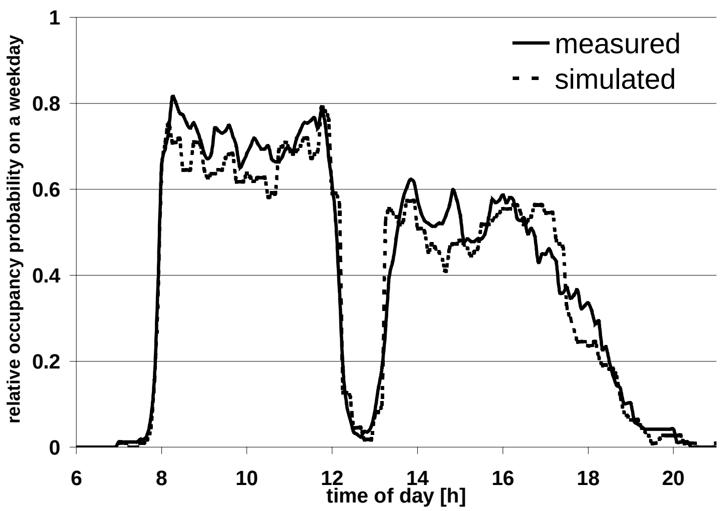

Fig. 8-3: Measured and simulated relative occupancy probabilities on a weekday for office 4 in the Lamparter building.

8.2. "LIGHTSWITCH 2001" – a preliminary Manual Lighting Control Model

In this section a preliminary *lighting control model* is proposed which determines the electric energy demand for artificial lighting based on simulated user occupancy profiles, simulated indoor illuminance distribution profiles and several behavioral patterns which have been discussed in the previous two chapters. The basic approach of the model is depicted in Fig. 8-4.

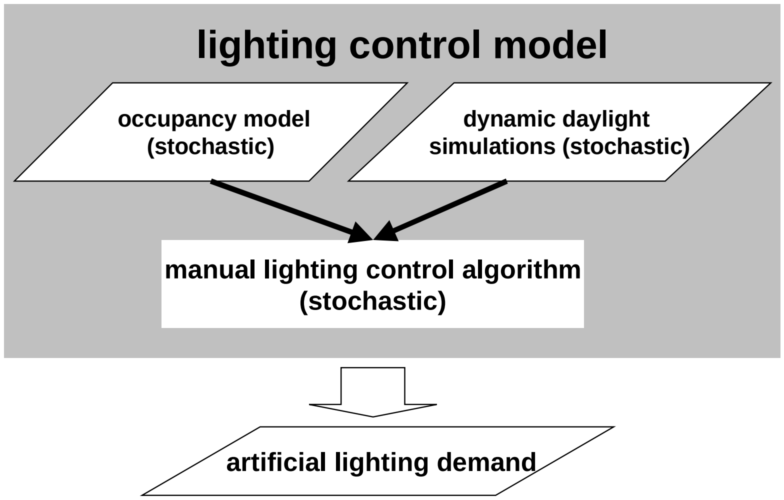

Fig. 8-4: Basic approach of the *LIGHTSWITCH 2001* manual lighting control model.

The new model is called *LIGHTSWITCH 2001* to reflect that it has been developed in the same spirit as Newsham's original model, i.e. to predict artificial lighting use in private offices based on probabilistic behavioral patterns which have been observed in actual office buildings. The manual lighting control algorithm is still "preliminary" as it will be refined in the future as behavioral research on manual lighting control advances.

The decisive innovation of the manual lighting control algorithm over former models is that each manual switching decision has a probability function assigned to it and a random process decides whether a switching event takes place or not. Opposed to that, Hunt proposed a model to predict artificial lighting use in an office in which the artificial lighting was switched on as soon as indoor illuminances fell below a static threshold [hun80]. Similarly, in an integrated artificial lighting and blind model by Newsham [new94] 150 lux were the static threshold below which the lighting was always switched on. Newsham also introduced a second static level of 233 W/m^2 facade irradiance above which the blinds were closed for the remaining of the day if the simulated work space was subject to direct sunlight.

In Fig. 8-5 the complete LIGHTSWITCH 2001 manual lighting control algorithm is presented. As explained above, it requires 5-minute data of user occupancy and minimum desk plane illuminances as inputs. At each time-step the outcome of the loop in Fig. 8-5 determines whether the artificial lighting status changes or not. The occupancy profile determines which switching decision applies. Afterwards a random process is carried out which determines whether the switching decision is followed by a switching event. Presently three switching decisions are implemented:

(1) individual switch-on probabilities upon arrival (Fig. 7-4)
(2) the intermediate switch-on probability from the Lamparter data (Fig. 7-7)
(3) switch-off probability with and without an occupancy sensor (Fig. 6-2) or a dimmable lighting system (Fig. 7-8)

While the latter two probability functions are only available for a group of users, individual values are available for the switch-on probability upon arrival. These individual functions are an additional model input to characterize user behavior. The model yields electric energy demands for artificial lighting for a purely manually operated lighting system as well as automated systems that feature an occupancy sensor and/or dimmed lighting. An exemplary application of the model is presented in section 8.3.

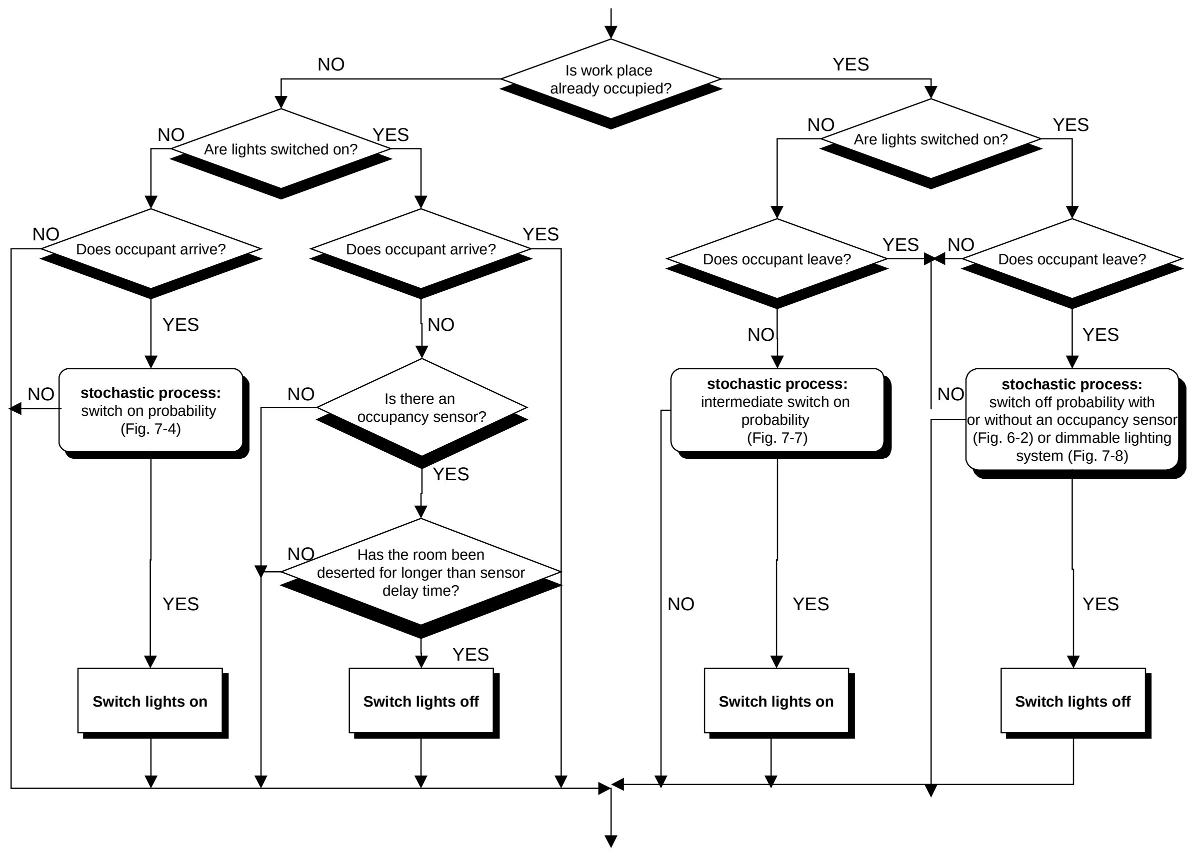

Fig. 8-5: The LIGHTSWITCH 2001 manual lighting control algorithm for artificial lighting.

The LIGHTSWITCH 2001 model as presented in Fig. 8-5 does not explicitly consider the status of the blinds and assumes that the artificial lighting is only activated when the blinds are fully retracted. The reason for this oversimplification is that presently no probability functions comparable to the ones for artificial lighting are available for blinds. It is also still unclear how regularly people manually operate their blinds. Despite these unresolved issues an extended manual lighting control model is proposed in 8.2.1 that incorporates blind usage.

The scenario that a user returns to the workplace after a temporarily absence and switches off the lighting is also not covered by the model in its present stage due to scarcity of supporting data from the Lamparter setup.

8.2.1. Incorporating Blind Usage

In Fig. 8-6 an extended version of LIGHTSWITCH 2001 is suggested which incorporates blinds. Changes with respect to Fig. 8-5 are colored in gray. The extensions shown in Fig. 8-7 based on the following assumptions:

close blinds: people avoid direct sunlight above 50 Wm^{-2}. Therefore, the blinds are completely closed whenever direct sunlight of sufficient intensity hits an occupied work place.

open blinds: even though section 7.4 suggests that the observed subjects in the Lamparter building usually preferred to retract their blinds rather than switching on their artificial lighting, there is no evidence that they would also have manually retracted their blinds in the absence of the automated system. A strong argument from Newsham[79] against such behavior is that people have no visual contact with the environment if the blinds are fully closed. Therefore, they are not aware whether direct sunlight would still disturb them at a latter point in time during the day. This hypothesis is backed by Lindsay who found that people tend to retract their blinds at departure or in the morning upon arrival [lin93]. Inoue also found that even though some

[79] private communication

users in his study retracted their blinds in the afternoon (in Fig. 6-3 the blind occlusion falls from 90% to 62% between 2 p.m. and 4 p.m.) the majority retracted their blinds in the morning upon arrival (blind occlusion falls from 60% to 10%). Based on these findings the extended LIGHTSWITCH 2001 model proposes that the blinds are only retracted once a day in the morning upon arrival.

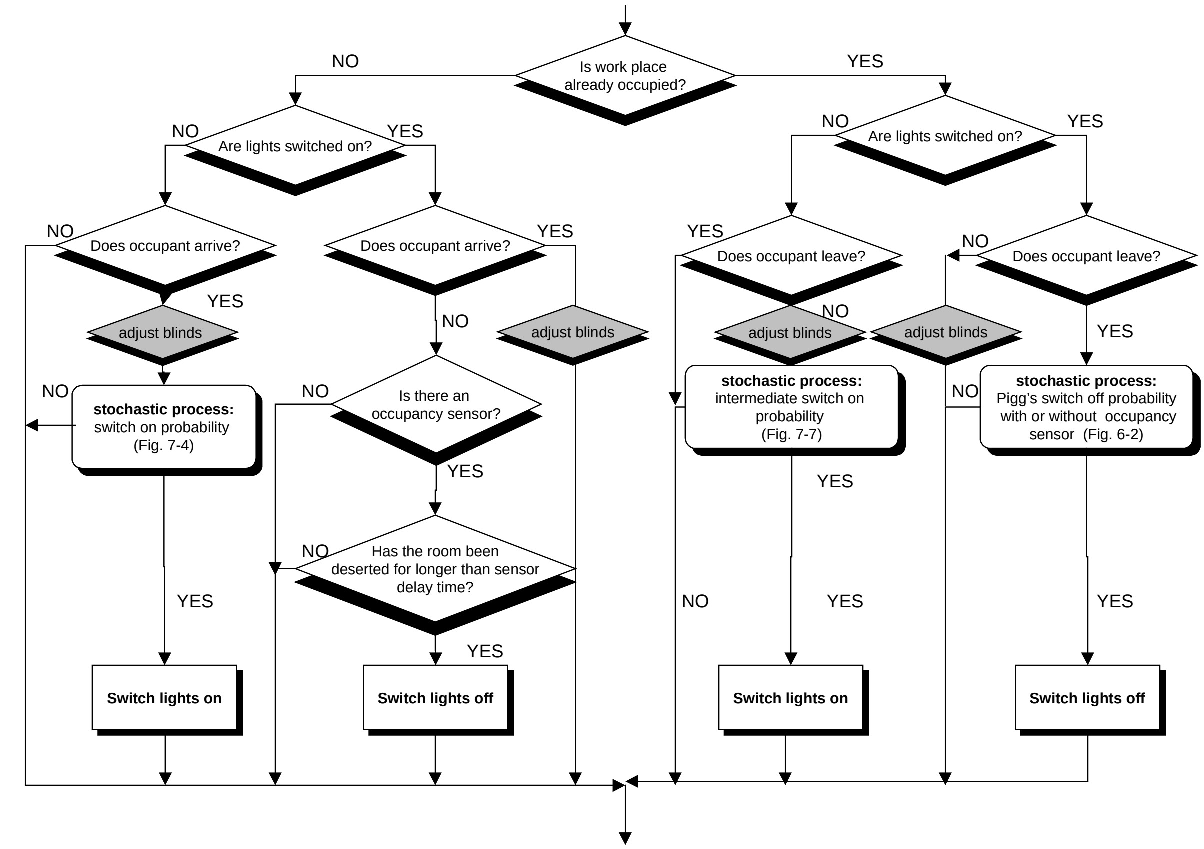

Fig. 8-6: integrated manual lighting control algorithm for blinds and artificial lighting.

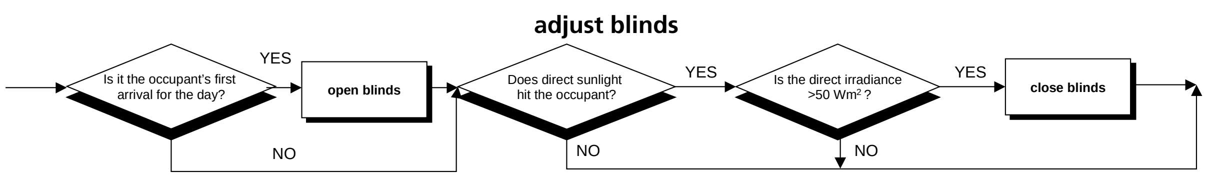

Fig. 8-7: The control algorithms for manual blind control which are implemented in Fig. 8-6.

While the first assumption is well established, the assumption that people retract their blinds once a day in the morning upon arrival is an obvious oversimplification of reality and still lacks supporting field data. The literature is undecided on this issue and actual user behavior is probably highly individual and strongly depends on the overall building design and the utilized solar shading device. An innovative shading device with semi-perforated blinds allows a user to maintain visual contact with the outside even when lowered. As consequence the user can principally always judge the exterior sky conditions and might operate the blinds more than twice a day. On the other hand, Rubin reported that blinds were often not used in single offices for weeks and months. There is an obvious need for further field data to resolve this issue.

The extended LIGHTSWITCH 2001 model also presently ignores any thermally driven mechanisms which might further trigger a closing of the blinds to avoid overheating.

8.3. Example Application of the Model

Fig. 8-8 presents LIGHTSWITCH 2001 simulation results of the annual electric energy demand for artificial lighting in an office with a southern facade. The geometry of the office corresponds to the test office in Fig. 4-1 and the simulated work place is situated at 2m distance from the facade. Indoor illuminances were simulated from measured 5-minute direct and diffuse irradiances from Freiburg, Germany, from 1998. The occupancy profile of the single occupant corresponds to the characteristics of the occupant of office 4 in the Lamparter building (Fig. 8-3). The installed electric power in the office for artificial lighting is 10 Wm^{-2} and four different lighting systems are considered:

- manual: a purely manual lighting system with a single on/off switch
- occ. sensor: the same system as *manual* with an occupancy sensor with a switch-off delay time of 20 minutes. The simulated occupancy sensor requires an extra installed power of 0.1 W/m^2 and is only activated when the lights are switched on. It switches the electric lighting and itself off when the room is vacated for more than 20 minutes. Switching on is always manual[80].
- dimmed: the same system as *manual* with an ideally dimmed lighting system that provides a stable 500 lux on the work plane if ambient daylight levels are low. At a dimming-level of zero, the electric power demand of the lighting system corresponds to 10% of its full capacity. According to the Swiss SIA Norm 380/4 [SIA95], around 2.5 W/m^2 of the installed power in the considered office would usually stem from the electronic ballast of the dimmable lighting system. This means that the energy savings due to dimming do only effect the remaining 7.5 W/m^2 of the lighting system.
- occ. sensor & dimmed: the same system as manual with an occupancy sensor with a switch-off delay time of 20 minutes and an ideally dimmed lighting system that provides a stable 500 lux on the work plane if ambient daylight levels are too low.

The energy performance of these four lighting scenarios has been calculated for three different individual switching characteristics:

- User type L2 with the individual switch-on probability of office 6[81] (Table 7.1)
- User type L2 with the individual switch-on probability of office 4 (Table 7.1)
- User type L1, i.e. a user that always switches on the lighting upon arrival.

The resulting twelve electric energy demands in Fig. 8-8 are based on 1000 realizations of the stochastic manual lighting control model and the error bars correspond to the standard deviation from these 1000 realizations. The required simulation time for all 12,000 annual simulations was about 32 minutes[82] on a Pentium Pro 450 MHz Linux Workstation.

---

[80] It is worthwhile to mention that if the considered occupancy sensor were permanently activated, it would have an annual standby energy demand of $0.1W/m^2*8760h=0.9\ kWh/m^2a$. This additional electric energy demand would significantly reduce the actually energy savings of the sensor, especially if the office is occupied by a type L1 user.

[81] Office 4 (6) were chosen because they correspond to occupants which switch their lighting on at relatively high (low) minimum desk plane illuminances compares to the other occupants in the Lamparter building.

[82] Not including the calculation times for the input annual daylight simulation.

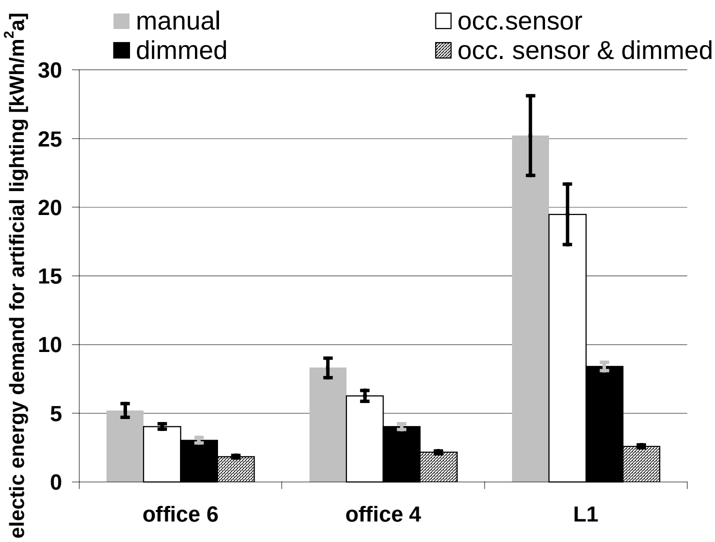

Fig. 8-8: Predictions of the annual electric energy demand for artificial lighting in an example office with a southern facade for a work place at 2m distance from the facade. 4 different lighting systems (manual, occ. sensor, dimmed and occ. sensor & dimmed) and 3 different individual switching patterns (office 6, office 4 and L1) are shown. The errors bars correspond to the standard deviation from 1000 individual annual simulations.

Fig. 8-8 provides a range of information that can help a designer to choose an adequate lighting system for the investigated work place.

The main differences between the predicted electric energy demands are caused by the underlying switching patterns: an occupant of Love's user type 1 requires 3 to 5 times more artificial lighting than a person that activates the artificial lighting only when daylight levels are low – even if both subjects work in identical offices and have identical occupancy schedules! The resulting annual energy savings range from 1 to 6 kWh/m^{2}a for an occupancy sensor and from 2 to 17 kWh/m^{2}a for the ideally dimmed lighting system. The reason for the enormous energy savings of a dimmed lighting system for user type L1 is the high daylight availability at the investigated work place. The real challenge for the lighting designer of this office would actually be to provide a glare protection device, that admits sufficient glarefree daylight into the office when ambient daylight levels are high.

Fig. 8-8 further reveals that from an energy savings point of view a dimmed lighting control system would be the system of choice in the investigated offices as it reduces the energy demand by between 42% and 62% and the resulting energy demand would lie below 9 kWh/m^{2}a *independent* of the underlying behavioral pattern. The latter information is useful if the cooling loads have to be kept low.

A cost benefit analysis of an automated compared to a manual lighting system yields that payback time crucially depends of the behavioral pattern of the occupant. Actual energy savings of a dimmed compared to a manual lighting system vary from 2 and 17 kWh/m^{2}a. For such an application, a practical approach would be to assume that in a building with many identical offices, user type L1 and L2 appear to equal parts. Unfortunately, this approach is not supported by the existing field data which – although scarce – suggests that the distribution of behavioral pattern is polarized in different buildings (see chapter 7).

8.4. Discussion

The preliminary lighting control model LIGHTSWITCH 2001 which has been proposed in section 8.2 combines several stochastic methods to yield more reliable predictions of the electric energy demand of manually operated lighting systems. Its main strengths are that it

- considers the short-time-step dynamics of natural daylight
- uses an advanced and validated RADIANCE-based daylight simulation method,
- features a dynamic user occupancy model which is able to model temporarily absence form the work place throughout the working day
- is based on established behavioral switching patterns which have been observed in the field

- has been implemented in a c-program that can be easily coupled with existing building simulations programs

The example application in section 8.3 has shown that the model provides a reference case of a manually operated lighting system against which more realistic estimates of the energy saving potential and hence the cost effectiveness of an automated shading or artificial lighting strategies can be tested. The model yields how stable a daylighting concept in a particular building is towards different behavioral user patterns. The resulting information on the kind of interaction of the building occupants with a lighting system can help a designer to decide what type of lighting system meets his or her expectations for a particular building.

As mentioned in the previous chapter, a limitation of any lighting control model which is based on behavioral patterns is that it cannot provide information on how satisfied different users would be with a given lighting concept in a building. Another limitation is that there is no conclusive data available to predict the frequency distribution of different behavioral switching patterns in a building to get its overall energy performance. Even though the model is based on scientifically sound methods and established behavioral patterns, future validations of the model in various office buildings will be necessary to ensure its quality. This is especially true for the extended LIGHTSWITCH 2001 model which includes blind usage.

8.5. Summary

A manual lighting control model has been proposed that couples dynamic daylight simulations with a stochastic occupancy model in order to predict the electric energy demands for artificial lighting at a work place for various behavioral patterns. The application of the model in an example southern office showed that

- the predicted energy savings for a dimmed lighting system ranged from 2 to 17 kWh/m^2a depending on the underlying behavioral pattern of the occupant
- a dimmed system could reduce the electric energy demand for lighting in the investigated single office below 9 kWh/m^2a independent of the underlying behavioral pattern of the occupant.

Chapter 9 Conclusion

In this chapter the hypothesises from section 1.5 are discussed on the basis of the findings of this work. The outlook identifies future work.

9.1. Feasibility

In part A of this thesis it has been shown that RADIANCE-based dynamic daylight simulation methods like DAYSIM are capable of simulating daylight autonomies with an accuracy as low as 2 percentage points for a rectangular office with an external venetian blind system. Concerning the required calculation times and accuracies, DAYSIM outperforms the other investigated methods. In combination with the statistical model which has been presented in chapter 5 the short-time-step dynamics of indoor illuminances were modeled based on widely available hourly mean direct and diffuse solar irradiances for five sites on earth. These findings reveal that

> the dynamic RADIANCE-based daylight simulation method which has been developed in this thesis is capable of efficiently generating accurate short-time-step indoor illluminance profiles due to daylight for a range of climatic boundary conditions, building geometries and daylighting elements.

The analysis from the field study in chapter 7 yielded that all subjects consistently followed one of Love's two behavioral patterns, i.e. they operated their artificial lighting in relation to ambient daylight levels or not. Within the former class, people switched on their lighting according to Hunt's probability correlation pattern although absolute illluminance threshold levels varied between individuals. There was a clear correlation between the time of absence from a work place and the probability that the artificial lighting was switched off. User occupancy could be modeled using a few input parameters that reflect the working habits of the simulated person. Artificial lighting tended to be only activated when the blinds were fully retracted. Whereas people rarely lowered the blinds after they had been automatically retracted, they disliked the blinds to be automatically closed. The main trigger for lowering the blinds was direct sunlight above 50 Wm^{-2} which was incident on the work place. All these results show that

> occupants consciously and consistently operate their lighting controls and tend to follow a number of basic behavioral patterns. Groups of people exhibit very similar switching probabilities whereas individual switching patterns somewhat vary. These individual patterns can be implemented into a manual lighting control model which predicts the annual electric energy demand of manually operated lighting systems.

9.2. Justifiable Effort

The most time-consuming part of a daylight simulation is usually to generate a three-dimensional model of the investigated building and its surroundings and to collect the optical properties of all involved surfaces. Once such a model is available, the additional effort for the architect or lighting engineer to carry out a dynamic instead of a static daylight simulation is marginal. A further-going analysis of annual daylight profiles can yield the daylight autonomy and the electric energy demand for artificial lighting for various manual and automated control systems.

> The required effort and working hours to produce and analyze dynamic daylight simulations can be justified by additional insight gained into the lighting situation of a future building. In combination with customer-tailored occupancy profiles these simulations can help identifying lighting concepts which consider user habits and energy efficiency to equal parts.

9.3. Relevance

According to chapter 8, differences due to individual behavior can lead to electric energy demands for artificial lighting in identical offices which vary between 6 and 26 kWh/m^2a. This shows that estimates of the saving potential of an automated lighting systems have to be treated with care and that

the implementation of behavioral patterns and short-time-step irradiance data series into daylight simulation programs leads to more accurate simulation results which can help to judge different daylighting strategies and products during the design phase of a building.

9.4. Outlook

While a number of advances have been realized during the course of this work, further steps are necessary to foster a wider usage of dynamic daylight simulations in the design process of a building.

advanced user interfaces: While the results of part A reveal the high simulation quality of dynamic daylight simulation methods like DAYSIM, this high performance standard can only be maintained in the *day-to-day* design process if the geometrical and optical properties of the investigated building and surroundings are sufficiently well described and if an adequate set of simulation parameters is chosen. Both aspects highlight that while the underlying methodology of dynamic daylight simulation packages is already mature, it is important to develop user-friendly interfaces which feature extended help menus and look-up tables to assist the casual user in setting the simulation parameters and material surface descriptions right.

larger user samples: While a few general correlations seem to exist between measurable external stimuli and user behavior, it is still unknown why people chose a certain behavioral pattern and in how far the building design influences their choice. In real office buildings the energy demand in identical offices spreads due to individual behavioral patterns. This spread can be estimated with the methods developed in this thesis. To be able to further estimate the total energy demand in a building, the frequency distribution of different behavioral patterns is required. Such statistical information can be gained from data sets which cover a larger number of occupants and buildings. In this context it will be crucial to understand, whether a behavioral pattern which has been observed during a few weeks already reflects the user behavior for the rest of the year.

investigation of a purely manually operated blind system: in the investigated building, most user-interferences with the blind system were not independent actions but triggered by the automated system. While the investigated system proved to be favorable for the artificial lighting demand of the offices, the measured data does not allow to extract information of how the users would have operated the blinds in the absence of the system. This issue deserves further attention in the future, as purely manually operated shading systems are presently more common than semi-automated systems.

behavioral patterns need to be refined: the literature review in chapter 6 and the results from the monitoring study in chapter 7 show that research on behavioral patterns which govern manual lighting control strategies are still at an early stage. While some obvious external triggers like user occupancy and indoor illluminance have been identified, future research should concentrate on how the luminance distribution within the view of a person contributes to his or her satisfaction with a visual situation. As this quantity is hard to measure in occupied offices new measurement procedures need to be developed to extract this information.

Appendix

Appendix A.2.1 Daylight Simulations with RADIANCE

All of the simulation results discussed in this work are based on the backward raytracer RADIANCE which has been developed by Greg Ward at Lawrence Berkeley National Laboratories in Berkeley, California, U.S.A.. The source code and binaries can be downloaded for free from the official RADIANCE web side at: http://radsite.lbl.gov/radiance/. The recently published book *The Art and Science of Lighting Visualization* written by Ward and Shakespeare is an excellent source of information which may serve as both, an introduction into daylight simulations with RADIANCE as well as a reference guide for detailed descriptions of the underlying simulation algorithms [war98].

This Appendix explains some RADIANCE features to help the reader appreciate how the daylight coefficient approach has been implemented into the RADIANCE simulation environment.

The raytracer RADIANCE

RADIANCE is a physically based lighting program which allows accurate calculations of luminance and illuminance distributions for arbitrarily complex building geometries. Various converters exist to export ArchiCAD or AutoCAD models into RADIANCE geometry and material input files. RADIANCE uses raytracing in a recursive evaluation of the luminance integral in a room. Contributions due to direct light sources and due to reflections from objects are treated separately in so-called direct and indirect (ambient) calculations. The latter "blends deterministic and stochastic ray-tracing techniques" to reduce the number of traced rays[83] [war98]. To further reduce the raytracing effort, the program incorporates interpolation and extrapolation schemes which allow to estimate the luminances on a surface point of interest from the luminance levels of nearby points.

Daylight Simulations with RADIANCE

Within RADIANCE the sky is not modeled as a geometrical element but instead as a solid angle [mar95]. Diffuse daylight and direct sunlight are treated as the RADIANCE materials *glow* and *light*, respectively [war98]. *Light* and *glow* mainly differ in that RADIANCE only carries out a *shadow testing* for all points of reflection for *light* sources, i.e. RADIANCE checks whether a point of reflection can "see" any *light* sources directly. As opposed to a *light* source, a *glowing* source is merely "found" if it happens to be hit by a ray from the mixed stochastic and deterministic ambient calculation. Since shadow testing is very time consuming, a growing number of *light* sources directly increases the required RADIANCE simulation times. This is why the celestial hemisphere is usually treated like a *glowing* material on which the diffuse sky luminance distribution pertaining to a considered sky condition is mapped. Merely the direct sunlight is modeled as an infinitely distant *light* source with an opening cone angle of 0.533° [84].

Technical limitations of RADIANCE

RADIANCE is a *backward raytracer*, i.e. light paths are traced backwardly from the spectator's eye to the light sources. Principally forward raytracing could be employed just the same, but for a great number of scenes the former approach is more economical considering the required

[83] During an ambient calculation in a first step disjoint directional ranges are defined for spawned rays which are emitted from a diffuse reflector. Afterwards single rays are emitted within these directional ranges according to a stochastic process [war88].

[84] See for example the RADIANCE programs *gensky* and *gendaylit* that model the CIE and the Perez sky luminance distributions respectively.

calculation times. In the following three scenes of rising complexity are discussed which show both the power as well as the limitations of RADIANCE.

scene 1: The goal is to calculate the illuminance due to daylight at a reference point behind a window in an office in a large building. Using forward raytracing the majority of traced rays would not even enter the room of interest, i.e. the rays would be worthless for the calculation as they cannot contribute to the illuminance at the reference point. In this situation, starting from the reference point is more economical.

scene 2: A venetian blinds system is pulled down in front of the window of the office of the previous scene with the slats in horizontal position. The surfaces of the slats are mostly diffuse. To calculate the illuminance at the reference point the number of required rays rises as some of the rare ray paths need to be identified which find their way in between the slats via multiple reflections. This complex geometry can be mastered by RADIANCE with an adequate choice of simulation parameters (see validation chapter 4).

scene 3: If the slats from scene 2 have highly specular surfaces, the capacity of RADIANCE is reached: The indoor illuminance distribution is not characterized to equal parts by all ray paths which find their way between the blinds but the specular direction under which direct sunlight is redirected to the ceiling is a preferred ray path with causes a bright spot at the ceiling. This spot is not recognized by RADIANCE as spawned rays which are emitted from a point at the ceiling need to hit the venetian blinds under a very narrow angle at a well-defined spot so that they – more or less accidentally – find the sun[85].

The shortcoming of conventional RADIANCE to correctly model daylight elements with highly specular components seriously limits its capabilities as an *all-round* daylight simulation tool. To overcome this limitation within RADIANCE, a *photon mapping* based approach is currently under development by Roland Schregle at the Fraunhofer Institute for Solar Energy Systems.

Barriers towards a wider usage

Advanced daylight simulation programs like RADIANCE require the setting of a large number of simulation parameters which have "few readily apparent absolute real world correlates". This puts the user in a situation with an "apparently infinite number of ways of getting it wrong or right" [don99] . The problem of finding a reasonable set of simulation parameters is an acknowledged barrier towards the widespread penetration of advanced daylight simulation tools like RADIANCE in today's design processes. It is a reason why "RADIANCE is still primarily viewed as a research tool" [jarv97]. To overcome this barrier various user interfaces are currently under development which aim to make the calculation power of advanced daylight simulation algorithms accessible to the casual user.

[85] For such scenes virtual light sources have been implemented into RADIANCE which place a *virtual* light source behind a mirror material for each primary light source. Virtual light source are very calculation intense as the calculation time is roughly linear to the product of the number of light sources and the number of *mirror* objects [war98]. The concept of virtual light source cannot be used if the considered mirror-like objects are bent – like most conventional slats.

Appendix A.2.2 Calculating Daylight Coefficients with an adapted "rtrace" Version

The *complete-year-run* method and the daylight coefficient method as implemented in ESP-R (see chapter 2) share a common problem. The reference point in the building as well as the building geometry, the materials descriptions and the simulation parameters remain unchanged during multiple raytracing runs under various sky conditions or different sky segments. Therefore RADIANCE repeats nearly identical same raytracing calculations a great number of times. Only the actual sky luminances for a ray hitting the celestial hemisphere changes with each investigated daylight condition[86]. To reduce these repetitive raytracing calculations for an annual daylight simulation, DAYSIM calculates the daylight coefficients with an adapted version of the backward raytracer RADIANCE.

Minor changes have been made to the output format of the original RADIANCE program *rtrace* to accelerate the calculation of a complete set of daylight coefficients. The raytracing algorithm itself has been left unchanged. Whereas a regular RADIANCE illuminance simulation yields integral illuminance values due to all light sources in a given scene, the adapted *rtrace*-version provides the contributions due to different light sources separately. With this new feature a complete set of daylight coefficients can be simulated in two *rtrace* runs:

1. To calculate the 148 diffuse and ground daylight coefficients, the building model is placed in a *glowing* sphere of constant luminance. No other light sources are admitted. During the raytracing illuminance contributions are grouped into 148 different bins according to the angular direction under which the backwardly traced rays hit the surrounding sphere.
2. For the calculation of the direct daylight coefficients, the building model is placed under some 65 angular light sources with a solar cone opening angle of 0.53°. The materials of the light sources are named *solar1* through *solar65*. The positions of the light sources correspond to the representative sun positions of the building site. During the raytracing the illuminance contributions are grouped according to the modifier names of the light sources [war98].

The drawback of the adapted *rtrace*-version is that even though the raytracing algorithm itself is identical to the conventional *rtrace*, the required RAM and necessary calculation times rise. The former effect stems form changes made to the caching structure in RADIANCE: during a conventional ambient calculation RADIANCE caches information like the color channel illuminances at already calculated points in the scene to allow for an interpolation or extrapolation of new values from already calculated neighboring points [war98]. The adapted *rtrace*-version further stores the illuminance contributions due to all light sources separately which increases the required memory per cached value by a factor of around 8. The calculation time rises due to the binning procedure by about 30% to 40%. The advantages of the new calculation procedure are that:

- both speed as well as stability of a daylight coefficient calculation are enhanced compared to individual raytracing runs for each daylight coefficient. This effect is pronounced for advanced building geometries and complicated daylight elements.
- redundant I/O processing between different programs can be avoided

[86] The raytracing calculations differ in the presence of direct sunlight, as a light source triggers direct shadow testing in RADIANCE, but under overcast sky conditions the ambient calculation remains virtually unchanged.

Appendix A.2.3 Conventional rtrace and DAYSIM: weighing the Benefits

This paragraph weighs the benefits and drawbacks of DAYSIM with respect to a conventional RADIANCE simulation. What are the additional planning efforts for the designer, the required calculation times, the suitable RADIANCE parameters and the hardware requirements, i.e. what is the price for simulating indoor illuminances under multiple instead of a single sky condition?

additional design work: DAYSIM uses the same material and geometry input files as a conventional RADIANCE simulation. This is important as the generation of the CAD model is usually the most time demanding part of a simulation. Direct and diffuse irradiance data are widely available in the form of test reference years (*see* chapter 2). Therefore, the additional design effort for running an annual daylight simulation is usually small and – as DAYSIM has been widely automated – mainly requires additional CPU times.

calculation times: Fig. A.2.3-1 compares calculation times for the three investigated blind settings from the validation chapter 4 which are required to calculate indoor illuminances under a single sunny sky or under arbitrary sky conditions. The columns correspond to the ratios between both calculation times while the actual calculation times are printed above the columns. While the ratio for retracted blinds lies around 8, it drops below 5 for closed blinds. This indicates that the significance of the daylight-coefficient-specific contribution to the overall calculation falls with growing complexity of the raytracing calculation.

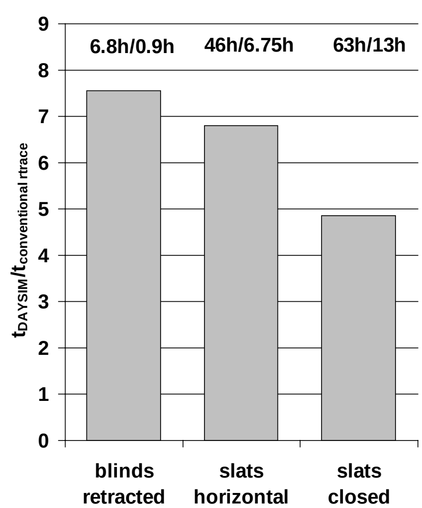

Fig. A.2.3-1: Comparison of the ratios of the calculation times for a DAYSIM simulation which yields a complete set of daylight coefficients to a conventional static RADIANCE simulation. All calculations involved the simulation of illuminances for 7 points inside the test office from chapter 4. Actual calculation times are printed above the columns. The ratios fall with rising model complexity.

RADIANCE parameters: a chosen set of raytracing parameters decisively influences the accuracy of a simulation and its calculation time. Therefore, the accuracy of simulation results for conventional RADIANCE and DAYSIM have been compared for various sets of raytracing parameters. The results were that the same set of simulation parameters yields very similar accuracies for both methods under various sky conditions and blind settings. Differences mainly arise under sunny sky conditions as DAYSIM has to estimate contributions from the direct sunlight from the available representative sun positions. This important finding implies that the same set of RADIANCE simulation parameters can be used for a dynamic daylight simulation as for the simulation of a single sunny sky condition. Again, no additional effort for the designer is required.

hardware requirements: As explained in Appendix A.2.2, the adapted *rtrace*-version demands about 8 times more RAM than a conventional *rtrace* simulation due to extended caching information. In the times of continuously rising hardware capabilities the 256 Megabyte RAM used for all simulations in chapter 4 should not constitute a severe financial barrier for a potential user of the simulation method.

Appendix A.2.4 Overview of the DAYSIM Subprograms

The dynamic daylight simulation method DAYSIM has been integrated into a user interface of the same name which generates shell scripts to simulate annual indoor illuminance profiles with underlying time-steps from hours to minutes. Fig. A.2.4-1 shows a diagram of the various DAYSIM subprograms[87]. A detailed manual, the latest version of the c source code as well as binaries for a LINUX system are available upon request from the author (christoph.reinhart@nrc.ca).

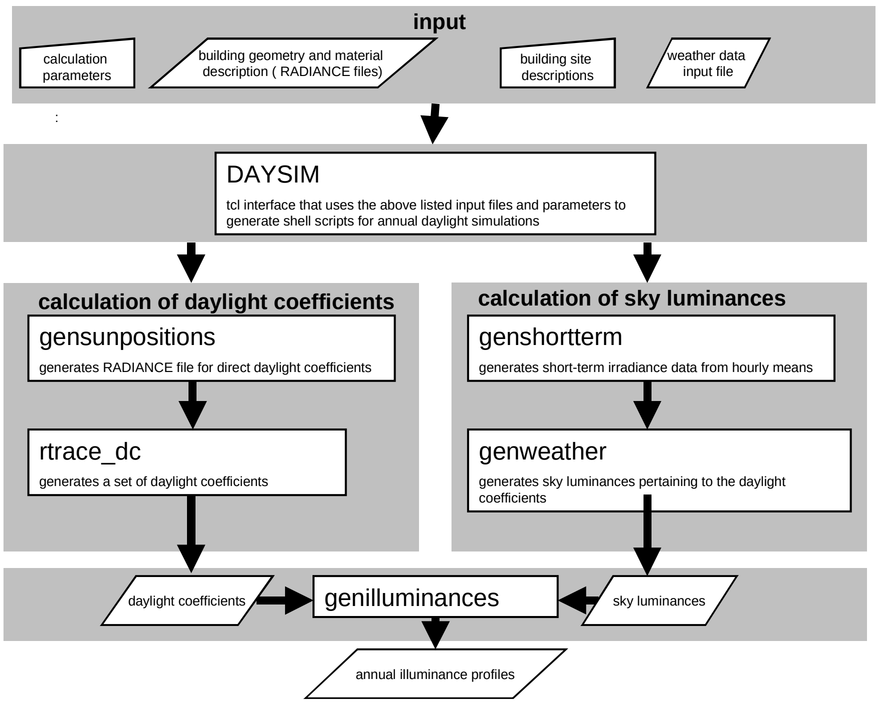

Fig. A.2.4-1: Diagram of the various DAYSIM subprograms.

[87] **rtrace_dc** is an adapted version of the RADIANCE program "rtrace" and described in detail in Appendix A.2.4. **genshortterm** has been written by Oliver Walkenhorst and is described in chapter5 and [wal01].

Appendix A.3.1 Simulation Results for a Cloudy and a Clear Day

This Appendix presents simulation results for the single office geometry (Fig. 3-2) on a cloudy and a clear day. Figures A.3.1-1(a) and A.3.3.1-2(a) show external horizontal illuminances while the Figures under (b) show internal illuminances at point 1 in the single office.

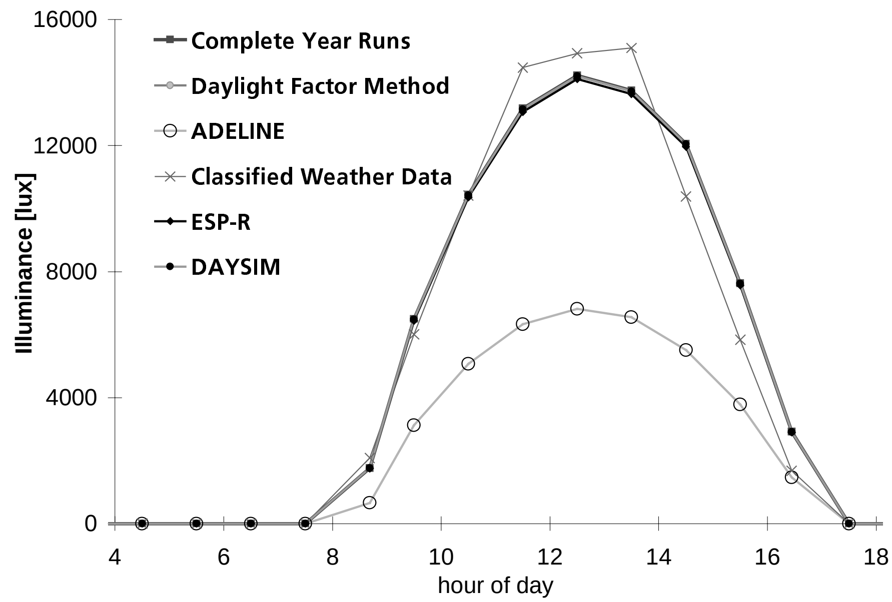

Fig. A.3.1-1: Comparison of the different methods for a cloudy day (March 13th)

(a) external horizontal illuminances

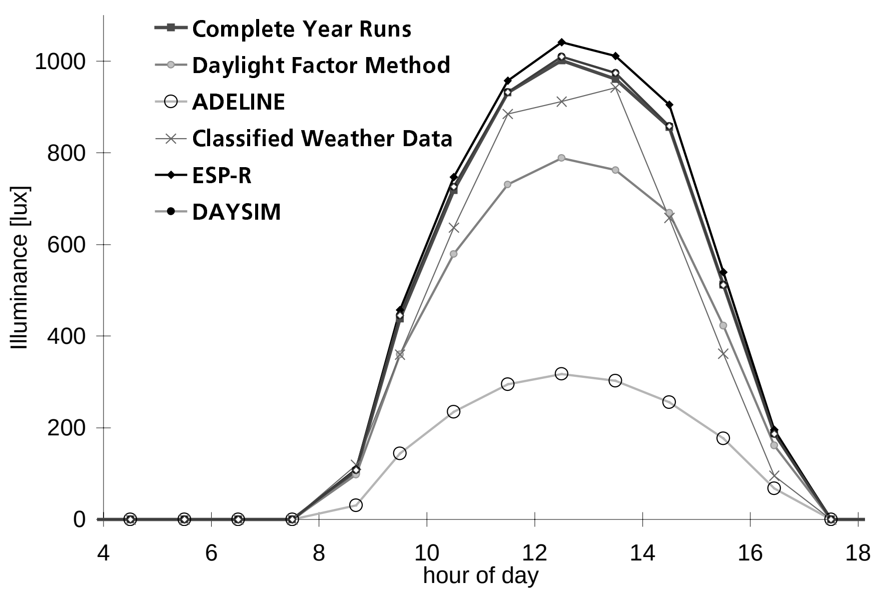

(b) work plane illuminance for point 1 in the single office

<u>Cloudy day</u>: For the cloudy day the simulation results of ESP-r and DAYSIM basically coincide with the reference case (Complete Year Runs) for both indoor as well as outdoor illuminances. The daylight factor method also coincides with the reference case for the external illuminances while it constantly underestimates the internal illuminances. The excellent results for the external illuminances are obvious since the daylight factor is 100% for this sensor position and since the Perez luminous efficacy model is used to calculate the external illuminances from the TRY data. The reason for the discrepancies of the indoor illuminances with the reference case is that the CIE overcast sky, under which the daylight factor is defined, tends to underestimate horizontal sky luminances which in turn have a significant contribution to indoor illuminances at deeper room depths. ADELINE constantly underestimates both indoor and outdoor illuminances. This clearly shows that ADELINE does not consider the given hourly mean diffuse illuminance values but always relies on the same CIE overcast sky of the corresponding month in the absence of

direct sunlight. The Classified Weather Data slightly overestimates the external illuminances around midday while the internal illuminances are underestimated. The magnitude of the errors can be reduced by increasing the number of diffuse weather classes at the expense of longer calculation times.

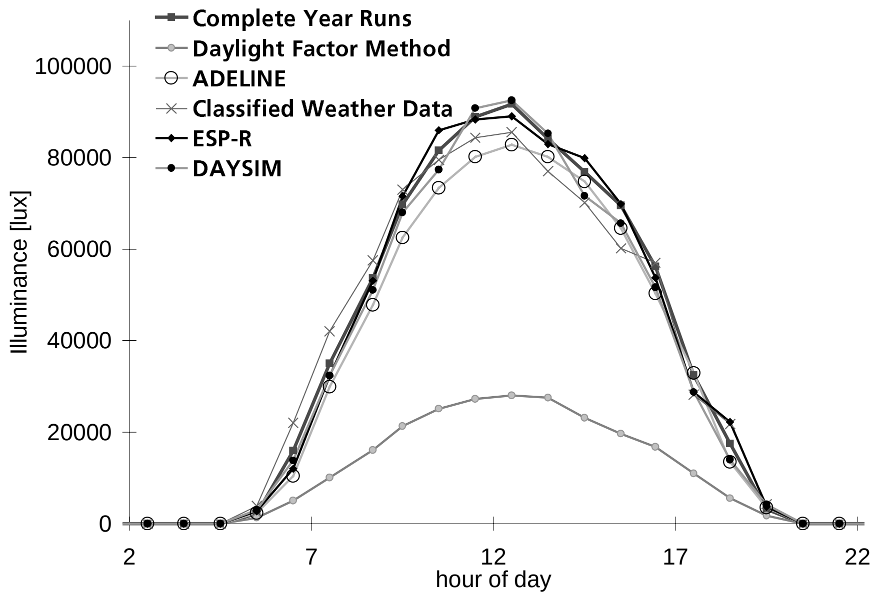

Fig. A.3.1-2: Comparison of the different methods for a clear day (August 11th)

(a) external horizontal illuminances

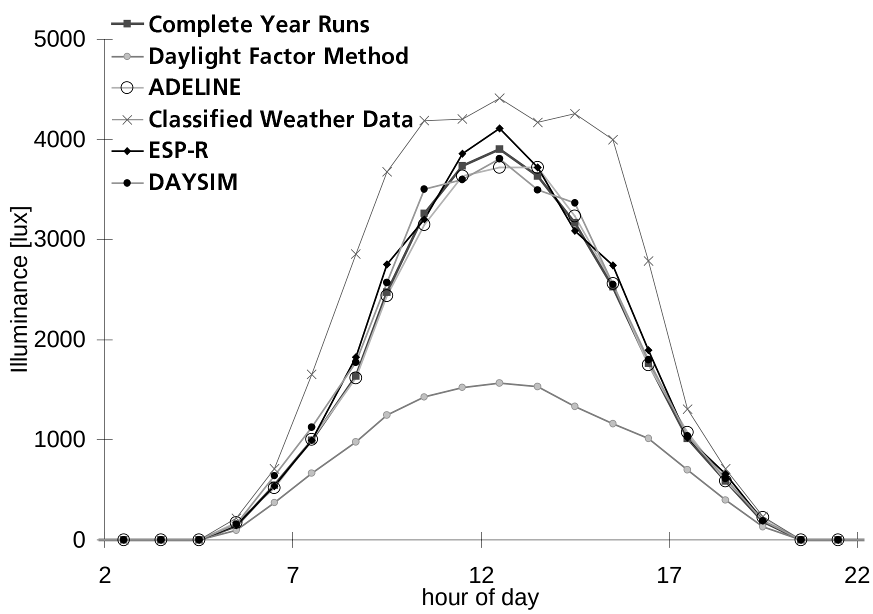

(b) work plane illuminance for point 1 in the single office

<u>Clear day:</u> Figure A.3.1.2 (a) and (b) present external and internal illuminances for a clear sky. As for the diffuse day, ESP-r, DAYSIM and the reference case lie very close together. The Daylight Factor Method only models illuminances due to diffuse daylight and accordingly lies below the reference case for indoor and outdoor illuminances. On the clear day, ADELINE approaches the reference case for external and internal illuminances since the Perez sky for a clear sky basically coincides with the clear CIE sky. The Classified Weather Data slightly underestimates the external illuminances while the indoor illuminances are modeled too large. The reason for this is that the actual mean hourly sun positions are approximated by sun positions of lower altitude, leading to lower external horizontal illuminances. On the other hand, a lower sun position around noon can cause higher indoor illuminances for a room with a southern window. As for the diffuse case, the number of direct classes would have to be increased to enhance the accuracy of the classified data.

Appendix A.4.1 RADIANCE parameters for external venetian blinds

In this Appendix the choice of RADIANCE simulation parameters used during the validation of DAYSIM simulation results in chapter 4 is briefly motivated. A deeper discussion of the meaning of these parameters can be found under [war98].

ambient bounces (ab=7): This parameter describes the number of diffuse interreflections which will be calculated before a ray path is discarded. A high ab-value significantly increases the required calculation time but is necessary in the case of closed blinds, as rays may be reflected several times between two adjacent slats before they pass through a blind system.

ambient division (ad=1500) and ambient sampling (ad=100): The ad-parameter determines the number of sample rays that are initially sent out from a surface point during an ambient calculation. This parameter needs to be high if the luminance distribution in a scene with a high brightness variation as is the case between blind slats. An as-parameter greater than zero determines the number of extra rays that are sent in sample areas with a high brightness gradient.

ambient accuracy (aa=0.1) and ambient resolution (ar=200): The combination of these two parameters with the maximum scene dimension provides a measure of how fine the luminance distribution in a scene is calculated. According to page 385 in [war98] the combination of aa=0.1, ar=200 and a maximum scene dimension of 10m yields a minimum spatial separation for cached irradiances of: (10m•0.1)/200=0.5cm. This resolution is sufficient to describe the investigated external blinds in chapter 4 as each slat was about 7 cm wide.

direct threshold (dt=0): This option switches off the selective source testing [war98], i.e. each light source is equally considered during each shadow testing. This option always needs to be set to zero when the direct daylight coefficients are calculated by DAYSIM.

direct subsampling (ds=0): This option switches off the direct subsampling threshold, i.e. only one ray is always send into the center of each light source. As during the calculation of the direct daylight coefficients only solar discs with an angular size of 0.5° are present. This procedure speeds up the calculation without impeding its accuracy.

Appendix A.4.2 Analysis of Simulation Errors

This Appendix aims to provide some insight into how the total simulation errors from Table 4-2 can be divided into errors due to the raytracing and to the sky model. Figures A.4.2-1 to A.4.2-3 presents the frequency distributions of the relative errors of all simulated illuminances at sensor #2 (Fig. 4-1) for the three blind settings separately.

For the retracted blinds (Fig. A.4.2-1) SHADOW TEST has a wide peak and the center of weight lies at 6%. The RMSE for this distribution is 22% (Table 4-2). After scaling[88] the peak narrows to a RMSE of 10% and shifts to a MBE of 0%. This behavior proves how exact the raytracing algorithm can model indoor illuminances in the absence of blinds. Our findings for this geometry are in accordance with the results of Mardaljevic [mar95] who found a MBE of 1% and a RMSE of 17.9 % for a point at 2.5 m distance to a facade with a single glazing.

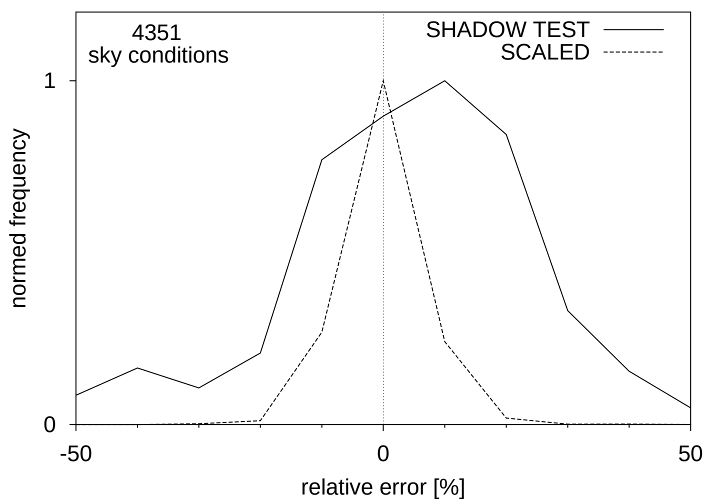

Fig. A.4.2-1: Frequency distribution of relative errors for sensor #2 for retracted blinds.

For the horizontal slats (Fig. A.4.2-2) the situation is similar: the wide SHADOW TEST peak with an associated RMSE of 25 % narrows down to 17% after scaling. The SCALED peak is not centered around 0% as the sensor is only partly exposed to the celestial hemisphere due to the slats. In that case the scaling cannot correct for all sky model errors.

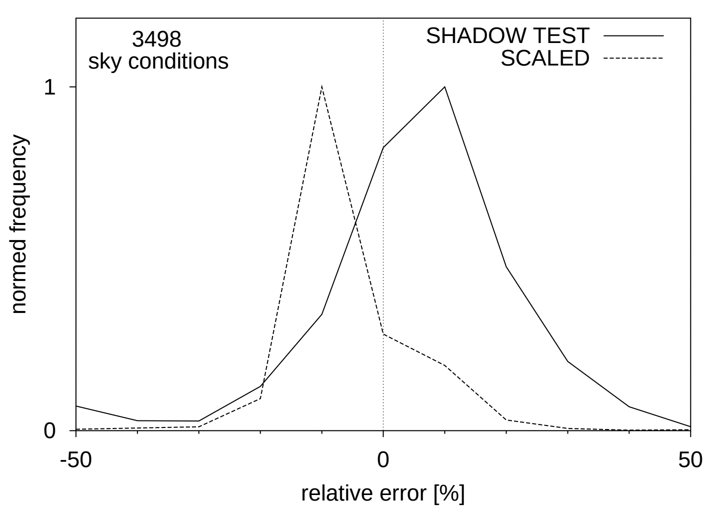

Fig. A.4.2-2: Frequency distribution of relative errors for sensor #2 for horizontal blinds.

For the closed blinds (Fig. A.4.2-3) the frequency distribution of SHADOW TEST features two peaks. The higher peak at about 10% stems from the cloudy skies (Fig. 4-3(c)) while the peak at –20% stems from the sunny skies (Fig. 4-6). The scaling merges the peaks and reduces the RMSE from 24% (Table 4-2) to 15%.

[88] see section 4.2.1

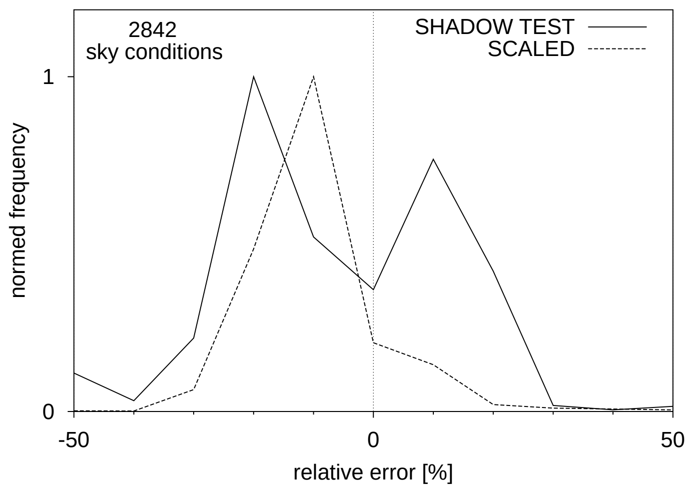

Fig. A.4.2-3: Frequency distribution of relative errors for sensor #2 for closed blinds.

These results for the three blind settings suggest that the overall simulation errors of DAYSIM for complicated facade geometries stem to roughly equal parts from the raytracing algorithm and the sky model.

Appendix A.6.1 Technical Details of the Experimental Setup

The data acquisition project *Lamparter* was carried out in cooperation with the Fachhochschule Stuttgart. While the Fachhochschule concentrated on the measurement of energy flows within the building, the setup which has been installed by the Fraunhofer Institute for Solar Energy Systems concentrated on the monitoring of manual control strategies. This Appendix provides details of the latter setup.

The monitoring techniques were focused on quantifying blind positions and artificial lighting status and continuously measuring the working environment of all rooms with south-facing windows. To achieve these ends, four different data collection systems were used:

HOBO & occupancy sensor: stand-alone data loggers with integrated illuminance and temperature sensors were coupled with two ultrasonic sensors for every office to determine user presence.

weather station: a central data acquisition system has been installed and is maintained by the Fachhochschule Stuttgart which records ambient temperatures, global and diffuse irradiances as well as vertical illuminances onto the southern facade [mül01].

EIB system: As blinds and artificial lighting are operated via an EIB system, the status of the switches could be directly recorded with a Linux PC which is connected to the EIB system.

video surveillance system: The blind positions were recorded by a video surveillance camera. The data acquisition system recorded a digital image of the facade if the status of any blind system changed. Afterwards, the blind positions were manually extracted from the collected digital images.

Table A.6-1 summarizes how the different physical quantities have been measured.

quantity	Appendix	short description
work place occupancy	A.6.1.1	stand-alone data acquisition system in each office
work plane illuminances		
indoor temperatures		
ambient temperature	A.6.1.2	central data acquisition system maintained by the Fachhochschule Stuttgart
global horizontal irradiance		
diffuse horizontal irradiance		
vertical illuminance in facade		
status of artificial lighting	A.6.1.3	Linux PC connected to an EIB system
status of external blinds	A.6.1.4	video surveillance and manual photo analysis

Table A.6.1-1: Overview of experimental setup.

A.6.1.1 User occupancy, Work Plane Illuminance and Indoor Temperatures

To measure the working conditions inside the Lamparter building, an onset HOBO data logger and two ultrasonic presence sensors were installed in every office with south facing windows. Each office contains two centrally located workstations joined together, with one PC per station, allowing for two users per room (see Fig. 6-6). The HOBO is a low-cost, stand-alone data logger which continuously measured the temperature and illumination at the workstations, while the ultrasonic sensors determine user presence. The HOBO and the two sensors were joined together as a single measuring device. Fig. A.6.1-1 shows a typical measurement setup in an office. The HOBO has four channels to acquire temperature, relative humidity, and light intensity. The fourth channel allowed for an external input to measure voltage. The battery operated, remote logger can store 7943 time-stamped measurements and operate for one year continuously between –20°C and 70°C before requiring battery replacement. It can be set to acquire data over time intervals ranging from 0.5 seconds to nine hours and with an optional time delayed start. A special software package included with PC interface cable is necessary to launch and read

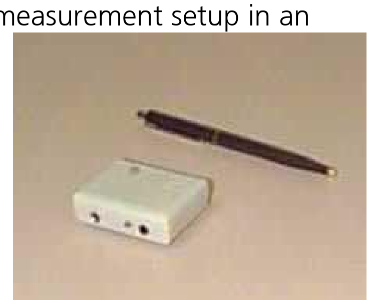

HOBO stand alone data logger

out the stored data. All loggers were simultaneously tested in a controlled climate to confirm the accuracy of every instrument. Running for 3 hours and 45 minutes with 15 second measurement intervals, the HOBOs underwent a temperature increase from 16°C to 30°C at constant humidity with a one degree increase every 15 minutes. The maximum difference in measurements between all loggers remained under 0.4°C at all times. The mean error between the average of the HOBOs and the temperature measured by the controlled climate apparatus was 0.7°C with a standard deviation of 0.18. The HOBO´s light intensity sensor measures illuminance in foot-candles (lumen/ft²) with a nominal range of from 2 to 600[89] with a manufacturer given error of ±20% of reading.

In the offices, every HOBO was programmed to record values every 15 minutes, allowing it to store data for 27 days. Three channels were activated: temperature, illuminance, and the external input to measure voltage. Each HOBO had to be individually retrieved from the separate rooms, downloaded and restarted at a Windows PC.

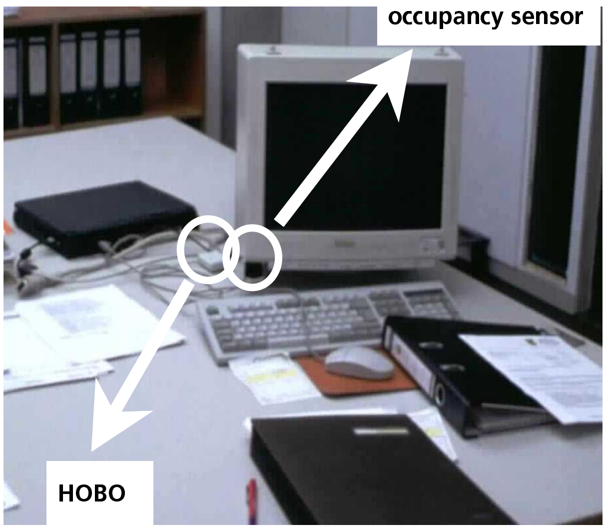

Fig. A.6.1.-1: Experimental setup in the offices: A HOBO stand-alone data logger with integrated illuminance and temperature sensor was placed at a central position between the two work places while the occupancy sensors were installed below the computer screens. The signal of two occupancy sensors was fed into a single HOBO.

In addition to the HOBO logger, two SWEL ultrasonic sensors[90] were attached directly to the underside of the monitors located at all workstations. Designed to determine the presence of a user at a workstation, the sensor sends out ultrasonic waves and detects the disturbances in the returning waves caused by human presence. Each sensor requires a 5V DC power supply and outputs a digital signal indicating presence. They can be adjusted to cover an angle of 60° over a distance of 2 meters. The reaction time can also be regulated between 20 seconds and 20 minutes. All sensors were set to cover the greatest possible area and to react in 20 seconds. As a HOBO logger contains only one external port, which can measure voltage between 0 and 2.5 DC volts, the sensors were grouped together to produce only one output between 0 and 2 volts .

A.6.1.2 Recording of ambient climatic Conditions

Details of the data acquisition system of the Fachhochschule Stuttgart can be found under [mül01].

A.6.1.3 Status of the Artificial Lighting System

The artificial lighting system in the southern offices is connected to a EIB (European Installation Bus) control system. Therefore, a Linux data acquisition PC was connected to the EIB system via a gateway from ELKA Elektronik GmbH[91] and the status of the manually operated artificial

[89] corresponds to 20 to 6500 lux
[90] http://www.swel.com
[91] ELKA-Elektronik GmbH, Postfach 15 04 , D-58465 Luedenscheid, Germany, http://www.elka.de/eib

lighting switches (on/off) could be directly recorded once every 5 minutes. Unfortunately, the dimmable lighting controls did not allow the setting or requesting of the dim level via the EIB system. Therefore, only on/off lighting levels could be collected.

A.6.1.4 Status of the Venetian Blinds

Fig. A.6.1-2 sketches the experimental setup for recording the venetian blind positions. The blinds are electronic—regulated by an EIB-Bus, which also controls the artificial lighting. The EIB system is intended to allow for automatic control of the blinds and artificial lighting, but can also be made for some or all manual control. The Lamparter EIB system can automatically control the blinds when the facade illuminance reaches a set limit or when the wind threatens to damage the blinds.

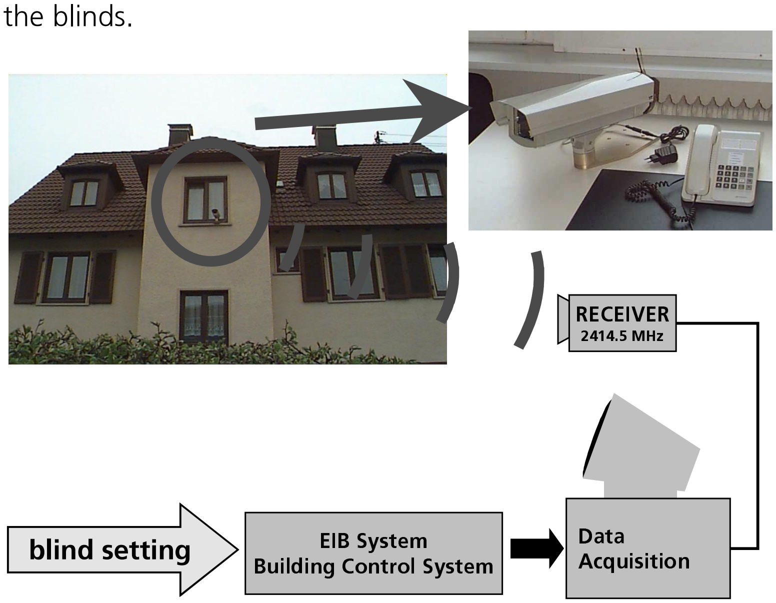

Fig. A6.1-2: Experimental setup for the recording of venetian blinds positions.

A video camera connected to a sender was mounted outdoors on the neighboring residential building facing the southern facade of the Lamparter building. The camera was continuously sending pictures to the data acquisition system which was situated on the top floor of the Lamparter building. Whenever a change in the any one of the southern blinds occurred, the data acquisition system noticed this event via the EIB system and saved a digital image from the camera was captured after pausing 90 seconds to allow the blinds to fully change positioning. The images were saved in jpeg-format according to date, time, room number and whether or not the blinds were moved automatically.

All images from one week were encoded into a MPEG film with names of the individual images, or frames, written into the image. Using the films, all individual pictures were evaluated manually. Fig. A.6.1-3 shows an example digital image.

Fig. A.6.1.-3: Example picture of the monitored facade with the 10 offices.

Appendix A.7.1 Considered Blind Settings

The following figure shows the 15 different blind positions which were assigned during the manual analysis of the pictures from the video surveillance camera. The blind occlusions associated with the 15 cases are also given.

case 1 **occl. 0%**

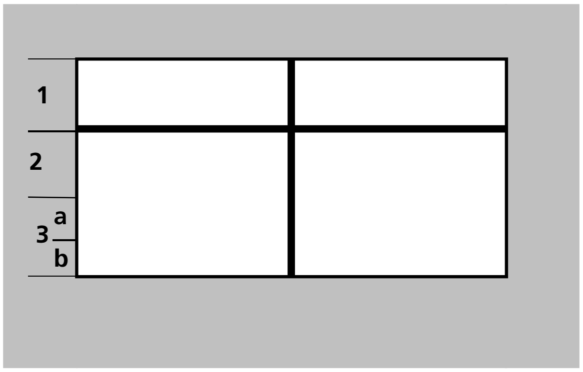

case 2 **occl. 30%**

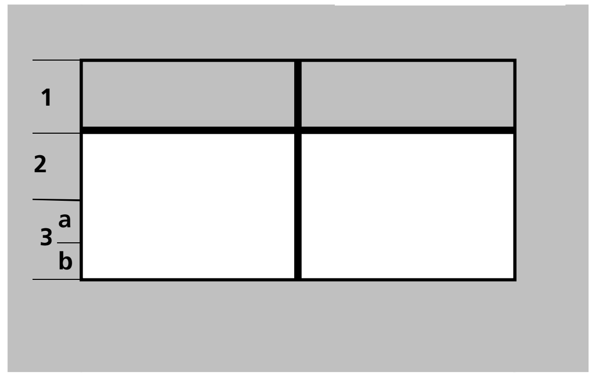

case 3 **occl. 30%**

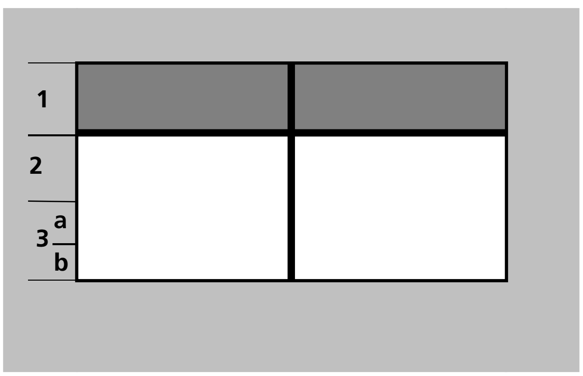

case 4 **occl. 60%**

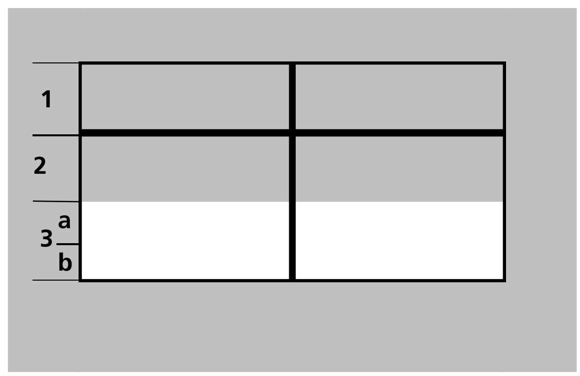

case 5 **occl. 60%**

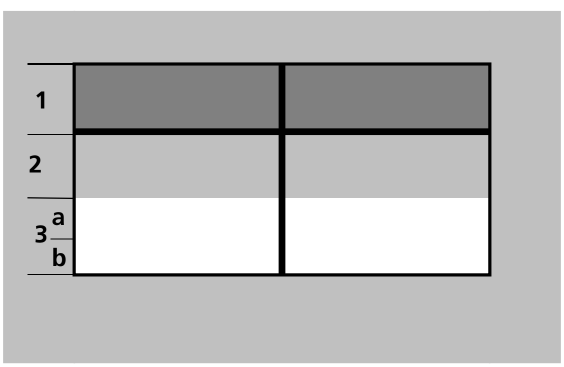

case 6 **occl. 60%**

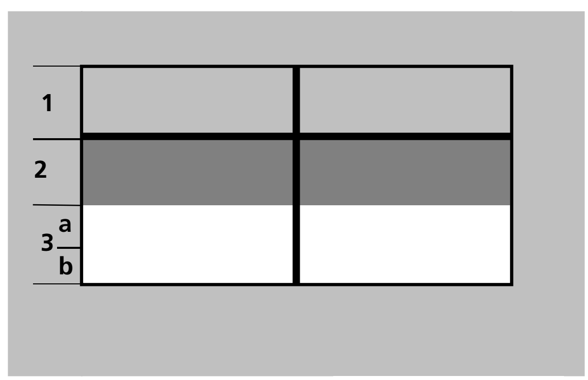

case 7 **occl. 60%**

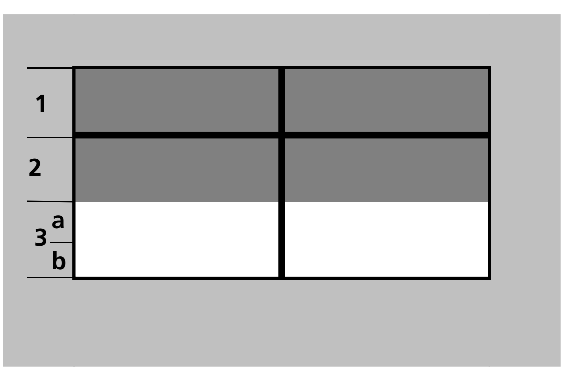

case 8 **occl. 75%**

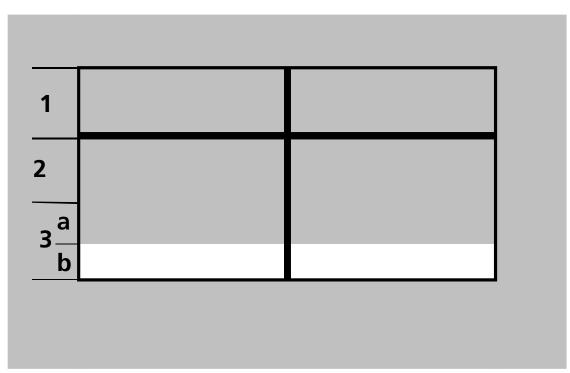

case 9 **occl. 75%**

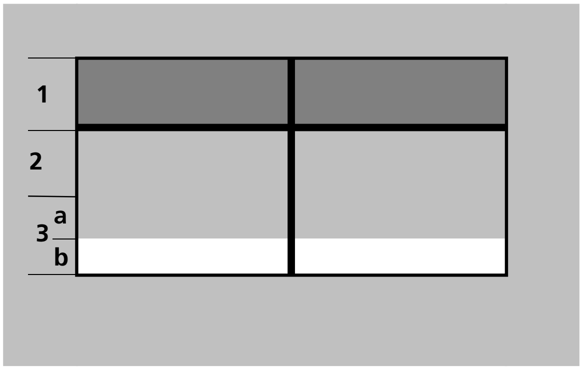

case 10 **occl. 75%**

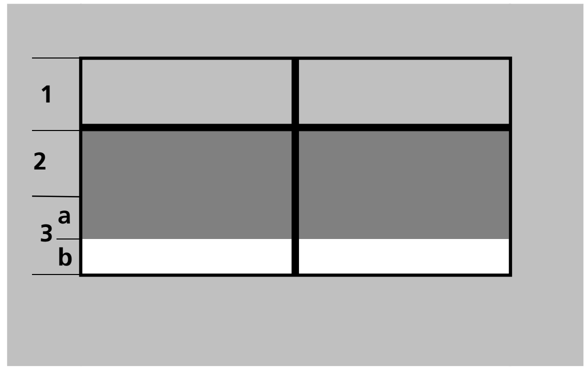

case 11 **occl. 75%**

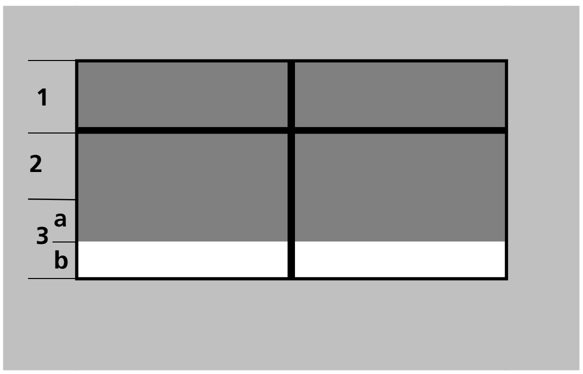

case 12 **occl. 100%**

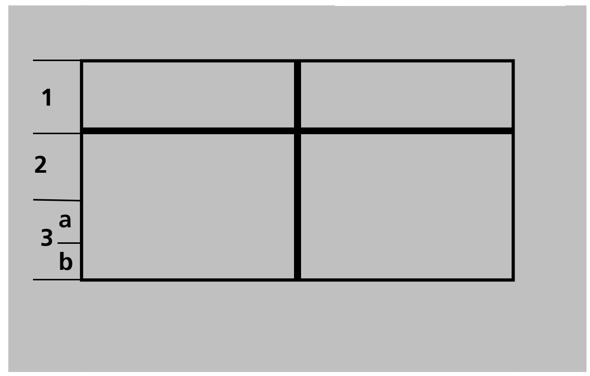

case 13 **occl. 100%**

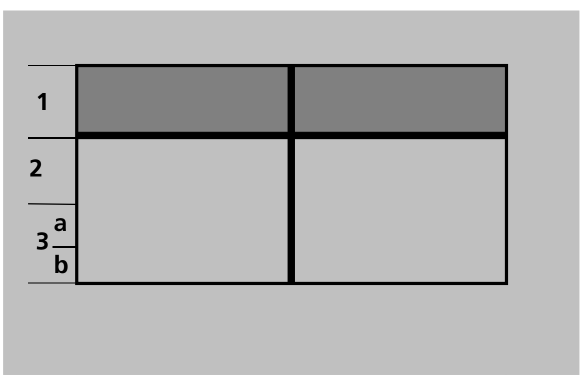

case 14 **occl. 100%**

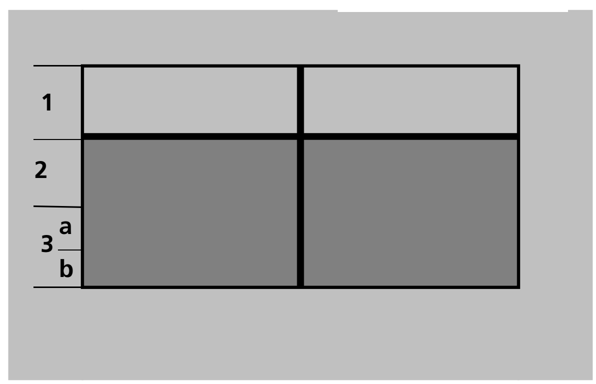

case 15 **occl. 100%**

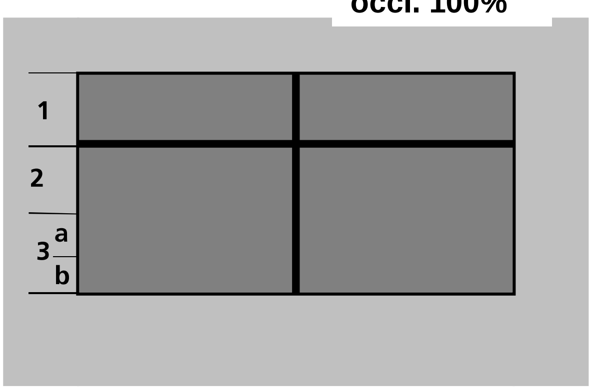

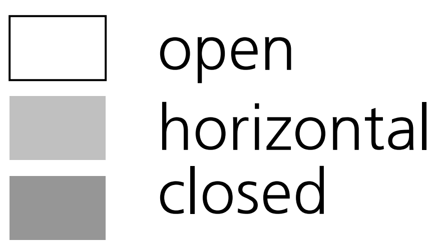

Appendix A.8.1 Measured and simulated occupancy Profiles for the 10 offices

This Appendix shows measured and simulated occupancy profiles in the 10 offices from the Lamparter setup.

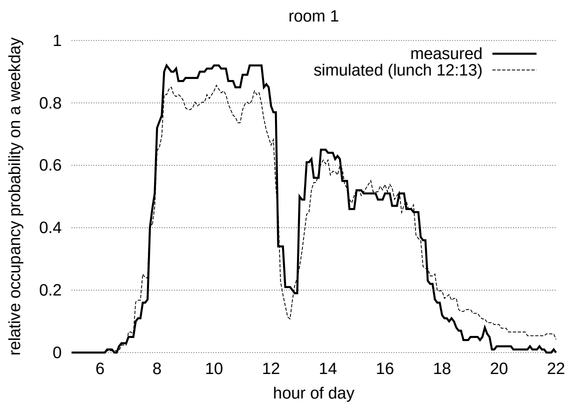

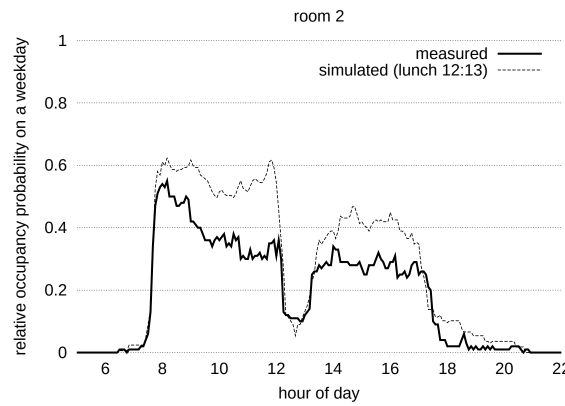

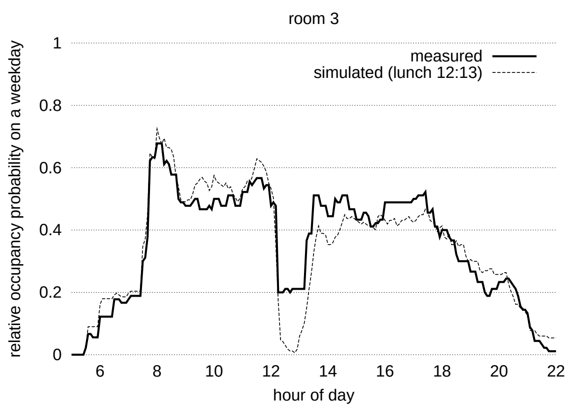

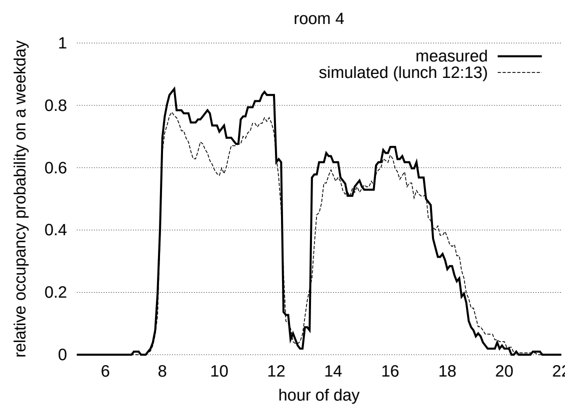

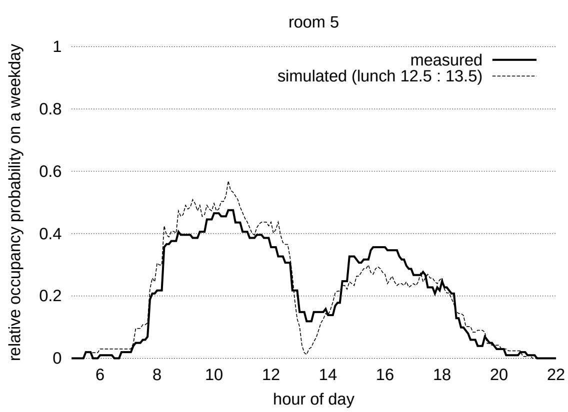

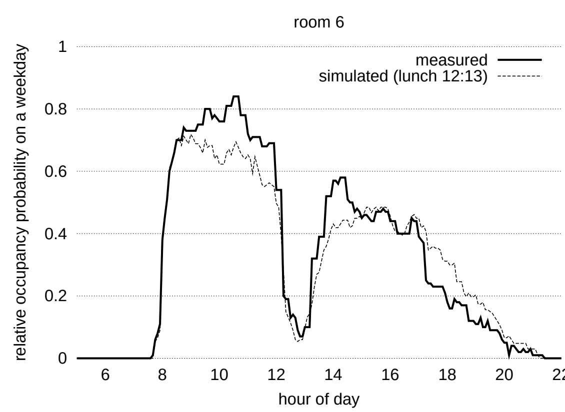

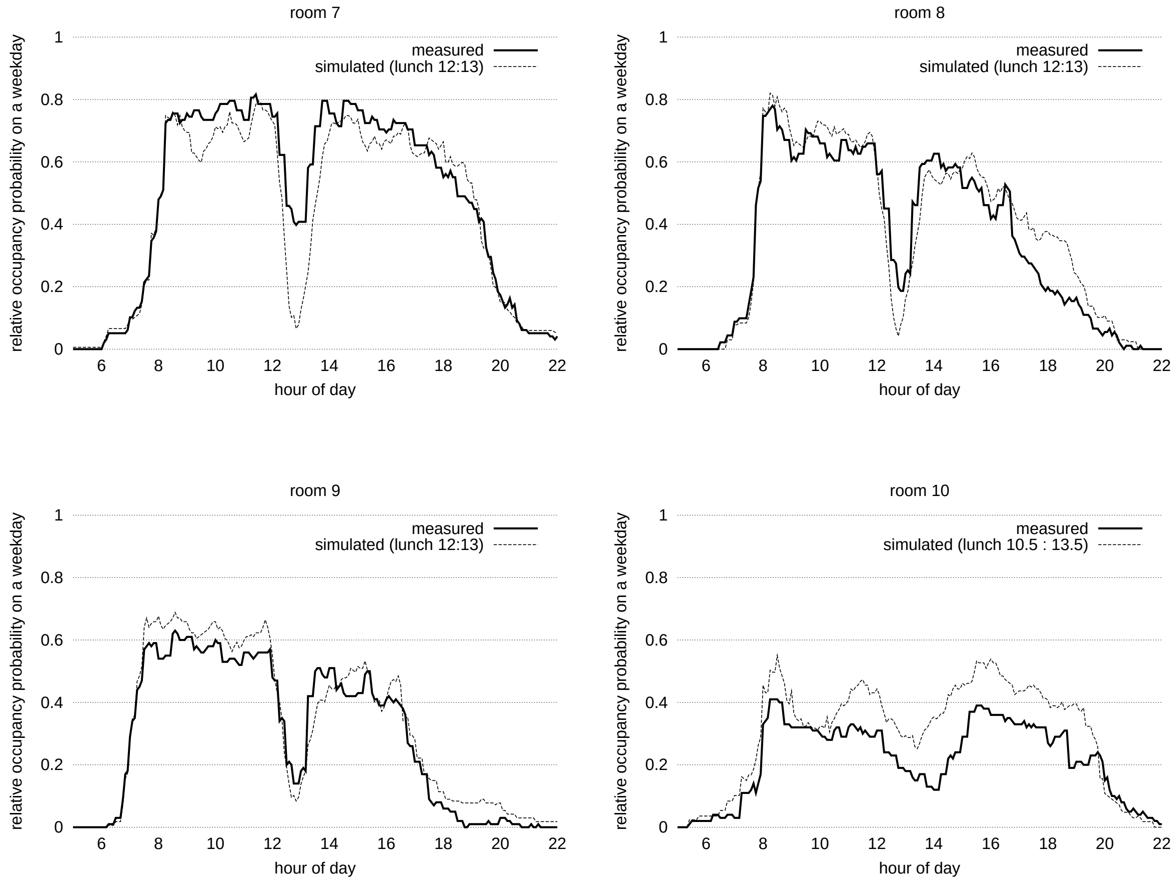
room 7
measured
simulated (lunch 12:13)
relative occupancy probability on a weekday
hour of day
room 8
measured
simulated (lunch 12:13)
relative occupancy probability on a weekday
hour of day
room 9
measured
simulated (lunch 12:13)
relative occupancy probability on a weekday
hour of day
room 10
measured
simulated (lunch 10.5 : 13.5)
relative occupancy probability on a weekday
hour of day

Glossary

atmospheric precipitable water content
: The atmospheric precipitable water content specifies the water content in the atmosphere which contributes to the amount of scattering in the atmosphere [ayd81].

closed/open-loop lighting control
: A closed–loop lighting systems usually consists of a indoor photo-sensor which considers the illuminated indoor environment, i.e. artificial lighting as well as daylight, in determining how to adjust/dim the artificial lighting. In contrast to that, an open looped system only measures incoming daylight, is usually facade mounted and makes lighting adjustments based on the estimated contribution that daylight makes on the controlled space.

daylight
: *Daylight* is the visible part of the electromagnetic radiation which reaches the earth's surface from the sun.

daylight autonomy
: The *daylight autonomy* a for a point in a building is a useful physical quantity to describe the annual daylight availability in a building. It is defined as the fraction of a considered time interval during which a minimum illuminance level can be maintained by daylight alone. Usually the considered time interval corresponds to the hours per year when a work place is occupied. Working hours – e.g. weekdays 7 a.m. to 6 p.m.- as well as the minimum illuminance levels – e.g. 500 lux – are set according to user demand.

The daylight autonomy is an intuitive parameter comparable to the daylight factor (see chapter 2) but it provides more insight as it varies for different facade orientations and describes the daylight availability under all possible sky conditions.

daylighting
: *Daylighting* describes the part of a building design which aims to optimize the annual availability of daylight in the building for lighting.

DHW
: domestic hot water

HVAC
: heating ventilation air-conditioning cooling

energy conversion factors
: A conversion factor specifies how many kWhs of primary energy are needed to provide 1 kWh of final energy in a building. As the generation of electrical energy in a power plant is accompanied by substantial conversion losses, costs as well as primary energy content of electrical power are higher than that of thermal energy. The following conversion numbers for electrical power are based on the German energy mix.

	$MWh_{primary}/MWh_{final}$	$kgCo_2/MWh_{final}$
natural gas, oil	1.1	210 – 290
electrical power	2.9	640

Primary energy factors and CO_2 emissions (TEMIS 1999*).*

illuminance
: The *illuminance* is one of the most important measures to quantify the amount of light/daylight at a point in space. It is defined as the total luminous flux per area which is incident on a plane. Accordingly, the illuminance is measured in lux=lm/m^2. Different tasks have well defined legal minimum illuminances which have to be maintained so that the task can be carried out safely and without tiring the working subject. Regular office work places usually necessitate minimum illuminances around 300 to 500 lux.

Linke turbidity
: The *Linke turbidity*, T, describes the amount of scattering of solar radiation in the atmosphere due to aerosols and water content [ayd81].

luminance
: The *luminance* is defined as the flux per unit area and solid angle which is emitted or reflected from a light source or a reflecting surface. It is measured in candela per unit area [cd/m^2]. For practical proposes the luminance from a given point of view quantifies the amount of luminous flux which is incident in the eye of a spectator from a certain direction. If a range of different luminances is within the view of a subject - i.e. a dark computer screen and a bright window -

	the subject is expected to experience difficulties in reading the content of the screen.
luminous efficacy	The *luminous efficacy* of a given light source is the ratio of the visible to the total electromagnetic radiation which is emitted from a given light source. It is measured in [lm/W]. Exemplary luminous efficacies for various light sources are given below. incandescent light 12 units heat : 1 unit light fluorescent light 3 units heat : 1 unit light daylight 2 units heat : 1 unit light
luminous flux	The *luminous flux* is the visible part of the total radiation which is emitted or reflected from a body. As opposed to the total flux which is measured in W the luminous flux is measured in lumen [lm].
ppd	Predicted person dissatisfied: measure weighted time intervals in which one is out of the comfort range
relative Mean Bias Error (MBE)	The relative Mean Bias Error (MBE) is a statistical measure to describe the similarity of two data series, i.e. $x_{sim,i}$ and $x_{mea,i}$ where j=1...N. The rel. MBE is defined as $$\text{rel. MBE} = \frac{1}{N}\sum_{i=1}^{N}\frac{(x_{sim,i} - x_{mea,i})}{x_{mea,i}}$$ It characterizes the relative size of the elements of a data series (x_{sim}) with respect to a references data series (x_{mea}). A positive (negative) MBE indicates that the considered data series tends to lie above (below) the reference data series. A vanishing MBE shows that the considered data series is scattered around the reference data series.
relative Root Mean Square Error (RMSE)	The relative ROOT Mean Square Error (RMSE) is a statistical measure to describe the similarity of two data series, i.e. $x_{sim,i}$ and $x_{mea,i}$ where j=1...N. The rel. RMSE is defined as $$\text{rel. RMSE} = \frac{1}{N}\sqrt{\sum_{i=1}^{N}\left(\frac{x_{sim,i} - x_{mea,i}}{x_{mea,i}}\right)^2}$$ It characterizes the average variance of the elements of a data series (x_{sim}) with respect to a references data series (x_{mea}). A small relative RMSE indicates that the considered data series lie close together.
sky model	A sky model is a theoretical model that yields the sky luminous distribution for a given sky condition based on different input parameters (see page 12)
solar zenith angle	The *solar zenith angle* specifies the angle between the vertical and the line to the sun [duf91].
VDT	visual display terminal

References

[api97] Apian-Bennewitz P, *Integral Visualization of buildings and simulation data in RSHOW*, Conf. Proc. of the IBPSA '99 Buildings Simulation, Vol. II, 1043-1050, Kyoto , Japan, Sep. 13 – 15, 1999

[api95] Apian-Bennewitz P, *Messung und Modellierung von lichtstreuenden Materialien zur Computersimulation von Tageslichtbeleuchtung*, Ph.D. thesis, Albert-Ludwigs-Universität Freiburg, Germany, 1995

[arc00] ArchiCAD 6.0 Manual, © GRAPHISOFT, http://www.graphisoft.com

[ati98] Atif M R , Love J A, Littlefair P, *Monitoring Protocols and Procedures for Daylighting Evaluation of Buildings*, Conference Proceedings CIE Symposium, Ottawa, Canada, Mai 9-10, 1998

[aut00] Autodesk 2000, http://www.autodesk.com

[ayd87] Aydinli S, Krochmann J, Seidl M, *Possibilities for energy saving for electrical light by daylighting of interiors in consideration of the visual task*, Conf. Proceed. of the European (CIE) Conference on Architecture in Munich , pp. 677- 680, 6th–10th of April 1987

[ayd81] Aydinli S, *Über die Berechnung der zur Verfugung stehenden Solarenergie und des Tageslichtes*, Ph.D. thesis, Technical University Berlin, Germany (1981)

[blü86] Blümel K *et al.*, Bundesministerium für Forschung und Technologie, *Entwicklung von Testreferenzjahren (TRY) für Klimaregionen der Bundesrepublik Deutschland*, scientific report of the Institute for Geophysical Sciences Technical University Berlin, Germany, 1986

[bak99] Baker N, *"Environmental Comfort- Optimization or Opportunity."*, Conf. Proceed. of Low Energy Building Conference ´99, September 17th to 18th in Hamburg, Germany, 1999

[beg97] Begemann S H A, van den Beld G J , Tenner A D, *"Daylight, artificial light and people in an office environment, overview of visual and biological responses"*, Industrial Ergonomics **20** 231-239, 1997

[beg94] Begemann S H A, Tenner A D, Aarts M, *"Daylight, artificial light and people"*, Proc. 39th Lighting Convention, Sydney Lights., 1994

[bek99] Beckmann W A, *TRNSYS – A Transient System Simulation Program*, Solar Energy Laboratory, University of Wisconsin-Madison, USA

[ben90] Benton C, *Daylighting in the U.S. Trends, Technology and Design*, Proceedings Second European Conference on Architecture. Dordrecht Khuwer Academic Publishers, Paris 1990. T. Steemers and W. Pfalz, Editors.

[bou91] Boubekri M, Hulliv R B, Boyer L L, *Impact of Window Size and Sunlight Penetration on Office Workers' Mood and Satisfaction: a novel Way of Assessing Sunlight*, Vol. 23 No. 4, 474-493, 1991

[boy80] Boyce P R, *Observations of the manual switching of lighting*, Lighting Research & Technology **12**(4) 195-205, 1980

[bül00] Bülow-Hübe H, *Office worker preferences of exterior shading devices*, Conf. Proceed. of the EUROSUN in Copenhagen, Denmark, June 2000

[CIBSE93] Chartered Institution of Building Services Engineers (CIBSE), *Lighting for offices*, Lighting Guide LG7:1993 (London: CIBSE), 1993

[cak00] Çakir A, *Light and Health*, can be downloaded from http://www.healthylight.de

[can00] Cannon-Brookes S W A, *Simple scale models for daylighting design: Analysis of error illuminance prediction*, Lighting Research & technology **29**(3) 135-142, 1997

[chu92] Chung T M, *A study of luminous efficacy of daylight in Hong Kong,* Energy and Buildings **19**(1), 45-50, 1992

[cla97] Clarke J *et al.*, *The ESP-R System for Building Simulation, User Guide Version 9 Series*, report number U97/1, University of Strathclyde, Glasgow, Scotland (1997)

[cla98] Clarke J, Janak M, *Simulating the thermal effects of daylight-controlled lighting*, Building Performance (BEPAC), issue 1 spring 1998

[co93] Cohen M F, Wallace J R, *Radiosity and Realistic Image Synthesis*, Academic Press Professional, Inc., first edition, 1993.

[col76] Collins B L, *„Review of the psychological reaction to windows"*, Lighting Research & Technology **8**(2), 80-88, 1976

[cra01] Crawley D B, Lawrie L K, Winkelmann F C , Buhl W F, Joe Huang Y, Pedersen C O, Strand R K, Liesen R J, Fisher D E , Witte M J, Glazer J, *EnergyPlus: creating a new-generation building energy simulation program*, Energy and Buildings **33** (4) pp. 319-331, 2001

[deb86] Debeir J-C, Deléage J-P, Hémery D, *Les servitudes de la puissance. Une histoire de l'énergie*, Flammarion, Paris, 1986

[del95] Delaunay J-J, *Contribution à la modélisation de la lumière naturelle en vue de son application a la simulation de l'éclairage de locaux*, Ph.D. thesis, Université Louis Pasteur de Strasbourg I, France, 1995

[del94] Delaunay J-J, Rommel M, Geisler J, *The Importance of the sampling frequency in determining short-time averaged Irradiance and Illuminance for rapidly changing cloud cover*, Solar Energy **52**(6) 541-545, 1994

[dia92] DIANE, Miklos M, Burkhardt P, *Tageslichtnutzung in Gebäuden - Denkanstöße, Bericht des Aktionsprogramms Energie 2000*, EWI Ingenieure und Berater 8034 Zurich, Switzerland, 1992

[doi73] Doigniaux R *et al.* , *Standardization of Luminance Distributions on Clear Skies*, Publication C.I.E. No. 22 (TC-4.2), 1973

[don99] Donn M, *Quality assurance – simulation and the real world*, Conf. Proc. of the IBPSA '99 Buildings Simulation, Vol. III, 1139 - 146, Kyoto , Japan, Sep. 13 – 15 1999

[duf91] Duffie J, Beckmann W, *Solar Engineering of thermal Processes*, 2nd edition, John Wiley sons INC. New York, 1991

[emp97] Breer D, Dorer V, Hopkirk N, Loschenz M, Lehmann B, Eber A, *Integrales Planen mit Gebbäudesimulationsprogrammen*, NEFF report, EMPA, Switzerland, http://www.empa.ch, 1997

[erh97] Erhorn H, Dirksmöller M, *ADELINE - An Integrated Approach to Lighting Simulation*, 5th Int. IBPSA Conf., 8.-10. Sept. 1997 Prague, Vol. II, 79 –85, 1997

[ESAP98] ESAP sa, *Energy in Europe: 1998- Annual Energy Review*, report for the European Communities, ISBN 92-828-4880-9, 1998

[esb98] Esbensen Consulting Engineers, *Energy Consumption and cost effectiveness of EC2000 buildings*, report for the European Commission, 1998

[eur97] eurostat (statistical office of the European communities), *Energy consumption in households*, ISBN 92-828-7589-X, 1999

[fan82] Fanger P O, *Thermal Comfort- Analysis and Application in Environmental Engineering*, Robert E. Krieger Publishing Company, Malabart, FL, U.S.A., 1982

[god98] Godish T, *Indoor Air Pollution Control*, Lewis Publishers, 1989

[gol00] Goller M, Reise C, *Über die Veränderlichkeit des Tageslichtes*, Conf. Proc. of the 6th Symposium on Innovative Lighting Systems in Buildings, pp. 85-90, Staffelstein, Germany, Jan 27th - 28th 2000

[gol98] Goller M, *The SAVE Program, Integration of Daylighting Technologies in Demand*

Side Management Programs: Estimation of the Energetical and Peak Load Potential", Final Report to the European Commission, 1998

[gul98] Gul M S, Muneer T, Kambezidis H D, *Models for obtaining solar radiation from other meteorological data*, Solar Energy **64** (1-3), 99-108, 1998

[her97] Herkel S, *Dynamic Link of Light and Thermal Simulation: On the Way to Integrated Planning Tools*, 5th Int. IBPSA Conf.,Con.f Proceed. Vol. II, 307 –312, Prague, 8.-10. Sept. 1997

[hes99] Heshong Mohane group and PG&E, *Daylighting in Schools: An Investigation into the Relationship between Daylighting and Human Performance*, report submitted to the Pacific gas and Electric Company on behalf of the California Energy Comission, http://www.pge.com/ (the daylighting initiative), 1999

[hes99] Hestnes A-G, *Building Integration of Solar Energy Systems*, Solar Energy **67,** 181-187, 1999

[heu91] Heusler W, *Experimentelle Untersuchung des Tageslichtangebotes und dessen Auswirkung auf die Innenraumbeleuchtung*, Ph.D. thesis, Technical University Berlin, Germany, 1991

[hör98] Hörner M, *Energiekennwerte und Benchmarking für Elektrizität in Bürogebäuden*, annual report Implusprogramm Hessen, Germany, 1998

[hun80] Hunt D R G, *Predicting artificial lighting use – a method based upon observed patterns of behavior*, Lighting Research & Technology **12**(1), 7 – 14, 1980

[hun79] Hunt D R G, *The use of artificial lighting in relation to daylight levels and occupancy*, Bldg. Envir. **14**, 21 – 33, 1979

[hüp00] http://www.hueppeform.de

[IDPM91] The measurement station of the Fraunhofer Institute for Solar Energy Systems is part of the International Daylight Measurement (IDMP) Network, official website http://idmp.entpe.fr/, 1991

[IESNA00] Illuminating Engineering Society of North America (IESNA), *Lighting Handbook,* ISBN 0-87995-150-8 (New York, NY:IESNA), 2000

[IESNA93] Illuminating Engineering Society of North America (IESNA), *American national standard practice for office lighting, ANSI*/IESNA –RP-1-1993 (New York, NY:IESNA), 1993

[ika99] Stein G, Wagner H F, *Das IKARUS-Projekt: Klimaschutz in Deutschland*, published by Springer Verlag, 1999

[ine94] Ineichen P, *Broad-Band Visible Radiation Data Acquisition and Analysis*, Technical report for the International Energy Agency , Taks 17 ,vol. 3 Satellite reports No. 4 and 5, 1994

[ino93] Inoue T, Ibamoto T, *Application of newly developed window system to office building*, International Symposium on Energy Efficient Buildings, Leinfelden-Echterlingen, March 1993, pp. 451-455, 1993

[ino88] Inoue T, Kawase T, Ibamoto T, Takakusa S, Matsuo Y, *The development of an optimal control system for window shading devices based on investigations in office buildings*, ASHRAE Transactions, Vol. 104, 1034 – 1049, 1988

[jan97] Janak M, *Coupling Building and Lighting Simulation*, 5th Int. IBPSA Conf.,8.-10. Sept. 1997 Prague, Vol. II, 313 – 319, 1997

[jar97] Jarvis D, Donn M, *Comparison of Computer and Model Simulations of a daylit Interior with Reality*, 5th Int. IBPSA Conf., 8.-10. Sept. 1997 Prague, Vol. III, 9-16, 1997

[jen99] Jennings J, Rubinstein F, Bartolomeo D, Blanc S, *Comparison of Control Options in an Advanced Lighting Control Testbed*, Proceedings of the IESNA 1999 Annual Conference, New Orleans, LA, August 10-12 1999

[jun94] Jung E G, Holick M F, *Biological Effects of Light*, Basel. Ed. plubl. Walter de

gruyter, Berlin/New York, 1994

[ken91] Kennaway D J, Van Drop C F, *Free-running rhythms of melatonin, cortisol, electrolytes, and sleep in humans in Antartica*, Am. Journal of Physiology, **260**(6) 1137-44, 1991

[kno98] Knoop T, *Tageslichtabhängige Beleuchtungssysteme auf der Basis von Installtions-bussen*, Ph.D. thesis Technical University of Berlin, Germany, 1998

[kra00] Kramer H, *Was bedeutet Lichtqualität in Gebäuden?*, 6th symposium on innovative lighting design in buildings, Jan. 27- 28, Staffelstein, Germany, 2000

[lam99] Lam K P, Mahadavi A, Ullah M B, Ng E, Pal V, *Evaluation of six sky luminance prediction models using measured data from Singapore*, Lighting Research & technology **31**(1), 13 – 17, 1999

[lin93] Lindsay C R T, Littlefair P J, *Occupant use of Venetian Blinds in Offices*, PD 233/92. Watford, Building Research Establishment,1993

[lit88] Littlefair P J, *Measurements of the luminous efficacy of daylight,* Lighting Research & Technology **20**(4), 177-188, 1988

[lit92] Littlefair P J, *Daylight Coefficients for practical Computations of internal Illuminances*, Lighting Research & Technology **24**(3), 127 – 135, 1992

[lit92_2] Littlefair P J, *Modeling Daylight illuminance in Building Environmental Performance Analysis*, J. of the Illuminating Engineering Society, 25 - 34, 1992

[lit90] Littlefair J P, *Predicting Annual Lighting use in Daylit Buildings*, Building & Environment **25,** 43 – 54, 1990

[loh98] Willbold-Lohr G, *Das Kölner Low Energy Office - ein Bürogebäude im Niedrigenergie-Standard*, annual report Implusprogramm Hessen, Germany, 1998

[lov98] Love J A, *Manual switching patterns observed in private offices*, Lighting Research & Technology **30**(1), 45-50, 1998

[lov95] Love J A, *Filed Performance of Daylighting Systems with Photoelectric Control*, Proc. Right Light Three, 3rd European Conference on Energy Efficient Lighting, 75 - 82, Newcastle UK, 1995

[lut96] Luther J, Voss K, *Solar Technologies for Future Buildings*, presented at the 4th European Conference on Solar Energy in Architecture and urban Planning, Berlin, March 26 – 29 1996

[man98] Maniccia D, Rutledge B, Rea M S , Morrow W, *Occupant use of manual lighting controls in private offices*, Journal of the Illuminating Engineering Society, Summer, 42-56, 1998

[mar01] Mardaljevic J, *Simulation of Annual Daylighting Profiles for Internal Illuminances*, Lighting Research & Technology **32**(3), 111-118, 2000

[mar97] Mardaljevic J, *Validation of a Lighting Simulation Program: A Study Using Measured Sky Brightness Distributions*, Lux, Conf. Proceed. The 8th European Lighting Conference, Amsterdam 11- 14 May, 555-569, 1997

[mar95] Mardaljevic J, *Validation of a lighting simulation program under real sky conditions*, Lighting Research & Technology, **27**(4), 181-188, 1995

[men97] Menzies D, Bourbeau J, *Building related illnesses*, The new England Journal of Medicine, **337**(21) 1524-1531, 1997

[met97] Remund J, Kunz S , *METEONORM 3.0: global meteorological database for solar energy and applied climatology*, Solar Engineering Handbook, published by METEOTEST, Fabrikstraße 14, CH-3012 Bern, Switzerland, 1997

[mic99] Michel L, *Méthode expérimentale d'évaluation des performances lumineuses de bâtiments*, PhD. thesis N° 2042, Ecole Federal Ploytechnique de Lausanne, Switzerland, 1999

[mit97] Mittelbach W, Henning H-M, *Seasonal Storage using Adsorption Processes*, IEA

workshop on Advanced Solar Thermal Systems, September 1997 in Helsinki, Finland, 1997

[mül01] Müller J F, Eicker U, Seeberger P, Bauer U, *Passiv-Bürohais Lamparter Weilheim/Teck:Konzept, Erfahrungen und Messergebnisse der ersten Heizperiode*, Conf. Conf. Proceed. of the 11th Symposium Thermal Solar Energy Usage, pp. 491-496, Kloster Banz, Staffelstein, Germany, May 9th –11th 2001 (ISBN: 3-934681-14-X)

[mül96] Müller S, *Simulation von Kunst- und Tageslicht mit dem Radiosity Verfahren*, Ph.D. thesis Technical University Darmstadt, Germany(1997)

[mun98] Muneer T, Gul M S, Kinghorn D, *Development of a meteorological Illuminance Model for Daylight Computations*, Applied Energy **59** (4), 235-260, 1998

[mun98_a] Muneer T, Kinghorn D, *Luminous Efficacy Models : Evaluation against UK data*, Journal of the Illumianting Engineering Society of North America **27** (1), 163-170, 1998

[new01] Newsham G, COPE (cost-effective open plan office environments) website http://www.nrc.ca/irc/ie/cope/index.html

[new97] Newsham G, *Clothing as a thermal moderator and the effect on energy consumption*, Energy & Buildings **26,** 283 – 291, 1997

[new95] Newsham G, *Lightswitch: A stochastic model for predicting office lighting energy consumption*, Proc. Right Light Three, 3rd European Conference on Energy Efficient Lighting, pp. 59 -66, Newcastle UK, 1995

[new94] Newsham G, *Manual Control of Window Blinds and Electric Lighting: Implications for Comfort and Energy Consumption*, Indoor Environment **3,** 135-144, 1994

[nil97] Nilson A, Upström R, Hjalmarsson C, *Energy Efficiency in Office Buildings- lessons from Swedish Projects*, Swedish Council for Building Research, ISBN 91-540-5787-6, 1997

[ols89] Olseth J A, Skartveit A, *Observed and modeled hourly luminous efficacies under arbitrary cloudiness,* Solar Energy Vol. **42**, No. 3, 221-233, 1989

[per93] Perez R, Seals R, Michalsky J, *All-Weather Model for Sky Luminance Distribution - Preliminary Configuration and Validation*, Solar Energy **50**(3), 235-245, 1993

[per90] Perez R, Ineichen P, Seals R, Michalsky J, Stewart R:, *Modeling daylight availability and irradiance components from direct and global irradiance*, Solar Energy **44**(5), 271 – 289, 1990

[pic91] Piccoli B, Parazzoli S, Zaniboni A, Demartini G, Fraschini F, *Non-visual effects of light mediated via the optical route: review of the literature and implications for occupational medicine*, Med. Lav **83**(3) 213-32, 1991

[pig96] Pigg S, Eilers M, Reed J, *Behavioral Aspects of Lighting and Occupancy Sensors in Privates Offices: A case study of a University Office Building*, Proceedings of the 1996 ACEEE Summer Study on Energy Efficiency in Buildings, **8** 8.161-8.171, 1996

[poh98] Pohl W, Scheiring Ch, *Integrative Planung von Tageslicht-Systemen*, 4tes Symposium Innovative Lichttechnik in Gebäuden, 380 – 384, 1998

[rea87] Rea M S, Jaekel R R, *Monitoring occupancy and lighting operation*, Lighting Research & Technology **9**, 45 – 49, 1987

[rea84] Rea M S, *Window Blind Occlusion: A Pilot Study*, Building and Environment **19**(2), 133 – 137, 1984

[red 97] Redlich C A, Sparer J S, Culllen M R, *Sick-building syndome*, THE LANCET **349** 1013-16, 1997

[rei90] Reindl D T, Beckman W A, Duffie J. A., *Diffuse fraction correlations*, Solar Energy **45** , 1-7, 1990

[rig00] Rigollier C, Bauer O, Wlad L, *On the clear sky model of the ESRA – European Solar radiation Atlas – with respect to the heliostat method*, Solar Energy **68,** 33-48, 2000

[rei01] Reise C, The measurement station of the Fraunhofer Institute for Solar Energy Systems is part of the International Daylight Measurement (IDMP) Network, official website http://idmp.entpe.fr/, 1991

[rub78] Rubin A I, Collins B L, Tibbott R L, *Window Blinds as a Potential Energy Saver- A Case Study*, NSB Building Science Series 112 , National Bureau of Standards, Washington, 1978

[SIA95] *Energie im Hochbau SIA 380/1-4* , guideline for energy use in commercial buildings, Association of Swiss Engineers and Architects (SIA) Zurich, Switzerland, 1995

[san94] Santamouris M, Argiriou A, *Renewable Energies and Energy Conservation Technologies for Buildings in Southern Europe,*. Solar Energy **15**, 69-79, 1994

[sch99] *Schweizer Energiefachbuch: Bundesamt für Statistik BFS: ein beispielhafter Bundesbau*, published by Künzler –Bachmann AG, St. Gallen, Switzerland, pp. 47-47, 1999

[sch96] Schaer A, *Teamorientiertes Planen*, published by Swiss Engineers and Architects (SIA), ISBN 3-905251-04-3, 1996

[sic99] Sick F, *Zur Beurteilung der Tageslichtqualität in der Praxis*, 5tes Symposium Innovative Lichttechnik in Gebäuden, Conf. Proceed. 178 – 197, 1999

[ska92] Skartveit A, Olseth J A, *The Probability Density and Autocorrelation of short-term global and beam irradiance*, Solar Energy **49**(6), 477-487, 1992

[sze96] Szerman M, Stoffel J, *ADELINE 2.0, Radlink Technical Manual*, IEA Solar Heating and Cooling, Task 12, 1996

[sze96_2] Szerman M, *Auswirkungen der Tageslichtnutzung auf das energetische Verhalten von Bürogebäuden*, Bauphysik, No. 4, pp. 97 - 109 und No.5, pp. 149 – 156, 1996

[sze94] Szerman M, *Auswirkungen der Tageslichtnutzung auf das energetische Verhalten von Bürogebäuden*, Ph. D. thesis University of Stuttgart, Germany, 1994

[tem97] TEMIS, *Total Emission Model of Integrated Systems, Version 3.x*, Öko Institut, Darmstadt, Germany, 1997

[ten97] Tenner A D, *Acceptance and Preference of illuminances in Offices*, Lux, Conf. Proceed. The 8th European Lighting Conference pp. 130-143, Amsterdam, 11- 14 May 1997

[tre87] Tregenza P R, *Subdivision of the Sky hemisphere for luminance measurements*, Lighting Research & Technology **19,** 13 –14, 1987

[tre84] Tregenza P R, Waters I M, *Predicting Daylight from Cloudy Skies*, Energy and Buildings **6,** 261 – 266, 1984

[tre83] Tregenza P R, Waters I M, *Daylight Coefficients*, Lighting Research & Technology **15**(2), 65-71, 1983

[tre83_2] Tregenza P R, *The Monte Carlo Method in lighting calculations,* Lighting Research & Technology **15**(4), 163 – 170, 1983

[tre80] Tregenza P R, *The daylight factors and actual illuminance ratios*, Lighting Research & Technology **12**(2), 64 – 68, 1980

[tsa97] Tsanrassoulis A, Santamouris M, *Daylight Modeling with Passport-Light*, 5th Int. IBPSA Conf.,8.-10. Sept. 1997 Prague, Vol. II pp. 73 – 78, 1997

[tsa96] Tsangrassoulis A, Santamouris M, Asimakopoulos D, *Theoretical and experimental analysis of daylighting performance for various shading systems*, Energy and Buildings **24,** 223 – 230, 1996

[tur00] Turnbull P, Loisos G, *Baselines and Barriers: Current Design Practices in*

Daylighting, Conf. Proc. of the ACEEE 2000 Summer Study on Energy Efficient Buildings, pp. 3.329 – 337, Pacific Grove, California, USA, August 20th –25th 2000

[var00] Vartiainen E, *Daylight Modeling and Optimization of Solar Facades*, Ph.D. thesis from the Faculty of Engineering Physics at the Helsinki University of Technology, 2000

[var00_a] Vartiainen E, *A Comparison of Luminous Efficacy Models with Illuminance and Irradiance Measurements*, Renewable Energy **20,** 265-277, 2000

[VBG95] *Arbeit an Bildschirmgeräten*, Grundentwurf März 1995, published by the Hauptverband der gewerblichen Berufsgenossenschaften (HVGB), 1995

[VDE92] Arbeitsausschuß VDEW*, Haushaltskundenbefragung 1991,* report of the association of German electricity providers (VDEW), May 1992

[vei01] Veitch J A, Newsham G R, *Preferred luminous conditions in open-plan offices: research and practice recommendations*, Lighting Research & Technology **32**(4), 199-212, 2000

[vei95] Veitch J A, Newsham G R, *Quantifying Lighting Quality Based on Experimental Investigations of End User Performance and Preference*, 3rd European Conference on Energy-Efficient Lighting, Newcastle-upon-Thyne, UK, June 1995

[vei96] Veitch J A, Newsham G R, *Determinants of Lighting Quality I: State of the Science*, 1996 Annual Conference of the Illuminating Society of North America, Cleveland, Ohio, August 5-7,1996

[vel99] Velds M, *Assessment of lighting quality in an office room with daylighting systems,* Ph.D. thesis Technical University Delft, Denmark, 1999

[vel97] Velds M, *An experimental approach to assess Discomfort Glare from Windows*, Lux, Conf. Proceed. The 8th European Lighting Conference, Amsterdam 11- 14 May 1997

[vin98] Vine E, Lee E, Clear R, DiBartolomeo D, Selkowitz S, *Office worker response to an automated venetian blind and electric lighting system: a pilot study*, Energy and Buildings **28**(2), 205-218, 1998

[vol98] Volz G, *Besseres Licht mit weniger Strom*, Deutsches Architektenblatt 10/98 pp. 1303-04, 1998

[vos01] Voss K, Energieeffizienz und Solarenergienutzung im Nichtwohnungsbau – Demonstrationsprojekte, SolarBau:MONITOR, Journal 2000. the official web page of the SolarBau:MONITOR program (in German) is: http://www.solarbau.de

[vos98] Voss K, *Bauen mit der Sonne*, Erneuerbare Energie, **2** 4-6, 1998

[wag98] Wagner A, *Zur sogenannten Solararchitektur*, Sonnenenergie **6** 20 -21 (1998)

[wag85] Wagner W F, (1985, April). *Round Table: Lighting – an art supported by a Technology*. Architectural Records, 173 (4), 156 – 163, 1985

[wal01] Walkenhorst O, Timmer J, Reinhart C, *Jahressimulationen des Tageslichtangebotes in Gebäuden auf der Basis von stündlichen und minütlichen Strahlungsdaten*, Conf. Proc. of the 7th Symposium on Innovative Lighting Systems in Buildings, Staffelstein, Germany, Jan 25th - 26th 2001

[wal01a] Walkenhorst O, Luther J, Reinhart C F, Timmer J, *Dynamic Annual Daylight Simulations based on One-hour and One-minute Means of Irradiance Data*, submitted to Solar Energy, June 2001

[war00] http://www.warema.de

[war94] Ward G, *The RADIANCE 2.4 Synthetic Imaging System*, University of California 1994

[war98] Ward G, Shakespeare R, *Rendering with RADIANCE. The Art and Science of Lighting Visualization*, Morgan Kaufmann Publishers, 1998

[war88] Ward G, Rubinstein F, *A New Technique for Computer Simulation of Illuminated*

Spaces, Jour. of the Illuminating Engineering Society **1** 80-91 (1988)

[web99] Weber L, Menti U-P, Keller I, *Energieverbrauch in Bürogebäuden*, ETH Zürich and Amsterin & Walthert AG, report of the Bundesumweltamt für Energie, Switrtzerland, 1999

[wie99] Wienold J, Schossig P, *Tageslicht am Arbeitsplatz – Messung, Bewertung und Nutzerakzeptanz von neuen Tageslichtsystemen"*, Conf. Proc.of the 5th Symposium on Innovative Lighting Systems in Buildings, pp. 56 -60, Staffelstein, Germany, Jan 29th 1999

[wie99a] Wienold J, Tenner A D, Zonneveldt L, Klingler M, *EULISP - Evaluation and User Assessment of Lighting Systems Performance*, Final Report for the European Commission, Contract No. JOR3-CT95-0016, 1999

Publications written in context with this thesis:

[rei01_b] Reinhart C F, Walkenhorst O, *Dynamic RADIANCE-based Daylight Simulations for a full-scale Test Office with outer Venetian Blinds*, Energy & Buildings **33**, 683-697, 2001

[rei01_a] Reinhart C F, Luther J, Witter V, Voss K, van der Weiden T C J, Santamouris M, Weiß W, *Energy Efficient Solar Buildings*, position paper in *The Future for Renewable Energies: Prospects and Directions*, European Renewable Energy Centers (EUREC) Agency, will be published by James & James, London, in October 2001 (32 pages)

[rei01] Reinhart C F, *Monitoring and Analysis of the Manual control strategies for Artificial Lighting and Venetian Blinds of 20 users – Experimental Setup and Preliminary Results*, Conf. Proc. of the 7th Symposium on Innovative Lighting Systems in Buildings, 208-212, Staffelstein, Germany, Jan 25th - 26th 2001

[rei00_b] Reinhart C F, Voss K, Wagner A, Löhnert G, *Lean buildings: Energy Efficient Commercial Buildings in Germany*, Conf. Proc. of the ACEEE 2000 Summer Study on Energy Efficient Buildings, Pacific Grove, California, USA, August 20th –25th 2000, pp. 3.287-3.298

[rei00_a] Reinhart C F, Herkel S, *The Simulation of Annual Daylight Illuminance Distributions- A state of the art comparison of six RADIANCE-based methods*, Energy & Buildings, **32**, 167-187, 2000

[rei00] Reinhart C F, Herkel S, *RADIANCE – Jahressimulationen des Tageslichtangebotes in Gebäuden – Ein Raytracer viele Ergebnisse*, Conf. Proc. of the 6th Symposium on Innovative Lighting Systems in Buildings, 189-194, Staffelstein, Germany, Jan 27th - 28th 2000

[rei99_a] Reinhart C F, Herkel S, *An Evaluation of RADIANCE-based Simulations of annual indoor Illuminance Distributions due to Daylight*, Conf. Proc. of the IBPSA '99 Buildings Simulation, Vol. II pp. 563 - 570, Kyoto , Japan, Sep. 13 – 15 1999

[rei99] Reinhart C F, Altmann K, Apian-Bennewitz P, Herkel S, Wienold J, Voss K, *Planung eines Büroneubaus – Tageslichtsimulation als Entscheidungshilfe in der Entwurfsphase*, Conf. Proc.of the 5th Symposium on Innovative Lighting Systems in Buildings, 193 – 197, Staffelstein, Germany, Jan 29th 1999

Curriculum Vitae

Personal Details

born	on the 27th of March1971 in Düsseldorf, Germany
citizenship	German

Professional Experience

since 2001	Research Officer with the Institute for Research in Construction of the National Research Council Canada, Ottawa, Canada
1997-2001	Member of the *Solar Building Design Group* at the Fraunhofer Institute for Solar Energy Systems in Freiburg, Germany Junior scientist (since 8/98) Research assistant (10/97 – 7/98)
1997-1998	Working Student in the pricing section of the Freiburg Energie- und Wasserversorgung (local energy provider)
1995 – 1997	Teaching and Research Assistant at Simon Fraser University, Vancouver, Canada
1994 –1995	Research Assistant at the Atmospheric Science Laboratory at Trent University, Ontario, Canada
summer 1994	Internship at the École Polytechnique in Paris, France

Education and Qualifications

1999 –2001	Enrollment in the Ph.D. program of the Department of Architecture at the Technical University of Karlsruhe, Germany
1997	Diplom-Physiker Albert-Ludwigs Universität, Freiburg, Germany Master of Science Simon Fraser University, Canada
1995	Bachelor of Science of Honours Trent University, Canada
1993 –1994	Studies in Physics at the Université de Paris XI in Paris, France
1991-1992	Studies in Physics and Mathematics at the Albert-Ludwigs-Universität Freiburg